ABSTRACT

Title of Document: VEGETATION-HYDRODYNAMIC INTERACTIONS AND THE STABILITY OF CHANNEL INLETS IN TIDAL FRESHWATER WETLANDS, CHESAPEAKE BAY SYSTEM

Anna Elizabeth Statkiewicz, Master of Science, 2014

Directed By: Karen L. Prestegaard, Associate Professor, Department of Geology

To maintain elevation, deposition of mineral and organic sediment in tidal freshwater wetlands (TFWs) must outweigh losses due to sea-level rise, erosion, decomposition, and compaction. Sediment loads into tidal marshes are controlled by inlet size and sediment supply, but interactions among vegetation, hydraulics, and geomorphology affect sediment retention. This study focused on these interactions in TFW inlets partially covered by aquatic vegetation (*N.luteum, Z.aquatica,* and *H.verticullata*). Measurements of hydraulic parameters and geomorphic change were correlated with observations of spatial and morphological characteristics for each vegetation type. The aquatic plants grew in significantly different water depths and well-defined platforms formed in areas occupied by emergent vegetation where effective shear stress is lowest. Net annual accretion data indicate an inverse relationship between maximum inlet depth and accretion rate. These results suggest

that initial vegetation colonization modifies channel inlet morphology; both vegetation and morphology generate the shear stress distributions, which maintain channel form.

VEGETATION-HYDRODYNAMIC INTERACTIONS AND THE STABILITY OF CHANNEL INLETS IN TIDAL FRESHWATER WETLANDS, CHESAPEAKE BAY SYSTEM

By

Anna Elizabeth Statkiewicz

Thesis submitted to the Faculty of the Graduate School of the
University of Maryland, College Park, in partial fulfillment
of the requirements for the degree of
Master of Science
2014

Advisory Committee:
Associate Professor Karen L. Prestegaard, Chair
Associate Professor Michael Evans
Assistant Professor Vedran Lekic

Acknowledgements

I would like to thank my advisor, Dr. Karen Prestegaard, for her guidance and assistance in the field, and all of my field assistants who generously donated their time to support my project:

Nathan Bailey
Chelsea DeMerice
C. Rosie Duncan
Eric Fowler
Kalev Hanstoo
Julia Gorman
Terrale Green
MeiMei Luhr
Phil Piccoli
Jenny Rewolinski
Robert Statkiewicz
Craig Velencia

Table of Contents

List of Tables

List of Figures

List of Symbols

τ_{tot}	*Total Shear Stress (N/m^2)*
ρ_w	*Density of Water (kg/m^3)*
g	*Acceleration of Gravity (m/s^2)*
R	*Depth (m)*
S	*Water Surface Gradient*
τ^*_{crit}	*Critical Dimensionless Shear Stress*
ρ_s	*Density of Sediment (kg/m^3)*
D_{50}	*Median Grain Size (m)*
$\overline{U}$	*Average Velocity (m/s)*
U*	*Shear Velocity (m/s)*
K	*VonKarmen's Constant*
z_o	*Roughness Height*
τ_{eff}	*Effective Shear Stress (N/m^2)*
m	*slope*
τ_{veg}	*Vegetation Shear Stress (N/m^2)*
F_r	*Flow Resistance*
L	*Length (m)*
D_o	*Maximum Inlet Depth (m)*
U_{crit}	*Critical Velocity (m/s)*
A_o	*Amplitude of Tidal Forcing*
W	*Tidal Angular Frequency*
M	*Relative Channel Depth (m)*
sl	*Distance between Water and Reference Level (m)*
Δg	*Change in Tidal Stage (m)*
d	*Apparent Depth (m)*
RL	*Reference Level (m)*

Chapter 1: Introduction

1.1 Statement of the Problem

Tidal freshwater wetlands (TFWs) contribute to the health of downstream estuarine and coastal waters through their ability to store sediment and promote denitrification (e.g., Boynton *et al.*, 2008; Seldomridge and Prestegaard, 2012). TFWs also serve as nurseries for young aquatic life and offer upland communities protection from storm surges (Michener *et al.*, 1997; Mitsch and Gosselink, 2000). It is important to understand how these ecosystems will adjust to future environmental changes, which may include: sea-level rise, higher salinity, increases in air and water temperature, and changes in length of the growing season. These changes will likely affect plant communities and the interactions among vegetation, hydraulics, and marsh geomorphology that influence ecosystem functioning (D'Alpaos, *et al.*, 2006; Mudd *et al.*, 2010). To preserve these valuable ecosystem services, TFW elevations must keep pace with accelerating sea-level rise, thus net accretion must equal or exceed subsidence and sea-level rise:

$$\Delta\text{Marsh elevation} = \text{net accretion} - (\text{subsidence} + \text{sea-level rise})$$

where,

$$\text{Net accretion} = \text{mineral sediment deposition} + \text{organic matter inputs} - \text{erosion}$$

$$\text{Subsidence} = \text{decomposition} + \text{compaction} + \text{geologic subsidence}$$

(Krone 1987)

Without positive net accretion on both marsh platforms and in channel networks, tidal inlets will widen and vast areas of open water will replace TFW, eliminating their ability to perform valuable ecosystem services (Kirwan and Murray, 2007). Previously, tidal marshes were thought to sustain themselves as net accretion matched the rate of sea-level rise (Redfield, 1965; Friedrichs and Perry, 2001). There are new concerns about the fate of tidal marshes as sea-level rise accelerates and riverine sediment loads are impounded by dams or levees (Kirwan *et al.*, 2011; Tambroni and Seminara, 2012). Recent modeling studies suggest that the minimum sediment load required to maintain positive elevation in these marshes will increase as sea-level rises; however, these studies also assume that sediment retention processes will remain constant as climate changes (Kirwan and Murray, 2007; Tambroni and Seminara, 2012). They do not consider alterations to marsh maintenance processes due to changes in vegetation cover, precipitation, storm magnitude, etc.

The amount of mineral sediment retained in tidal marshes depends on external variables, such as the supply of sediment from upstream watersheds, as well as internally-adjusted variables such as the geomorphology of marsh channel networks, channel hydraulics, and the distribution of aquatic vegetation in the channels. Inlet channel morphology determines the amount of sediment entering the wetland, the residence time of water in the system, and the depth and frequency of overbank flooding (Fagherazzi *et al.,* 1999; Seldomridge, 2009). Changes to channel morphology, especially inlet shape and size, could significantly affect marsh maintenance processes and the flux of sediment in these tidal freshwater marshes.

In TFW, inlet geomorphology is affected by emergent vegetation that grows in the channel, thereby increasing flow resistance and enhancing deposition. As discussed by Marani *et al.* (2013), aquatic plants engineer their habitat, creating channel depth distributions specific to the dominant vegetation species. The amount of deposition in these channels depends upon the availability of mineral sediment, but also on the alteration of channel hydraulics by individual plant species. Vegetation hydraulic characteristics, such as stem density, height, and growth depth, produce variations in bed roughness, and therefore flow resistance, velocity distributions, and ultimately sediment deposition (Palmer *et al.,* 2004; Nepf and Ghisalberti, 2008; Larsen *et al.*, 2009). Each dominant plant species has a range of specific depth habitats, stem densities, and other characteristics that affect sediment trapping differently during the growing season.

The seasonality of marsh vegetation growth, and thus the biogeomorphic relationships between vegetation coverage and inlet morphology impacts the ability of TFW to accrete sediment and prevent flooding of the marsh platform. The presence of dense monocultures of vegetation in the summer and complete absence of plants in the winter create two distinct end-member states in TFW channels as shown in figures 1.1-1.2. Constriction of flow and vegetation roughness at growth maxima may greatly enhance deposition rates and improve the ability of the marsh to maintain positive elevation as sea-level rises. Dieback of vegetation during the winter months increases effective flow widths, velocities, and thus discharge, promoting greater boundary shear stress and erosion. Because of these relationships, net annual marsh accretion likely occurs due to the combination of these alternate channel states.

Species-specific differences in plant dieback dynamics (e.g. how stem density changes with dieback, whether flow resistance persists due to standing dead vegetation, etc.) could affect the timing and rate of accretion in marshes with different

Figure 1.1 Summer state of TFW. Google Earth imagery from Summer 2008 showing a tidal freshwater marsh channel on the Patuxent River, MD. The thin, blue line in the center of the channel represents open water, greenish-brown edges represent area occupied by vegetation.

Figure 1.2 Winter state of TFW. U.S. Geological Survey imagery accessed through Google Earth from Winter 2010 showing the TFW from figure 1.1. White lines represent frozen edges of the channel. No vegetation is present to restrict the flow of water through the channel.

dominant channel vegetation. The seasonal alternation between vegetated and non-vegetated states will result in net channel accretion, if summer accretion is greater than winter erosion.

1.2 Previous Work

1.2.1 Biogeomorphic Relationships

Previous studies (D'Alpaos *et al.,* 2006; Tambroni and Seminara, 2010, etc.) have examined the dynamics of marsh maintenance by modeling the interactions among vegetation, hydrology, and geomorphology of marsh platforms. Other studies scrutinized specific aspects of these relationships such as the contribution of biomass to marsh accretion (Mudd *et al.,* 2010) or the variation of hydraulic properties with vegetation characteristics (Nepf and Ghisalberti, 2008; Larsen *et al.*, 2009). Few of these experiments couple simulations with observations, and even fewer focus on the importance of channel inlets. As a result, many of these models apply empirical relationships based on values measured in other marshes to quantify variables such as biomass, flow resistance, etc. (e.g. Palmer *et al.*, 2004; D'Alpaos *et al.,* 2006). Most authors provide little or no validation of their models; thus their models can only provide simplified explanations of relationships among channel hydraulics, vegetation, and channel morphology (e.g. Kirwan and Murray, 2007; Mudd *et al.,* 2010). These models could be improved through field data collection that identifies important processes and variables, and also tests model assumptions.

Although many studies recognize the importance of vegetation, few studies acknowledge that vegetation can vary seasonally, that *both* vegetated and non-vegetated states occur *each year.* Many modeling studies evaluate whether a

vegetated marsh has higher net accretion rates than non-vegetated counterparts (e.g. Marani *et al.*, 2007; Tambroni and Seminara, 2010). Generally, these studies indicate that water depth over non-vegetated marsh platforms will increase until the wetland is transformed to open water. Because they do not evaluate the effects of hydraulics, geomorphology, and vegetation equally, these studies may place a disproportionately large value on vegetation in terms of net accretion, particularly if they do not consider the nature of the material accreted (organic versus mineral; decomposition rates; the fate of accreted material during erosion cycles). Furthermore, seasonal variations in upland vegetation density also affect the supply of sediment. In seasonally cold watersheds, mineral sediment supply may be higher and/or coarser grained during winter months, which in turn creates seasonal variations in the erodability of accreted channel sediment (Wolman, 1967).

Currently little is known about the relationships among vegetation attributes, accreted sediment characteristics, and channel morphology, particularly for plant species common in TFW. These gaps in our understanding reflect the extensive study of tidal saltwater marshes compared with TFW systems. Salt marsh systems differ greatly in both structure and function from their freshwater counterparts. Saline marshes often have lower plant diversity than TFW, as many plants cannot sustain themselves under the dual stresses of inundation and high salinity (e.g. Zedler, 1977; Nixon, 1982). TFW vegetation flourishes easily under the single stress of anoxic conditions produced by frequent flooding; therefore, TFW maintain a higher diversity of plant species, especially at channel margins (Odum and Hoover, 1987). Salinity also affects the location of plant growth: in saltwater marshes, vegetation generally

colonizes the marsh platform, whereas TFW plants grow along channel margins and shallow reaches of the channel (Odum, 1988).

Seasonality also contributes to major structural and functional differences between these marshes. Salt marsh platform vegetation and some freshwater platform vegetation remains on the marsh surface throughout the year (as standing dead cover in the winter) (Odum, 1988). Emergent vegetation in tidal channels, however, usually dies back during cold seasons, which may affect vegetation flow resistance and the capacity for accretion. These three factors, plant diversity, plant cover, and seasonality vary along salinity gradients; such variations could result in different mechanisms of erosion and sediment delivery among tidal marshes. The recent focus on tidal saltwater wetlands, where these factors seem to create simpler biogeomorphic relationships, leaves the effect of these variables on flow regime, sediment deposition, and erosion in TFW largely uninvestigated.

1.2.2 Hydrodynamics

Erosion depends on the ability of flow to entrain particles off the channel bed. Sediment entrainment requires a shear stress in excess of a critical value that varies with grain size and density. Shear stress (τ), the force per unit area acting on the bed, results from the shearing of fluid caused by the interaction of gravitational and frictional forces along the bed as water flows along a channel bottom. Assuming that the resisting force equals the gravitational force (i.e. the flowing water does not accelerate and the width of the channel is much greater than depth), we can calculate the total boundary shear stress (τ_{tot}) acting on the bed using the duBoys equation:

$$\tau_{tot} = \rho_w g R S \tag{1.1}$$

where ρ_w is the density of water, g is gravitational acceleration, R is flow depth, and S is slope, or gradient.

The critical dimensionless shear stress (τ^*_{crit}), or Shields stress, is the ratio of the shear stress exerted by the fluid to the grain resisting forces (chemical attraction among particles; frictional forces with the bed) that impede erosion:

$$\tau^*_{crit} = \frac{\tau}{(\rho_s - \rho_w) g D_{50}} \tag{1.2}$$

where ρ_s is the density of the bed material and D_{50} is the median surface grain size of sediment particles. For erosion to occur, the force acting on the bed must equal or exceed the critical dimensionless shear stress specific to the sediment in the channel.

The effective shear stress, the proportion of the force that is applied to entraining bed particles, varies due to the amount of friction between the bed and the down slope movement of water. The magnitude of this frictional force depends on the roughness of the bed, which in practical terms refers to the uniformity of particle size and bed topography, but can also be affected by the presence of vegetation. These roughness characteristics dissipate a portion of the flow energy, reducing the amount of force devoted to erosion and sediment transport.

We can measure the effective shear stress at a specific location and moment in time using the von Karman-Prandtl Law of the Wall, which relies on the logarithmic relation between flow depth and velocity to estimate bed shear stress:

$$\frac{\overline{U}}{U_*} = \frac{1}{K} \ln\left(\frac{R}{z_o}\right) \tag{1.3}$$

$$\text{where } U_* = \sqrt{gRS} \tag{1.4}$$

$$\text{thus, } \tau_{eff} = \rho_w U_*^2 \tag{1.5}$$

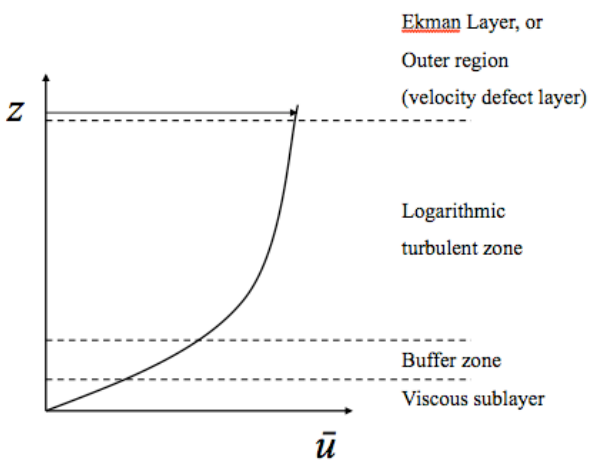

Figure 1.3 Logarithmic velocity profile. According to the Law of the Wall, velocity in a channel varies logarithmically with depth. Figure by Dr. Karen Prestegaard.

where $\overline{U}$ is average flow velocity, U_* is shear velocity (a parameter that states shear stress in terms of velocity), K is von Karman's constant, and z_o is the depth at which velocity reaches zero. The ideal flow is divided into distinct subsections: a thin, viscous sublayer with laminar flow, a turbulent, logarithmically defined layer, and an outer velocity defect layer (see figure 1.3). The Law of the Wall describes how velocity changes as boundary shear forces and the transfer of momentum cause turbulent eddies to alter flow logarithmically with depth. We can derive τ_{eff} by linearly regressing on the measured vertical velocity profile within the turbulent zone; in this case, the slope (m) of the line is proportional to shear velocity ($m=K/U_*$). Because shear velocity is a mathematical construct used to relate velocity and shear stress, we can apply equation (1.5) to derive the effective shear stress at a specific location.

Previous studies (e.g. Larsen *et al.,* 2009) have employed this idea of shear stress partitioning to specifically explore the impact of vegetation on flow regime. We define vegetation shear stress (τ_{veg}) as the difference between the overall total and effective shear stresses, evaluated across the entire channel:

$$\int \tau_{veg}\, ds = \int \tau_{tot}\, ds - \int \tau_{eff}\, ds \qquad (1.6)$$

Using this relationship, we can estimate how much energy has been dissipated by flow through vegetation and therefore the degree to which biomass inhibits erosion or

enhances deposition in a channel. As demonstrated by Larsen *et al.* (2009), the reduction of effective shear stress is due to the frictional resisting forces introduced by vegetation in the water column. The reduction of effective stress depends on the vegetation architecture, or the area of the water column occupied by vegetation, and therefore varies with the geometry and spatial distribution of plant species. Vegetation shear stress also changes seasonally and may approach zero as vegetation disappears in the winter, allowing greater effective shear stresses and therefore erosion (see figure 1.4).

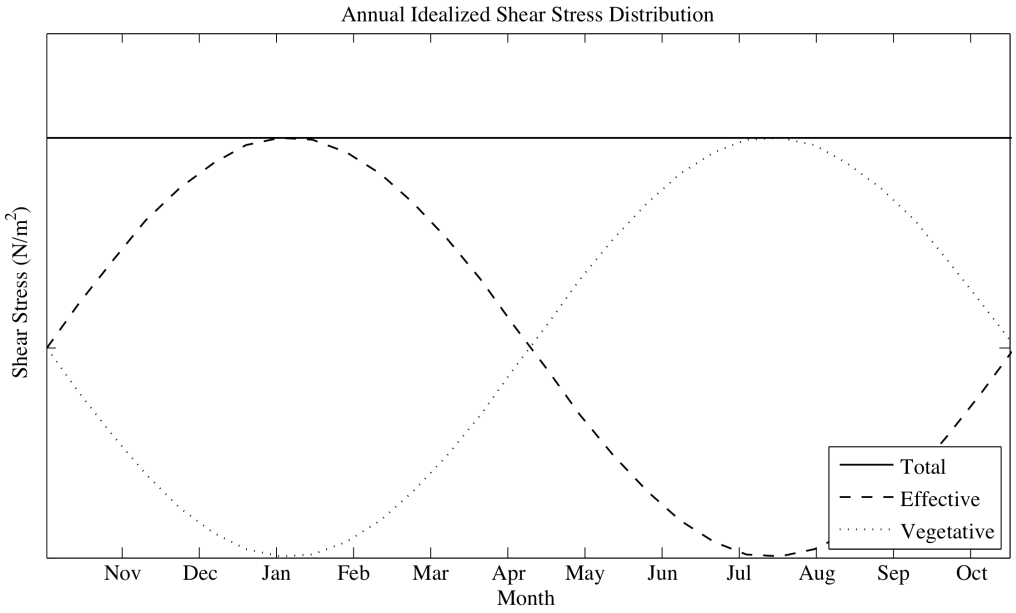

Figure 1.4 Idealized shear stress distribution for Q_{max} over an annual cycle of vegetation growth and dieback. If the total shear stress is constant, the partitioning of shear stress into the component dissipated by vegetation and the effective shear stress, varies with vegetation growth. As shown, effective shear stress peaks during times of vegetation minima while vegetation shear stress crests during the summer growth maxima.

Keulegan (1938), Leopold and Wolman (1957), Limerinos (1970), and others explored the effect of bed roughness on flow by relating roughness height to resulting flow resistance. The authors derive these variables from empirical relationships described by the Law of the Wall, where flow resistance (F_r) is the ratio of average velocity to shear velocity:

$$F_r = \frac{\overline{U}}{U_*} \tag{1.7}$$

and the roughness height is equal to the depth at which velocity is zero (z_o). In this formulation, a larger value of F_r actually indicates greater bed smoothness. Hydraulic roughness of the channel boundary can be expressed as the ratio of flow depth to roughness height (d/Ks, where roughness height Ks is proportional to z_o). The relationship between relative roughness and flow resistance has been evaluated for flume channels (Keulegan, 1938) and natural streams (Leopold and Wolman, 1957) (fig.1.5). Due to the large roughness height and density of emergent vegetation in tidal channels, these systems might be significantly hydraulically rougher than gravel-bed streams.

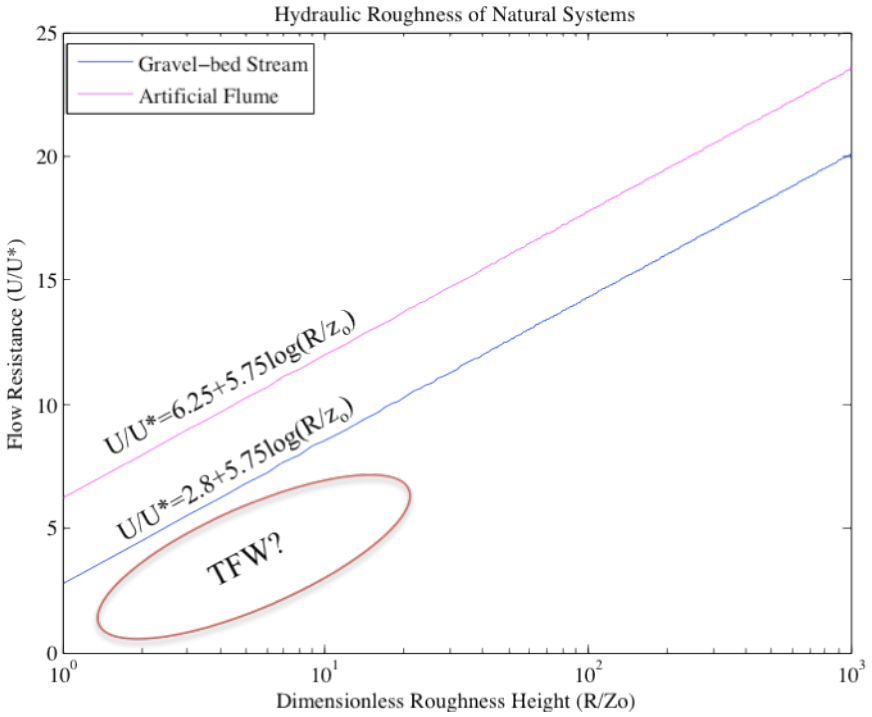

Figure 1.5 Relationship between depth and roughness height ratio (R/z_o) and flow resistance for flume, natural channels, and tidal channels with vegetation. Smooth systems, such as Keulegan's flume study, plot above (smoother than) hydraulically rough systems, such as Leopold and Wolman's equation for gravel-bed streams. We hypothesize that TFW channels are among the most hydraulically rough systems. Note that R/z_o is actually a measure of relative smoothness; as this ratio increases, the system roughness height decreases relative to depth.

1.2.3 Marsh Channel Equilibrium

The concept of an equilibrium channel form was initially developed for terrestrial channels, and has been defined as a channel that neither aggrades nor degrades over time (Mackin, 1948). Hydraulic definitions of an equilibrium channel suggest that the effective shear stress at bankfull flow (or channel-forming discharge) is in equilibrium with the critical shear stress required to move material along channel boundaries (Parker, 1978; Dietrich and Smith, 1984). Fluid shear stress is proportional to depth and gradient; therefore, at a given location the equilibrium channel has a depth distribution (shape) dependent upon the grain size distribution (Parker, 1978). These hydraulic considerations imply that the equilibrium form varies with the size-distribution of bed material, vegetation that affects effective shear stress, and the frequency of bankfull discharges. Changes to these variables generate adjustments to a new equilibrium form.

Terrestrial channels are considered to be in dynamic or quasi-equilibrium: although the channel form is stable, the channel migrates across the floodplain (Langbein and Leopold, 1968). There is less evidence that tidal channels undergo significant lateral movement, and thus they may achieve a static equilibrium (Hickin and Nanson, 1984). Tidal marsh channels have a finite length, but a discharge that varies periodically with tidal forcing. Previous studies have defined marsh equilibrium from several different perspectives: sediment mass balance, equilibrium channel geomorphology, and marsh hydrodynamics. The classic idea of marsh equilibrium is the Krone (1987) mass balance approach (see section 1.1), in which the positive elevation inputs (mineral and organic sediment deposition, biomass

production) balance negative elevation impacts (sea-level rise, decomposition, erosion, compaction) to preserve the marsh platform. Unlike definitions of terrestrial channel equilibrium and other definitions of tidal marsh equilibrium, this formulation requires a positive net sediment flux to keep pace with changing environmental factors and makes few specifications about channel form.

Friedrichs and Aubrey (1996) refined the idea of marsh equilibrium, using marsh-scale relationships between channel geometry and discharge magnitude to define the expected equilibrium form. They define the static equilibrium channel as one for which channel length (L) is proportional to inlet depth (D):

$$L = \frac{D_o U_{crit}}{A_o W} \tag{1.8}$$

where D_o is inlet maximum depth, U_{crit} is the critical velocity required to move sediment, A_o is the amplitude of the forcing (spring) tides, and W is the angular frequency of the tides.

Seminara *et al.* (2010) adapted the idea of an equilibrium channel to tidal marsh studies by describing the hydrodynamic characteristics required to achieve no annual net flux of sediment. They define the static equilibrium state as a channel in which the effective shear stress equals the critical shear stress at all locations at each instant. Unlike the other formulations of marsh equilibrium, this definition does not consider the marsh area as a whole, but instead is evaluated continuously across the marsh. This definition is problematic, however, as it ignores the possibility of variation in parameters contributing to the effective shear stress such as variation in tidal amplitude, flow depth, vegetation cover, and flow resistance.

1.3 Study Objectives

In this study, we utilize field-based observations to evaluate the effects of vegetation on marsh channel morphology and net annual accretion through the following objectives:

1. *Identify species-specific spatial and morphological vegetation characteristics in tidal freshwater inlets.*
2. *Determine how vegetation type affects effective shear stress distributions and flow resistance in tidal freshwater inlets.*
3. *Determine how vegetation type affects inlet channel geometry and the capacity for net annual accretion in tidal freshwater marshes.*

1.4 Study Area and Approach

This study focused on tidal marsh inlets extensively (30-60%) covered by aquatic vegetation in the freshwater portion of the Patuxent River, MD (fig. 1.6). Inlets were selected based on both size and vegetation cover. Several species occupy these inlets in monocultures, including the emergent *Nuphar luteum* (L.) and *Zizania aquatica* (L.), and submerged aquatic vegetation (SAV) (commonly *Hydrilla verticullata* (Royle)) (fig. 1.7). Seldomridge and Prestegaard (2012) found that the largest marshes make up ~10% of the TFW community, but perform ~90% of the nitrate retention. Retention of sediment is also likely based on inlet size and channel vegetation that may affect sediment deposition. Therefore, in this study, we examined the large tidal inlet-marsh systems in the upper Patuxent River estuary, north of Jug Bay Wetlands Sanctuary. Each inlet was occupied by one of the three principal vegetation species.

In each entrance reach, we established two permanent cross sections at which vegetation, morphology, flow dynamics, and channel accretion were monitored. The

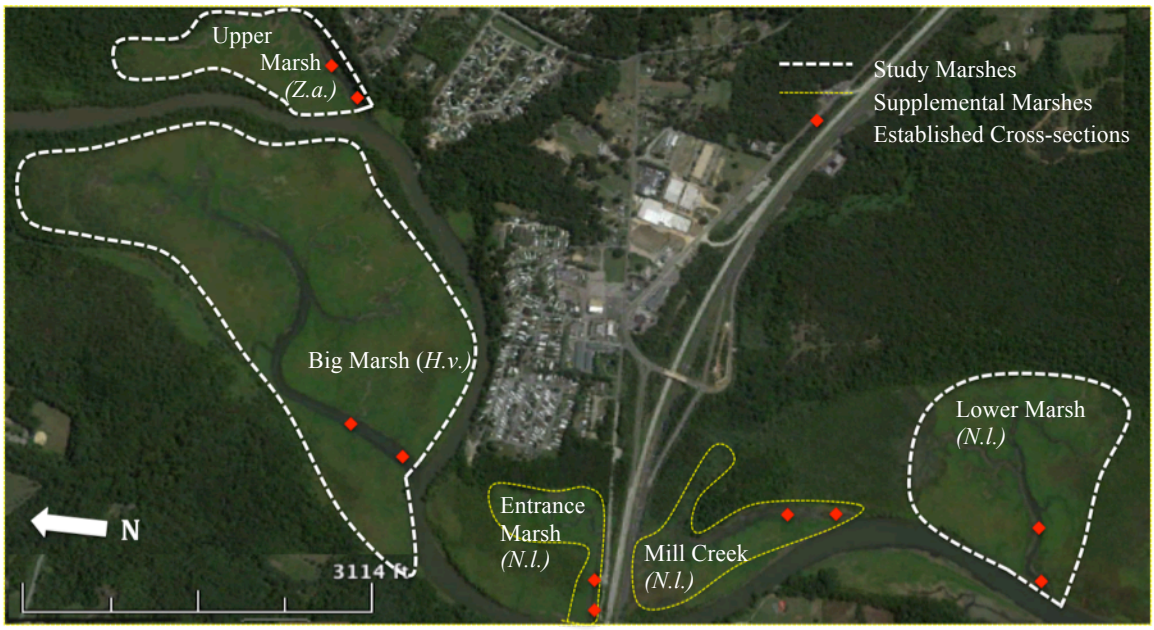

Figure 1.6 Map of study sites. Google Earth imagery from 8/28/2010 showing TFW sites on the upper Patuxent River, MD. Main study marshes outlined in red, supplementary marshes shown in yellow. Red diamonds indicate location of established cross-sections where the majority of measurements were repeated. Future references to study sites will include marsh code (initials of marsh name) and an Arabic numeral denoting cross-section within marsh (1 for inlet, 2 for upstream). Italics indicate plant species present.

ends of each cross-section were anchored by PVC pipe installed >1m into the marsh soil at the channel margins. The marsh channel-platform boundary was delineated by changes in elevation and species diversity. Channel vegetation typically forms monocultures of emergent or submerged vegetation, whereas marsh platform vegetation is composed of diverse plant communities, including herbaceous emergent vegetation, shrubs, vines, and even trees.

Subsequent chapters will seek first to characterize each of the three dominant types of vegetation by spatial distribution and unique plant morphology. Such information will highlight differences in plant growth and habitat, but also indicate how each plant could affect channel hydraulics. Vegetation studies will also analyze seasonal changes in vegetation community. Patterns of growth and dieback, including

length of dieback, decomposition rate, etc., could influence the long-term storage of sediment accreted over the summer period.

Chapter 3 will expand upon this investigation, exploring the specific influences of each vegetation type on shear stress distributions and flow resistance. Here we can learn which vegetation growth parameters best predict a species' influence on flow. Comparison with critical shear stress in each channel will indicate which locations are most susceptible to erosion and deposition both during the vegetated summer period and subsequent non-vegetated winter season.

Chapter 4 will examine how vegetation growth and its affect on channel hydrodynamics feedback on inlet channel accretion and deposition. We will investigate whether channel hydraulics predict the changes in channel morphology shown by our time series of geomorphic measurements. Trends in accretion under various plant types and channel geometries will also be investigated.

Chapter 5 will revisit ideas of marsh equilibrium and net annual accretion presented in chapter 1 to evaluate assumptions made by previous studies. We will also explore the implications of our findings as they apply to marsh maintenance processes and the effects of climate change. Finally, we will address topics, which require more study and outline avenues for future work.

Figure 1.7 Dominant plant species found at Patuxent Study Marshes. *N. luteum* (top) is a fleshy, erbaceous lily-pad, which becomes partially or fully submerged at high tide. *H. verticullata* (center) is a waxy, submerged aquatic plant, which fills channels with large mats of weeds. *Z. aquatica* (bottom) is a fibrous grass, which is partially submerged at high tide.

Photo credits: Anna Statkiewicz (top left), Carefree Enzymes: Natural and Eco-safe Products, carefreeenzymes.com (top right), Virginia Plant Atlas, vaplantatlas.org (bottom left)

Chapter 2: Spatial Distribution and Morphological Characteristics of Emergent and Submerged Aquatic Plants

2.1 Introduction

Emergent plants in tidal inlets impact flow resistance, and therefore sediment deposition and erosion processes. The submerged surface area of the plant reduces flow area and increases hydraulic roughness, thus creating resistance to flow (Larsen *et al*., 2009). The widely used Palmer *et al.* (2004) model of particle capture by plants depends on plant morphology, but also considers spatial relationships such as stem density. In order to evaluate the effects of different plant species on marsh maintenance processes, both the spatial distribution and morphological characteristics of plants need to be measured. These morphological characteristics may change with the growth state of the plant; therefore, repeated vegetation sampling will track the hydraulic characteristics of channel vegetation over the lifecycle of each species.

2.2 Methods

2.2.1 Field Data Collection

Previous studies indicate that stem density, stem diameter, stem height, width of vegetated channel area, and water depth beneath vegetation are important parameters that can be used to determine the submerged surface area of a plant, and thus flow resistance it creates (Larsen *et al*., 2009) and to model particle capture (Palmer *et al.*, 2004). For the present study, we measured these vegetation parameters

in the inlets of *N.luteum* and *Z.aquatica* marshes. Previous studies (Jenner, 2011) indicate that *H.verticullata* creates a distinct vegetation boundary layer with most of the flow going above the dense, matted vegetation; therefore, we measured only flow depth and vegetation boundary layer height for *H.verticullata*.

At each inlet transect, stem height and growth depth (relative to maximum high tide) were measured at 1 m intervals across the channel with a USGS-style wading rod. The channel width occupied by *N.luteum* and *Z.aquatica* vs. distance upstream was determined from U.S. Geological Survey air photos by measuring vegetated width at 20m intervals up the main marsh channels. Stem density (stems/ m^2) and stem diameter for each emergent species were determined using a quadrant sampling method. Quadrants were established by tossing a $1m^2$ PVC square into monocultures of each species at random distances along the channel. Within each square, the number of stems was recorded and the diameter of 10 randomly selected stems was measured. Stem density measurements were taken seasonally, while stem diameter was measured at peak growth height.

2.2.2 Data Analysis

Mean and standard error of stem density and stem diameter for *N.luteum* and *Z.aquatica* as were calculated, and t-tests ($p<0.05$) were used to investigate whether statistically significant differences in stem height or stem densities exist between these species. Growth curves for *N.luteum* and *Z.aquatica* were generated by plotting plant height (as a box plot) versus date of measurement. Channel depth ranges (relative to the marsh platform) were identified from cumulative probability distributions of growth depth for each species and further confirmed using a model I,

single-factor ANOVA and subsequent a posteriori (Tukey) testing. Time-series plots of channel width occupied by each species were developed to track the rate of dieback of each species.

2.3 Results

As shown in figures 2.1-2.2, both emergent species exhibited peak growth during different time intervals: *N.luteum* reaches its maximum height of 0.9-1.1m in late June-July, while *Z.aquatica* reaches its maximum growth height of 2.0-2.5m in late August-September. Although these data accurately reflect the timing and peak growth height of *N.luteum*, these measurements do not capture the bimodal nature of the *N.luteum* growing season; however, we do not expect this to affect conclusions of the study. As observed in the field, *N.luteum* dies shortly after peak growth, replacing broad leaves (~15-18cm in diameter) with smaller fist-sized leaves (~10-12cm in diameter).

Each of the three plant species inhabits distinct depths and therefore areas of TFW inlets. Cumulative probability curves of occupied channel depth (relative to high tide), reveal different growth ranges for each species (fig. 2.3): *Z.aquatica* occupies the shallowest depth (0-0.7m, mean ~0.45), *N.luteum* the intermediate portion of the channel (0-0.8m, mean ~0.6m), and *H.verticullata* the deepest depths (0.4-1.8m, mean ~0.8m). Differences in preferred depth were further confirmed by a model I, single-factor ANOVA and subsequent a posteriori testing as shown below in table 2.1. While the favorable growth depths for each species overlap, aquatic vegetation grows in monocultures in each TFW channel. In inlets dominated by *N.luteum, Z.aquatica* was relegated to the marsh platform and *H.verticullata* (if

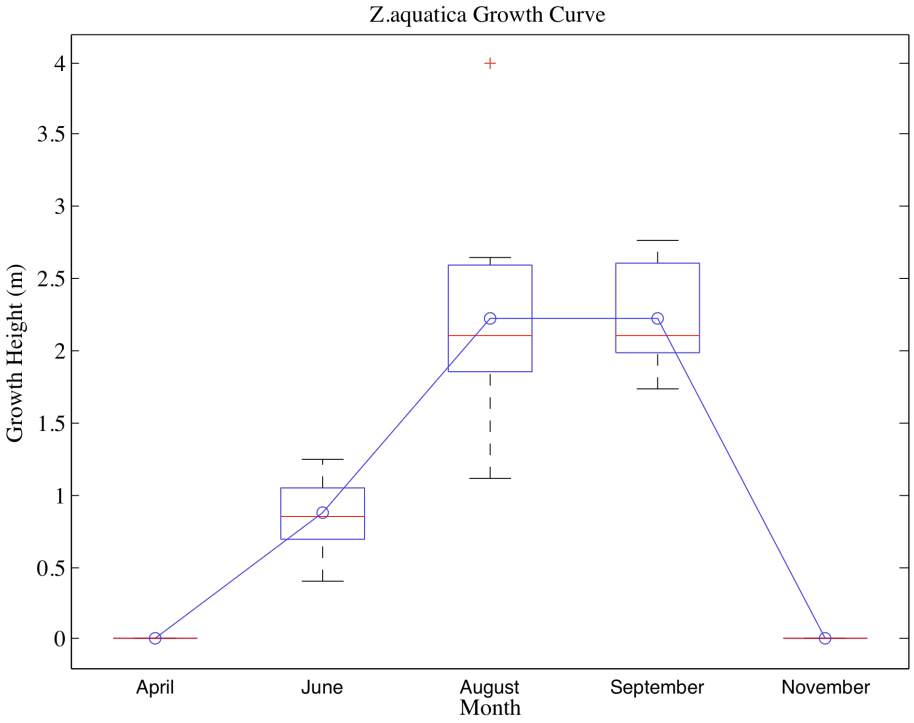

Figure 2.1 Growth curve for *Z.aquatica* constructed using monthly to bimonthly measurements of plant height. Horizontal red lines mark distribution mean, while blue boxes include data, which falls between the lower and upper quartiles (75% of the data). Whiskers include 99% of the data, while red crosses designate outliers. Average growth height (m) indicated by the solid blue line connecting monthly box plots. These conventions will be followed for box plots throughout the remaining text.

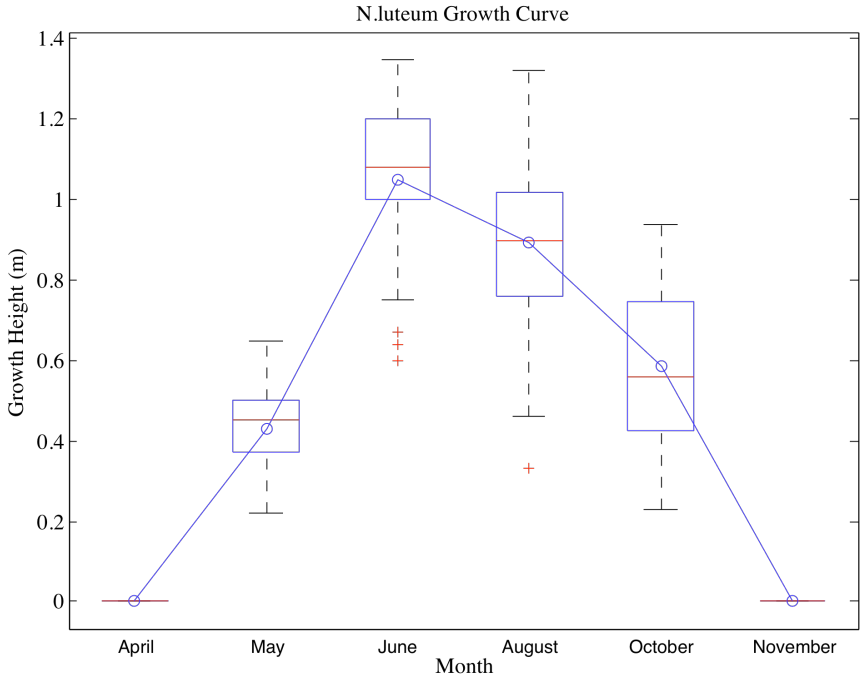

Figure 2.2 Growth curve for *N.luteum* constructed using monthly to bimonthly measurements of plant height.

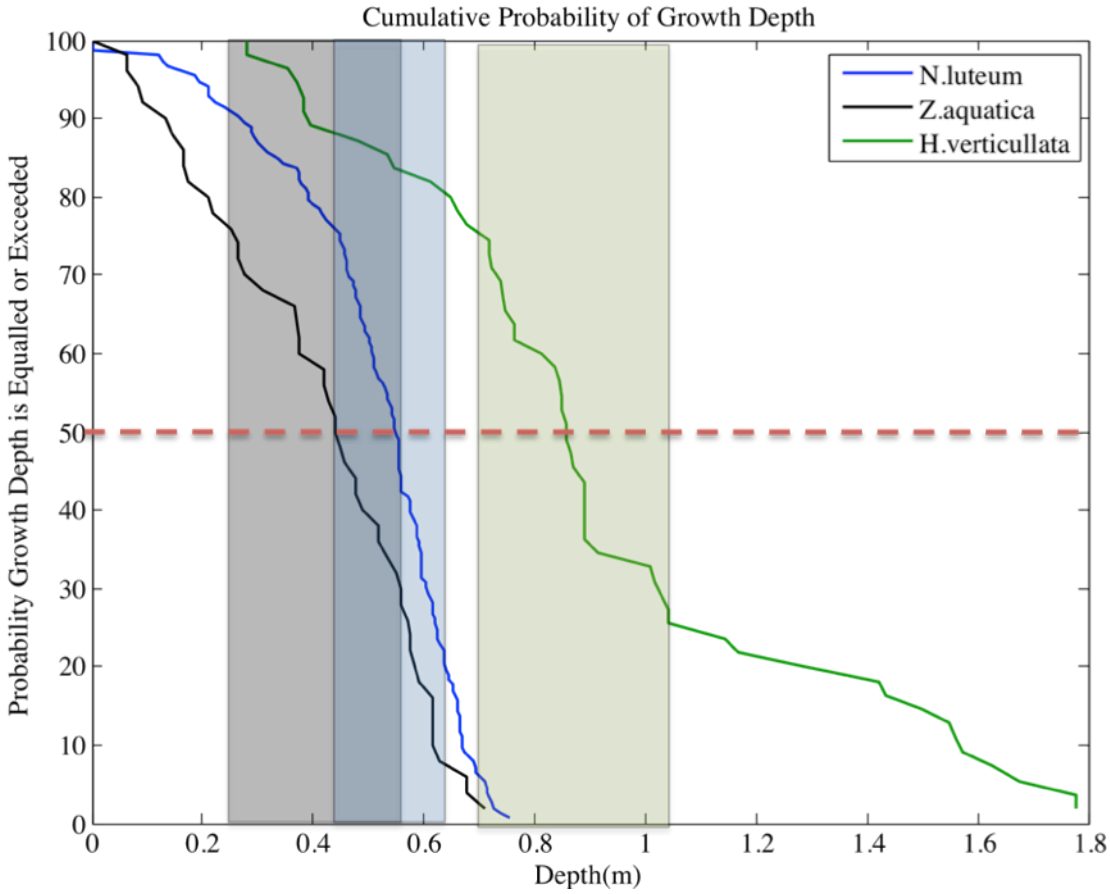

Figure 2.3 Cumulative probability of growth depth for each species found at Patuxent TFW. Shaded region indicates the depth range of each species (25th to 75th percentile). Red dashed line designates the median growth depth of each species.

Source of Variation	Sum of Squares	Degrees Freedom	Mean Square	F
Among Vegetation Types	8.42	2	4.21	76.22***
Within Vegetation Types	14.09	255	0.06	
Total	22.51	257		

Table 2.1 Summary table for ANOVA comparing depth at which aquatic vegetation grows for three dominant types of plants. *=0.05<p≤0.1, **=0.01<p≤0.05, ***=p≤0.01. These conventions will be followed throughout the remaining text.

Growth Depth			
Species	*N.luteum*	*Z.aquatica*	*H.verticullata*
N.luteum	———	3.83**	15.49***
Z.aquatica		———	15.66***
H.verticullata			———

Table 2.2 A posteriori summary table for comparison of growth depth for three dominant types of aquatic vegetation.

present) was restricted to greater depths adjacent to the central channel. In *Z.aquatica*-dominated inlets, both *Z.aquatica* and *H.verticullata* together occupy the full extent of the channel width without overlap. Only in the marsh where emergent macrophytes are absent did *H.verticullata* occupy a wide range of depths, including the shallower ranges preferred by the emergent plant species.

In addition to distinct differences in growth-depth preferences and plant heights, the two emergent species also occupy varying widths of the channel the inlet. As shown in figure 2.4, *N.luteum* fills more than half the inlet channel width, while *Z.aquatica* occupies ~30% of the channel, and *H.verticullata* <15% of the inlet width. The SAV estimations were based on field measurements, as these submerged species are not visible at the resolution of available air photos. The submerged nature of these species makes accurate measurement of the occupied width difficult.

The hydraulic properties of these plants—those applied to estimate particle trapping in models (Palmer *et al.*, 2004; Larsen *et al.,* 2009)—are significantly different ($p<0.1$) (table 2.3). A two-tailed t-test comparing frontal areas of each species, the area of the water column occupied by each plant type, reveals a significant difference between *N.luteum* and *Z.aquatica* ($p<0.01$).

In addition to describing plant habitat, these measurements also inform about the dieback characteristics of the emergent species. As discussed previously, *N.luteum* reaches peak growth before *Z.aquatica*. Data showing the fraction of inlet width occupied by emergent vegetation can be expressed as a time series. These data

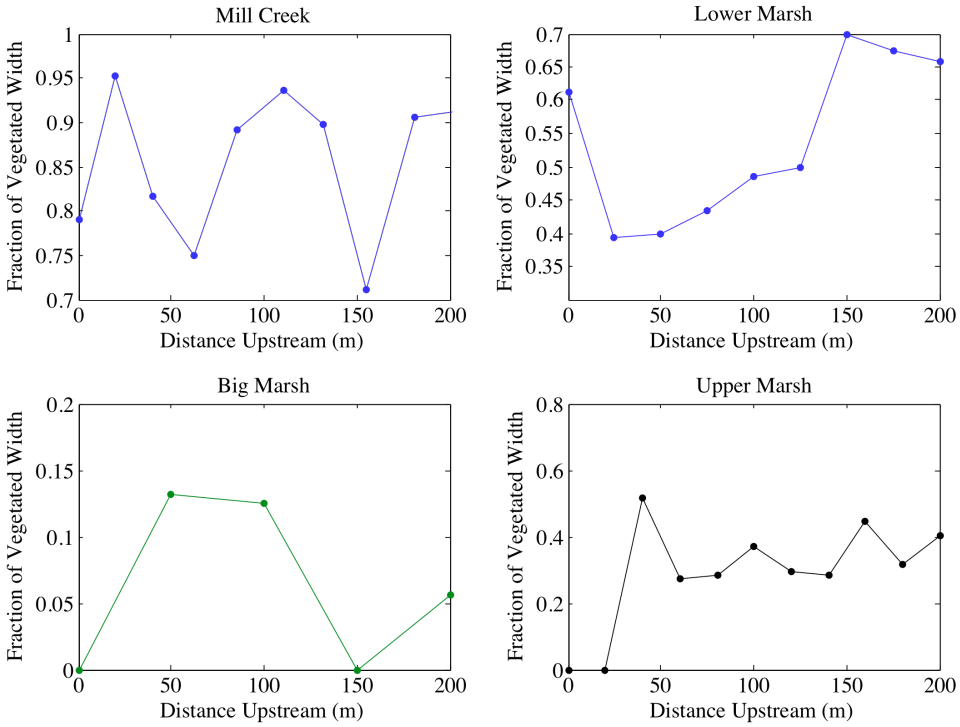

Figure 2.4 Fraction of vegetated width vs. distance upstream for each dominant plant species. Line colors correspond to previous diagrams: blue representing *N.luteum,* black *Z.aquatica*, and green *H.verticullata.*

Species	Mean Stem Diameter (cm)	Mean Stem Density (stems/m^2)		Frontal Area (m^2)
		Summer	Fall	
N.luteum	1.54±0.049	34.0±1.48	2.2±0.61	0.52
Z.aquatica	1.37±0.034	40.5±3.10	———	0.55

Table 2.3 Hydraulic vegetation growth characteristics of *N.luteum* and *Z.aquatica*. All measurements were taken at peak growth height except the fall measure of stem density. *Z.aquatica* has no listed fall stem density as this grass falls over and remains in place for several weeks after dieback. *N.luteum*, on the other hand, thins out gradually. Mean values followed by calculated standard error.

indicate that the majority of *Z.aquatica* stems remain as standing dead long after peak growth, and thus width and stem density remain steady through the end of the growing season (Fig. 2.5). *N.luteum* occupies >50% less area two months after peak growth, and its stem density decreases >90% during the same time period (fig. 2.6).

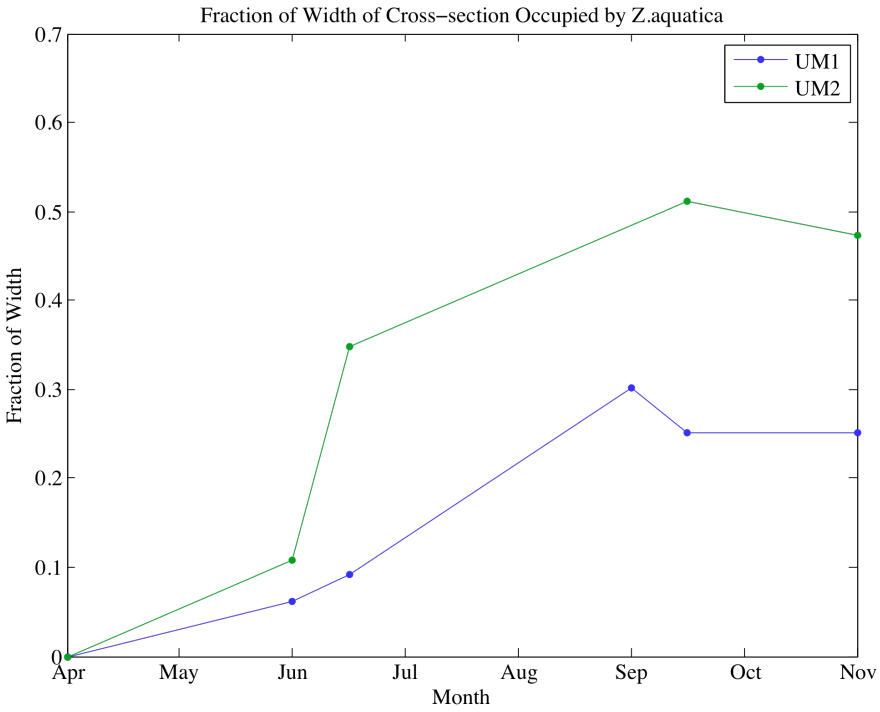

Figure 2.5 Time series of fraction of vegetated width of *Z.aquatica*-dominated channel cross-sections.

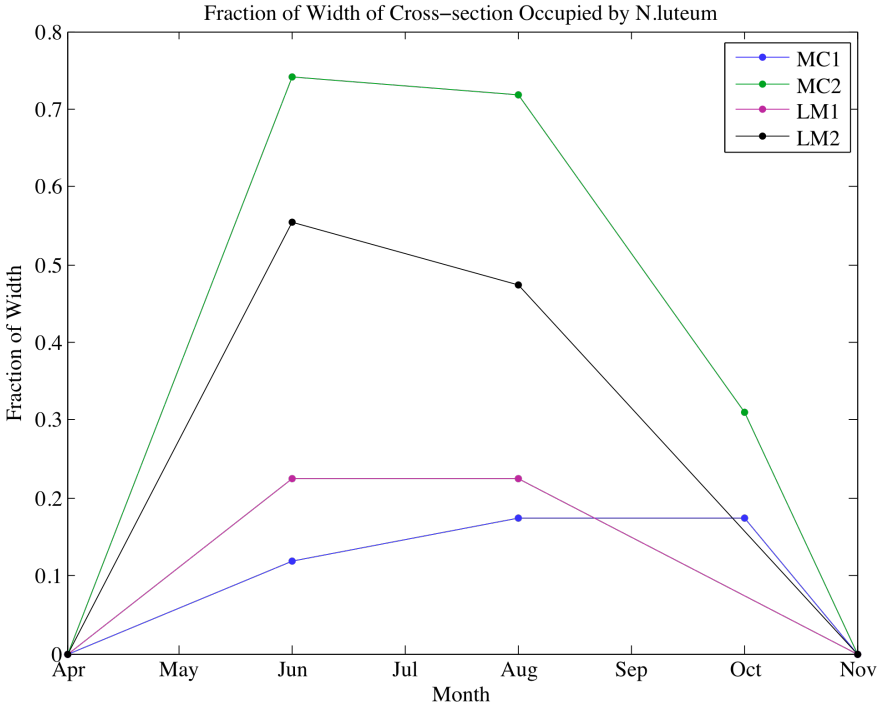

Figure 2.6 Time series of fraction of vegetated width of *N.luteum*-dominated channel cross-sections.

2.4 Discussion

The emergent and submerged species present in TFW inlet channels occupy distinct portions of inlet channels and dominate different inlets. The spatial and morphological characteristics of these plants are intimately related to the relationships between vegetation, hydrodynamics, and geomorphology. *Z.aquatica* grows in the shallow margins of the channel, and thus restricts itself to a smaller width and may have a limited capacity to engineer the channel. This plant does not fully develop until late summer, and dies back slowly. Similar to salt marsh vegetation, *Z.aquatica* remains as standing dead long into the fall season. As a result, effective shear stresses will be reduced long into the fall, both enhancing deposition and preventing erosion. The ideal shear stress distribution shown in figure 1.4 would have an elongated summer vegetation shear stress peak and an abbreviated winter vegetation stress minimum. While *Z.aquatica* may have a longer period of influence on the channel it occupies, it is easily flattened by wind gusts and storms. As a result, it is less adaptable to wide, open marsh areas and marshes on the downstream extent of the TFW system. It is also an annual that must reproduce from seed, thus the extent of *Z.aquatica* may vary greatly on an annual basis.

In contrast, *N.luteum* can grow at a greater mean and maximum depth than *Z.aquatica*, and therefore occupies larger portions of TFW channels. *N.luteum* is a perennial plant, which propagates through tubers (rhizomes) that remain in the marsh year round. This species, which is often submerged at high tide, is much more flexible, bending with the flow of water as well as gusts of wind. These characteristics allow *N.luteum* to outcompete *Z.aquatica* in most of the Patuxent

TFW. In *N.luteum*-dominated marshes, the rare instances of *Z.aquatica* growth occur only on the marsh platform where other species protect it from high winds. The wide extent of this plant and its dominance over other species allow *N.luteum* to have a significant affect on marsh processes; however, its quick disappearance after peak growth (in occupied width, stem density, and growth size) could affect its influence on channel form.

Previous studies have explored the effect of SAV, such as *H.verticullata* on channel hydrodynamics (Jenner, 2011). These species effectively reduce the cross-sectional area of the channel, thus greatly increasing the opportunity for accretion. As demonstrated above, these SAV species occupy relatively small fractions of the channel, but have the ability to grow over the widest depth range. *H.verticullata* has the shortest channel occupancy of Patuxent TFW species, growing quickly from late June-July and dying back in mid-August. Typically SAV species, such as *H.verticullata* do not remain in the channel, but instead release great netted masses downstream. The fate of sediment accreted under SAV is thus largely unknown—does it remain in the channel after the vegetation leaves, or is it eroded with the SAV?

2.5 Conclusion

Z.aquatica, which reaches peak growth (~2-2.5m) in late August, grows at mean water depths of ~0.45m. Due to this restriction, the vegetated width of Z.aquatica-dominated channel inlets is small relative to the other emergent species present in these TFW. During dieback, this plant remains as standing dead late into the fall season, which may affect its ability to trap sediment likely varies annually.

Based on hydraulic parameters and its persistence as standing dead, it could have the most significant effect on flow per m^2 of channel.

N.luteum reaches peak growth (~1m) in July, growing at a mean water depth of ~0.6m. Because of its relatively large mean depth and ability to outcompete other aquatic plants, *N.luteum* occupies a significant extent of TFW channels, dominating >50% of the inlet channel width. The occupied width and stem density of this plant decreases quickly after peak growth, potentially limiting its ability to permanently trap sediment in the marsh.

H.verticullata grows in deep sections of TFW inlet channels and has great potential to affect flow as it occupies large cross-sectional areas (Jenner, 2011). Its short growth period and manner of dieback potentially limits its ability to accrete sediment permanently. Sediment deposits on SAV masses, thus when plant segments float out of the channel in mid to late summer, much of the accreted sediment likely leaves the channel with it.

Chapter 3: The Effect of Aquatic Vegetation on Flow Resistance and Shear Stress Distribution in Tidal Freshwater Inlets

3.1 Hypotheses

H1: The combination of long occupation time and larger frontal area will allow *Z.aquatica* to affect flow more significantly than other aquatic vegetation types.

3.2 Rationale

Differences in stem density, diameter, and height among plant species affect flow resistance and thus the effective shear stress in the channel. Plants, which occupy larger areas of the channel (that have greater densities and frontal areas), will have a greater ability to impede flow. Greater flow resistance and resultant low velocities will translate to significant deposition in the channel, provided sediment is available. Erosion will likely occur in areas with higher flow depths and shear stresses during non-vegetated periods.

3.3 Methods

3.3.1 Hydraulic Measurements

Measurements of vegetation roughness, gradient, depth, and velocity are used to calculate total shear stress, effective shear stress, and flow resistance. Summer distributions of roughness height (z_o), flow resistance (U/U_*), and effective shear stress (τ_{eff}) for each inlet cross-section were measured in collaboration with Dr. Karen

Prestegaard. Due to weather in the winter-spring of 2014 (frozen river in winter, high winds in early spring), we could not measure velocity for the non-vegetated state. Therefore, we compared the hydraulics among vegetated channels during summer maxima. At each inlet, we also analyzed differences between the summer effective shear stress to total shear stress, which would be the maximum possible shear stress without vegetation (comparable to the winter state).

Hydrodynamic measurements were conducted during peak growth of vegetation to calculate total channel shear stress at each established cross-section. All of these measurements coincide with the maximum erosive capacity of the channel, which occurs as the flow reaches the steepest gradient and maximum depth on the outgoing tide. Gradient is measured with 3 staff gauges, one at each inlet cross-section, and the third halfway between the two cross-sections; gauge heights are continually recorded during the measurement time interval (2-5 hours). Cross-sectional depth (R) is measured at the beginning of data collection, but adjusted to depths that correspond with the maximum energy gradient at each station.

3.3.2 Data Analysis

To compare the effect of each vegetation type on erosion and flow, we partitioned total shear stress into shear stress expended on vegetation (τ_{veg}) and effective shear stress (τ_{eff}). Larger τ_{veg} values indicate greater dissipation of flow energy by vegetation, and therefore a reduction in erosive capacity. Recall that,

$$\int \tau_{veg}\, ds = \int \tau_{tot}\, ds - \int \tau_{eff}\, ds, \qquad (3.1)\ \text{(from 1.6)}$$

$$where\ \tau_{tot} = \rho_w g R S \qquad (3.2)\ \text{(from 1.1)}$$

Variations in τ_{veg} were compared among the three vegetation types (*N.luteum,* *H.verticullata,* and *Z.aquatica*) at varying stages of growth and dieback.

Flow resistance and roughness height also reveal the impact of vegetation on flow. By examining the relationship between these variables (expressed as a dimensionless ratio: d/z_o and U/U^*), we can compare the hydraulic roughness of the three vegetation types (see eqn. 1.3-1.5). If the relationship between roughness and resistance is systematic, it might be used to predict variations in flow resistance based on vegetation type. To test the robustness of these inter-vegetation comparisons of vegetation shear stress, flow resistance, and flow roughness, we performed an model I analysis of variance (ANOVA) followed by a posteriori testing (Tukey test).

After comparing among vegetation types, we used the critical shear stress values (from Friedrichs and Aubrey, 1996) to highlight the portion of each cross-section where erosion can theoretically occur. These predictions will be compared with actual morphological measurements of accretion and erosion in the next chapter. With these results, we can identify seasonal variations in deposition and compare how susceptible each cross-section under each vegetation type is to erosion.

3.4 Results

3.4.1 Shear Stress Distributions

Results of the shear stress partitioning calculations are shown in figures 3.1-3.4. In all marshes, the effective shear stress approached a minimum where aquatic vegetation was present in the channel. Inlets dominated by the emergent vegetation *N.luteum* or *Z.aquatica* experienced effective stress that equaled or exceeded the total stress in the central channel. This is possible because the integral of $(\tau_{tot}-\tau_{eff})$ across

the channel must always be greater than or equal to zero, but this relationship does not have to hold true at each interval across the channel. In other words, the total vegetation shear stress plus the effective shear stress must equal the overall total shear stress in the channel. The emergent vegetation redistributes the energy unequally across the channel, thus allowing the vegetation shear stress to exceed the total shear stress in certain areas of the channel. In the SAV-dominated marsh, the effective stress did reach a maximum in the central channel; however, it did not exceed the total shear stress.

Although weather prevented local measurement of effective shear stress during the winter, we can still make some seasonal comparisons. As discussed previously, during the non-vegetated state, the vegetation shear stress should approach a minimum, thus the total shear stress and the effective shear stress will approach a shared value. Because we did not see significant change in channel forms (see Ch. 4), the total summer shear stress distributions will likely be close to the winter effective stress. In this case, the winter distributions also reach a minimum under the previously vegetated areas of the channel. While these stresses do not approach zero, those over previously vegetated platforms are much smaller than the critical shear stress required to erode the sediment.

In some channels where summer effective stress exceeded critical in the central channel, the effective winter stresses do not follow the same trend. The shallower, *Z.aquatica*-dominated cross-sections experience shear stresses that barely exceed critical in the central channel and remain below critical over vegetated platforms. This marsh has very low maximum effective shear stresses in both the

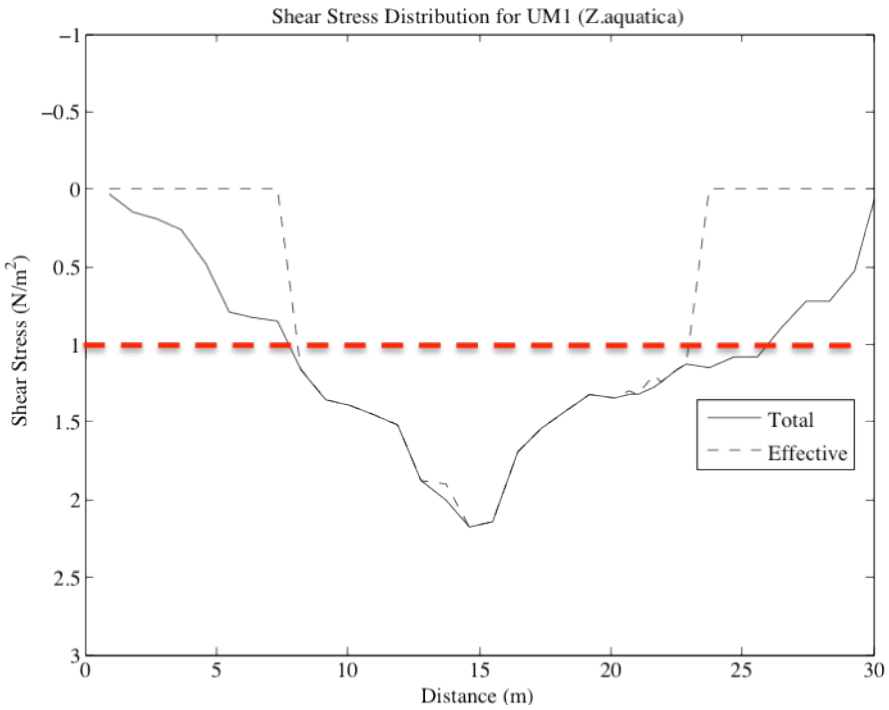

Figure 3.1 Shear stress distribution at UM1 cross-section, dominated by *Z.aquatica,* from September 2013. Notice y-axis scale is reversed. In all diagrams, the dashed red line indicates the critical shear stress value from Friedrichs and Aubrey, 1996. In areas where τ_{tot} or τ_{eff} exceeds τ_{crit}, erosion can occur.

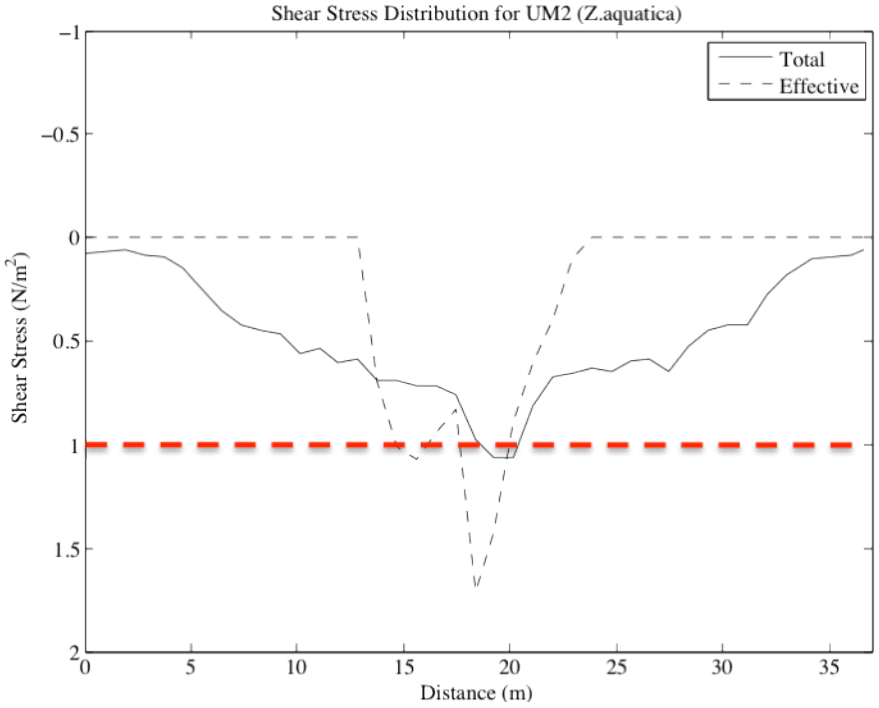

Figure 3.2 Shear stress distribution at UM2 cross-section, dominated by *Z.aquatica,* from September 2013. Notice y-axis scale is reversed.

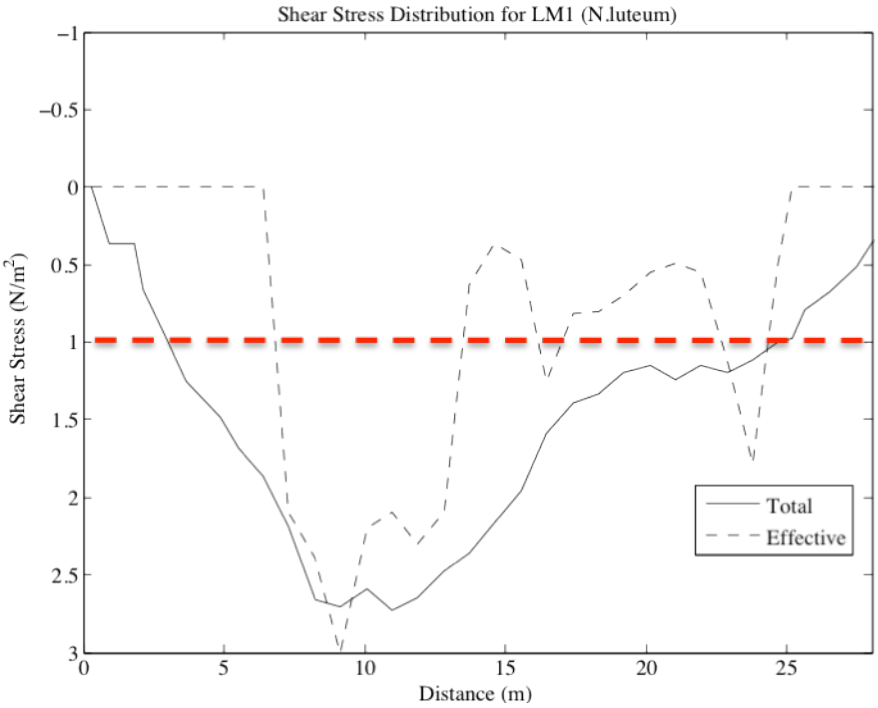

Figure 3.3 Shear stress distribution at LM1 cross-section, dominated by *N.luteum,* from September 2013. Notice y-axis scale is reversed.

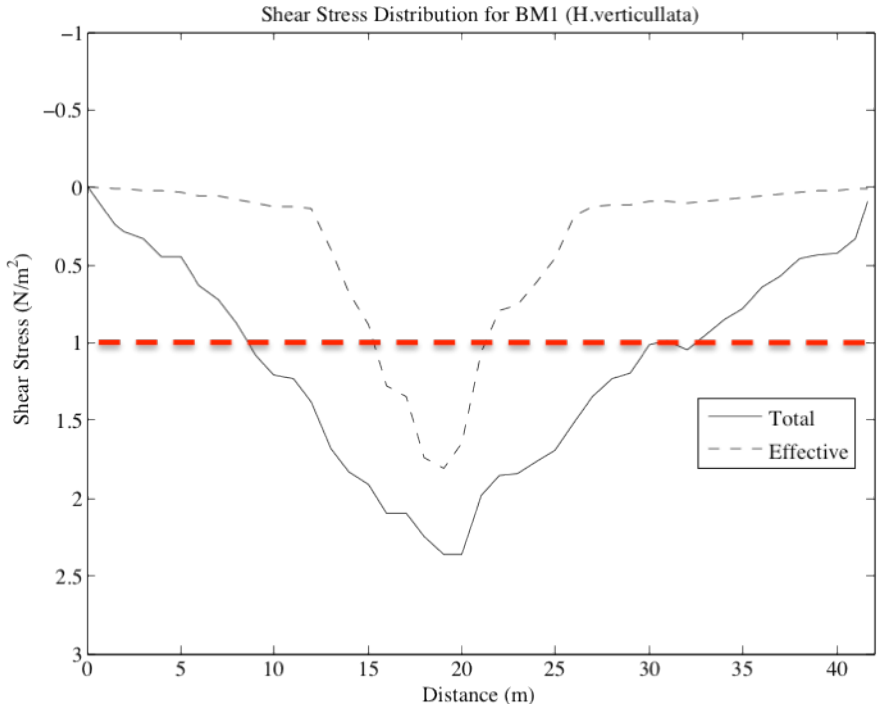

Figure 3.4 Shear stress distribution at BM1 cross-section, dominated by *H.verticullata,* from September 2013. Notice y-axis scale is reversed.

summer and winter case, so we expect to observe positive overall accretion at this inlet. At the *N.luteum* inlet, the maximum effective winter and summer stresses are both large, thus, we expect to measure little significant channel change. Some deposition can occur on the vegetated platform over the summer, but effective stress causes erosion in this area during winter. In the SAV-dominated marsh, the winter stresses exceed the summer effective shear stresses, which would suggest that erosion may occur. The channel margins remain below critical conditions at all times.

3.4.2 Flow Resistance

Flow resistance is another way to investigate how individual plant species will affect flow and deposition in each channel. We calculated flow resistance under each vegetation type from local velocity measurements. Observable differences in roughness do exist among the vegetation types as shown by the box plots in figure 3.5. The *Z.aquatica*-dominated marsh appears to be the most resistant to flow and SAV the smoothest, with the *N.luteum* marsh falling between them. A single-factor ANOVA confirms that each vegetation type has a characteristic distribution of observed flow resistance (see tables 3.1-3.2).

To understand the magnitude of influence imposed by these aquatic vegetation types, we compared the hydraulic roughness of these TFW to other well-studied hydraulic systems. Figure 3.6 shows hydrodynamic data from marshes dominated by each of the three vegetation types superimposed on figure 1.5, which depicts the hydraulic roughness of several systems and our prediction of the relationship between these vegetated TFWs and other hydraulic networks. Recall that large values along the x and y-axes represent a smoothing of the system, with decreasing resistance to

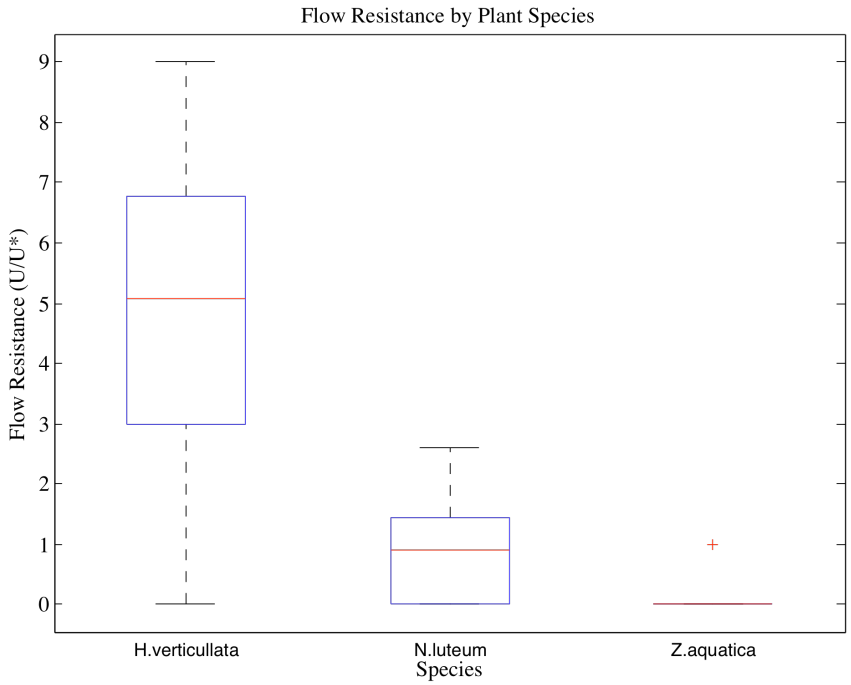

Figure 3.5 Flow resistance by plant type as represented by box plots. Only values measured directly beneath/above each plant type are included here.

Source of Variation	Sum of Squares	Degrees Freedom	Mean Square	F
Among TFW	459.5	2	229.7	85.13***
Within TFW	256.4	95	2.70	
Total	715.9	97		

Table 3.1 Summary table for ANOVA comparing flow resistance through three dominant types of aquatic vegetation.

Flow Resistance			
Species	*N.luteum*	*Z.aquatica*	*H.verticullata*
N.luteum	———	2.44*	11.87***
Z.aquatica		———	17.88***
H.verticullata			———

Table 3.2 A posteriori summary table for comparison of flow resistance through three dominant types of aquatic vegetation.

flow (y-axis) and area of the channel occupied by surface features, i.e. ripples, large clasts, vegetation (x-axis).

In figure 3.6, the data appear perfectly correlated with each other because the method used to calculate dimensionless roughness relies on measurements of flow resistance. Despite this artificial relationship, these results indicate that TFW channels are extremely hydraulically rough, significantly rougher than natural gravel bed

streams or laboratory flumes. Marsh inlets dominated by emergent and submerged vegetation experience greater interruption of flow along vegetated zones, but exhibit a smooth central core.

3.5 Discussion

3.5.1 Shear Stress Distributions

In most of the inlet cross-sections, the central channel was characterized by a maximum summer effective shear stresses, which equaled or exceeded the total shear stress. These shear stress distributions likely result from the funneling of water through the center of the inlet channel when emergent vegetation is present. During vegetation maxima, emergent vegetation acts like a wall, forcing more water through the center and generating large effective stresses in the central channel. This hypothesis is supported by the observation of minimum effective shear stresses under emergent vegetation. The edge of emergent vegetation fields generates an eddy fence that forces flow into the center of the channel. In this scenario, only a small portion of the discharge can then flow over vegetated platforms, and thus only small shear stresses can be generated over these fields.

The SAV-dominated channel is the only marsh in which the effective stress does not exceed the total stress in the central core; however, we still observe the maximum stress in the central channel. These effects stem from the nature of flow through *H.verticulllata,* which does not create lateral boundaries that funnel water toward the center as effectively as the emergent vegetation. As observed by Jenner (2011), the SAV reduces the channel area; water flows slowly through the vegetation as porous media flow (i.e. like groundwater flows through soil). The residual

discharge is forced over the SAV, but is subjected to greater flow resistance than flow over bare sediment.

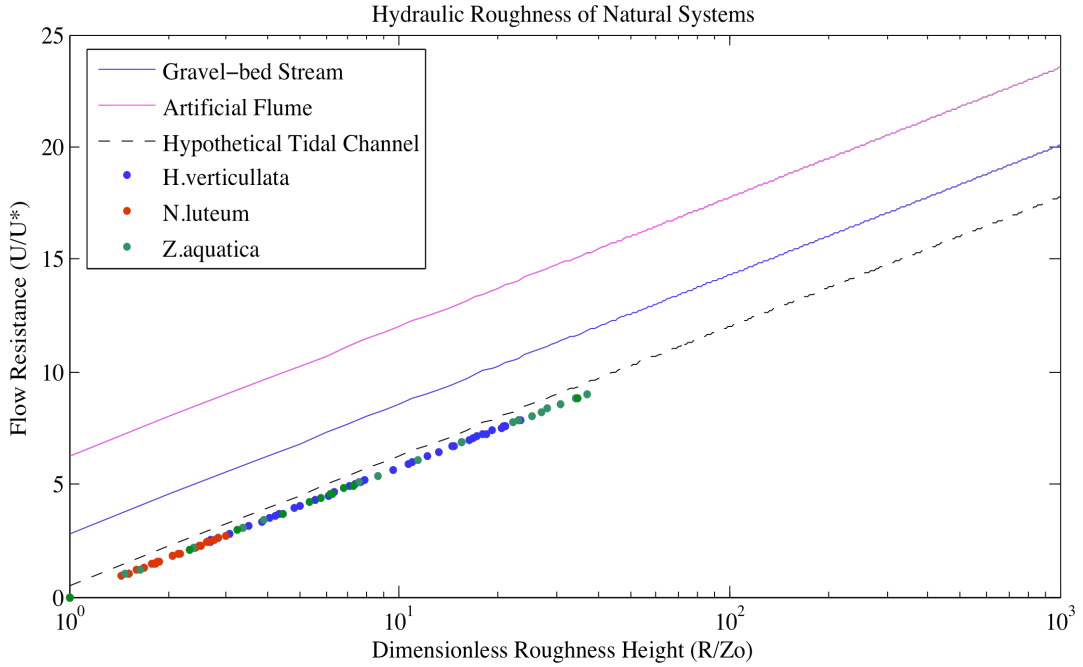

Figure 3.6 Hydraulic roughness of TFW systems by vegetation type. Study data are superimposed on introductory figure showing the relationships between dimensionless roughness height and flow resistance for previously studied systems.

3.5.2 Seasonal Variations in Shear Stress

If we compare the theoretical non-vegetated (winter) stresses (the summer total shear stress distribution) to the effective summer stresses, we can see a few notable differences. On vegetated platforms and SAV-dominated areas, the winter stresses are significantly larger than the summer stresses. In the central channel, the winter stress decreases compared to the summer state. These relationships would suggest significant summer deposition over vegetated platforms and erosion in the central channel, which would switch to winter erosion over the platforms and potentially deposition in the central core.

Observations reveal that some cross-sectional shear stress distributions deviate from this trend, and thus measurements of channel accretion may diverge from this

hypothesis. To explain these discrepancies, we must consider the relationship between the effective stresses and the critical shear stress at each inlet. The critical shear stress has a variable relationship with the effective stress distribution at each cross-section. In shallow inlets, the critical stress required to erode sediment is only achieved in the central portion of the channel where the effective stress reaches a maximum, thus only a small area of the channel will experience erosion. This relationship is not seasonally dependent. Conversely, deep inlets have large shear stresses in both summer and winter, so the channels have high erosive capacities.

3.5.3 Flow Resistance

In addition to revealing the interaction of vegetation with flow, shear stress distributions also indicate the capacity for net annual accretion in these marshes. Relationships between critical shear stress and effective shear stress indicate that some marshes will only erode in limited areas of the channel. In all channels, the vegetated platform remained below critical during the summer; however, the smaller cross-sections (UM1, UM2) remain in this state year-round. Only the central channel can experience erosion. For larger cross-sections (BM1, LM1), parts of the vegetated platform have effective shear stresses, which exceed critical when vegetation is not present. As a result, the larger marshes likely experience less overall marsh channel change than the shallow ones.

The resolution of our effective shear stress measurements is not precise enough to compare among vegetation types, thus we only examined the relationship between vegetation type and flow resistance. Figure 3.5 suggests that each type of vegetation does affect flow uniquely: *Z.aquatica* being the most rough and

H.verticullata the least. These observations correlate with measurements of stem density, diameter and frontal area, which support our hypothesis that vegetation which occupy the largest region of channel area will create the greatest flow resistance.

3.6 Conclusions

In addition to the individual effect of each plant species, shear stress distributions revealed two important characteristics of TFW hydrodynamics: (1) when emergent vegetation is present, effective shear stresses exceed total shear stresses in the central channel, and (2) effective shear stress approaches a minimum when flowing through/over aquatic vegetation. The increase in effective shear stress in the central channel results from the funneling of water through the system. When emergent vegetation populates channel margins, it forms an eddy fence that prevents discharge from flowing evenly through the channel, thus increasing shear stresses in the center. The high effective stresses appear impossible at first; however, as demonstrated by eqn. 3.1, the total shear stress must equal the vegetation and effective shear stresses across the entire channel. Deviation from continuity at intervals across the channel is possible, as long as stresses balance out across the entire system. The SAV decreases the available channel area (allowing minimal flow through vegetation), thus concentrating some flow in the center, but the effect is less pronounced than in the case of emergent vegetation.

Total (non-vegetated) stresses were systematically larger than summer stresses (with the exception of the central channel), but these stresses were still not always above critical. Channels with deeper depths can generate winter shear stresses, which

exceed critical over parts of the vegetated platform. These channels may not experience net annual accretion, whereas shallow channels, where effective stress can only ever exceed critical in the central channel, will experience positive elevation changes over the annual cycle.

While shear stress measurements did not allow differentiation among aquatic vegetation types, calculations of flow resistance revealed significant variation in the hydrodynamic effects of these plant species. Figure 3.5 reveals that *Z.aquatica* creates the roughest channel with the greatest flow resistance while *H.verticullata* allows the smoothest flow over vegetation. This pattern is related to stem density, but the relationship between flow resistance and frontal area is poorly defined. High stem density translates to increased flow resistance.

Chapter 4: The Effect of Aquatic Vegetation on Patterns of Accretion and Geomorphology of Tidal Freshwater Inlets

4.1 Hypotheses

H1: Larger channel erosion rates will be associated with vegetation that exhibits earlier dieback.

H2: Due to seasonal variations in vegetation cover and its effect on shear stress distributions, inlet channel form oscillates between two potential equilibrium end members.

4.2 Rationale

H1: Variations in vegetation hydraulic characteristics throughout plant lifecycles will likely affect net annual accretion in these marshes. Different mechanisms of dieback will produce varying rates of channel erosion; those patterns of dieback, which preserve summer hydrodynamic features, may protect a marsh channel from erosion long into the next season or even encourage deposition for longer periods. Vegetation that dies back soon after its summer peak will have less ability to stabilize channel boundaries as the marsh erodes and moves toward its winter equilibrium. Such patterns have important implications for marsh maintenance and a channel's ability to produce net annual accretion.

The style of vegetation dieback varies for different species, especially those in this study. The three types of plants found at the Patuxent TFW sites (*N.luteum,*

H.verticullata, and *Z.aquatica*) experience peak growth and dieback on different timescales (fig. 2.1-2.2;2.5-2.6). *Z.aquatica,* which dies back in late summer, but leaves a slowly decomposing residue, may prevent erosion further into the fall than *H.verticullata* and *N.luteum,* which begin dieback in late July. *N.luteum* degrades quickly after dieback; vegetation dies one stem at a time, slowly decreasing in density throughout the fall (see table 2.3). *H.verticullata*, which grows as a matted mass of submerged vines, does not remain in the channel; dead vines are instead exported from the channel in large clumps.

H2: In this study, we define channel equilibrium as the channel form in equilibrium with bankfull shear stress distributions. Seasonal changes in vegetation cause changes in effective shear stress distributions; therefore, the equilibrium channel form should also change seasonally. In winter, the non-vegetated channel experiences higher velocities and greater shear stresses in the previously vegetated parts of the channel. This increase in effective shear stress enables erosion of the bed unless standing dead vegetation remains to prevent this. The growth of summer vegetation alters channel hydrodynamics, resulting in low velocity/shear stress zones where sediment can accumulate.

Based on these vegetation-induced variations in shear stress, we hypothesize that two end member equilibrium channel forms exist for tidal marsh channels. Similar to equilibrium ideas for terrestrial channels, channel forming or bankfull discharge, is assumed to occur during spring tides (the upper 5% of high tides) experienced by the channel. At these discharges, the equilibrium channel will have the gradient and depth to generate the critical shear stress required to entrain the bed

material. Winter and summer channel shear stress distributions could cause variations in morphology and grain-size distribution. The tendency for these channels to oscillate between these two equilibrium forms drives expansive summer deposition and significant winter erosion. Net accretion occurs when winter erosion is less than summer deposition.

4.3 Methods

4.3.1 Field Data Collection

Sequential inlet cross section measurements were made at permanently anchored sites to track channel change over an annual cycle. These measurements were conducted at two locations in each of the five study inlets. In order to accurately measure channel change, each measurement was taken relative to a permanent reference elevation. All measurements at each cross-section were then normalized to the same elevation; therefore, changes in depth reflect erosion or deposition relative to the elevation of the marsh platform (see fig. 4.1). Normalization procedure is:

$$M = sl + \Delta g + d - RL \tag{4.1}$$

where M is the depth relative to the marsh platform, sl is the distance between the reference level and water surface, g is the tidal gauge height, d is the water depth, and RL is the reference level.

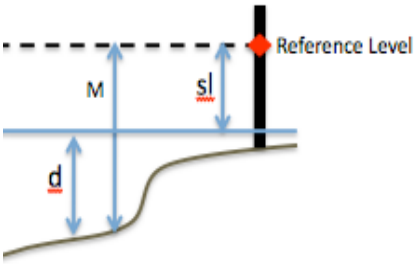

Figure 4.1 Schematic representation of reference level cross-section measurements.

Geomorphic sampling occurred monthly to bimonthy during the summer and winter periods. As demonstrated by figure 4.2, channel change measurements bracketed several flood events. The relationship between river hydrograph and sampling scheme will allow us to

investigate TFW response to major flood events and compare these to observed seasonal changes. Measurements immediately before and after the April 2014 spring event, one of the largest on record, will indicate the magnitude of the effect of seasonal changes to the vegetation community. If this even causes little change, than seasonal changes are also likely to be negligable. Alternatively, flood events could transform channel form more significantly than seasonal changes, thus extreme discharges would be considered the mechanism for TFW channel maintenance. While we were unable to collect winter hydraulic measurements, the effect of this event on the non-vegetated marsh will demonstrate whether the vegetated state or geometry of the inlet channel has a greater effect on marsh maintenance.

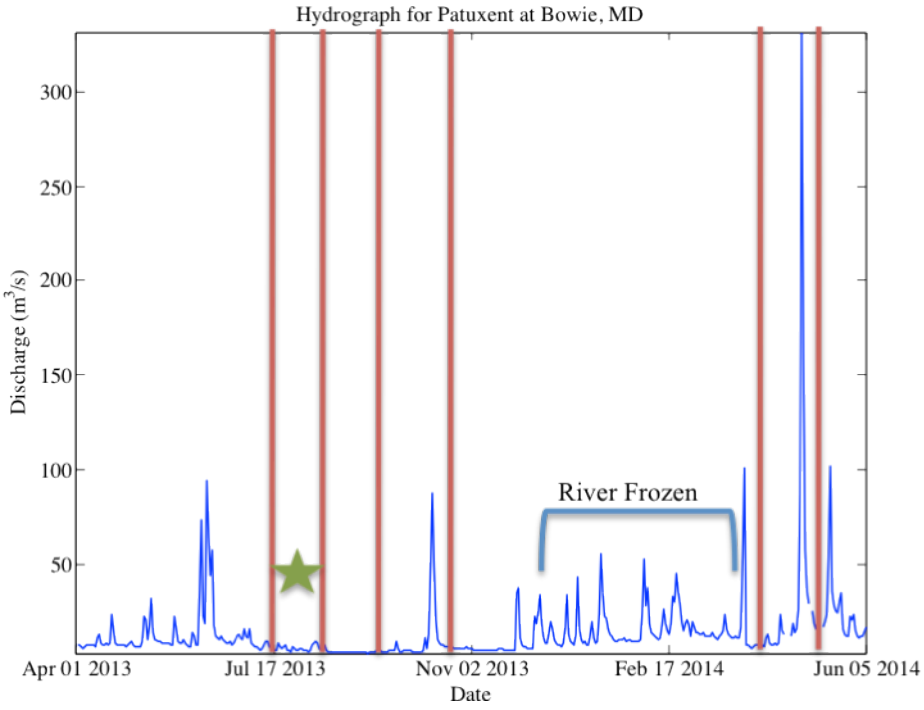

Figure 4.2 Hydrograph from Patuxent at Bowie, MD, located just upstream of TFW study sites. Red lines represent sampling dates. Blue bracket indicates period of time during which river was frozen. Star represents timing of sediment sampling. Hydrograph produced from U.S. Geological Survey WaterWatch data (http://waterwatch.usgs.gov).

4.3.2 Laboratory Analysis

Sediment characteristics influence hydraulic conditions in TFW channels and the capacity of these channels to produce net annual accretion. Determining the amount of organic matter and mineral sediment accreted in a marsh channel has important implications for marsh elevation maintenance. Organic matter has a lower bulk density, or mass of particles/volume, than mineral sediment. Sediment with a high percentage of organic matter may produce a large initial accretion rate; however, decomposition may diminish its contribution to marsh elevation in the long term. Differences in decomposition rate and timing of dieback of *N.luteum, H.verticullata,* and *Z.aquatica* could affect the amount of organic material incorporated into marsh sediments and the residence time of this organic material.

Sediment was sampled across the established channel inlet cross-sections in July 2013. Using an Eijkelkamp peat sampler, I collected 5cm sediment cores from 0-5cm depth at 1.5m intervals across each channel cross-section. This core represents the most recently deposited material, not yet compacted, and rich in organic material.

To determine bulk density, samples were dried at 70^{o}C for ~48hrs to remove moisture. Bulk density is calculated with the following equation:

$$\rho_b = \frac{W_d}{V} \tag{4.2}$$

where ρ_b is bulk density, W_d is sample dry weight, and V is wet sample volume.

Percent organic matter was determined by loss on ignition with a 2-3g homogenized aliquot of each dried sample. Any large vegetation fragments (e.g. roots) were removed at this juncture to avoid measurements of material that has not been incorporated into the sediment. Organic matter is burned off in a muffle furnace

by heating the samples at 400°C for ~8hrs (Schulte and Hopkins, 1996; Wang *et al.,* 2011). Weight lost during ignition was then used to calculate percent organic matter:

$$O = \left(\frac{\left(W_d - W_I\right)}{W_d} \right) * 100 \tag{4.3}$$

where W_I is weight after ignition, and O is % organic matter.

4.3.3 Data Analysis

To validate our hydraulic results, we compared the morphological change data with calculated shear stress distributions to identify whether observed erosion coincides with calculated maximum shear stresses. In chapter 3, we plotted effective channel shear stress vs. channel width for each cross-section and highlighted the portion of the channel where erosion can theoretically occur (based on literature $\tau_{crit.}$). We compared these predictions with actual morphological measurements of accretion and erosion. With these results, we can identify seasonal variations in deposition and also determine whether the hydraulic effects unique to each vegetation type affect annual accretion.

Variations in erosion and deposition were evaluated by comparing the sequential, normalized cross-sectional elevation data. Linear regression was used to explore relationships between accretion (seasonal and annual) and plant type, maximum channel depth, and individual marsh configuration. With these data, we evaluated how effectively each vegetation type restricts the loss of sediment and whether the effects of vegetation persist after dieback due to its engineering of cross-sectional morphology.

To determine whether morphological change responds to seasonal changes in effective shear stress, we compared the geometry of each summer and winter cross-section. To compare cross-section shape, dimensionless cross-sections, normalized by maximum depth and width, were calculated. These results will show whether an oscillation in form occurs, but also indicate whether the path of oscillation differs depending on vegetation type rather than merely presence or absence of plant cover.

With the *Matlab* statistical package, we ran a model I ANOVA with a posteriori testing (Tukey tests) to compare percent organic matter and bulk density of sediment accreted under different vegetation types.

4.4 Results

4.4.1 Geomorphic Change

As shown by measurements of channel form over time, the *H.verticullata*-dominated marsh (figures 4.3-4.4) exhibited accretion at the inlet and erosion upstream, but these fluctuations generally remain within measurement error (±2.5cm). The *Z.aquatica* (and *H.verticullata*)-dominated marsh (figures 4.5-4.6), experienced significant accretion over the study period. The two *N.luteum* marshes (figures 4.7-4.10) revealed differing accretion trends: the smaller, shallower Mill Creek experienced net annual accretion, while the larger, deeper Lower Marsh revealed some erosion, but little net elevation change (most was within measurement error). Note that the upstream Lower Marsh site is missing an initial June measurement. This resulted from loss of the established reference level between June and August, thus making June measurements incomparable to subsequent data. Significant overall

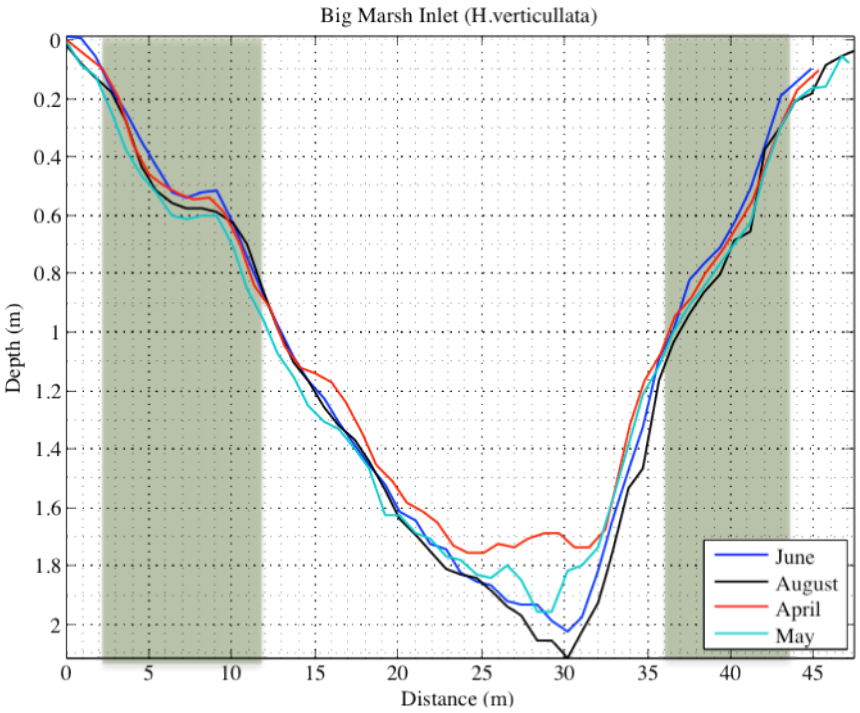

Figure 4.3 Time series of channel form measurements for the Big Marsh inlet station, normalized to marsh platform elevation. Green shading denotes approximate location and extent of *H.verticullata* in the cross-section. Locations are only approximate due to turbidity limitations. Note only significant cross-sectional change occurs in the central portion of the channel.

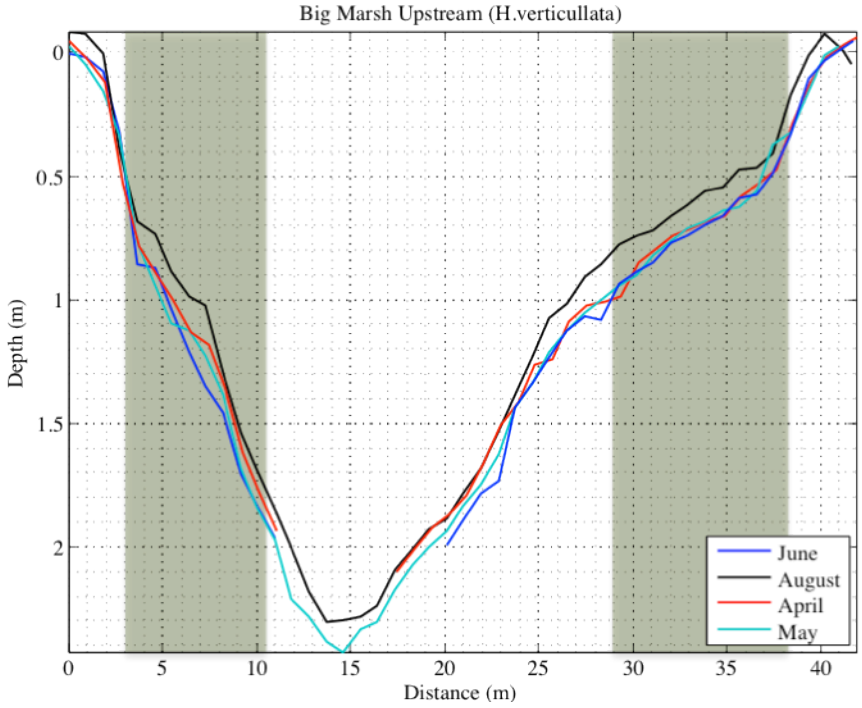

Figure 4.4 Time series of channel form measurements for the Big Marsh upstream station, normalized to marsh platform elevation. Green shading denotes approximate location and extent of *H.verticullata* in the cross-section. Locations are only approximate due to turbidity limitations. Note, missing measurements of central channel because depth greatly exceeded measurement instrument.

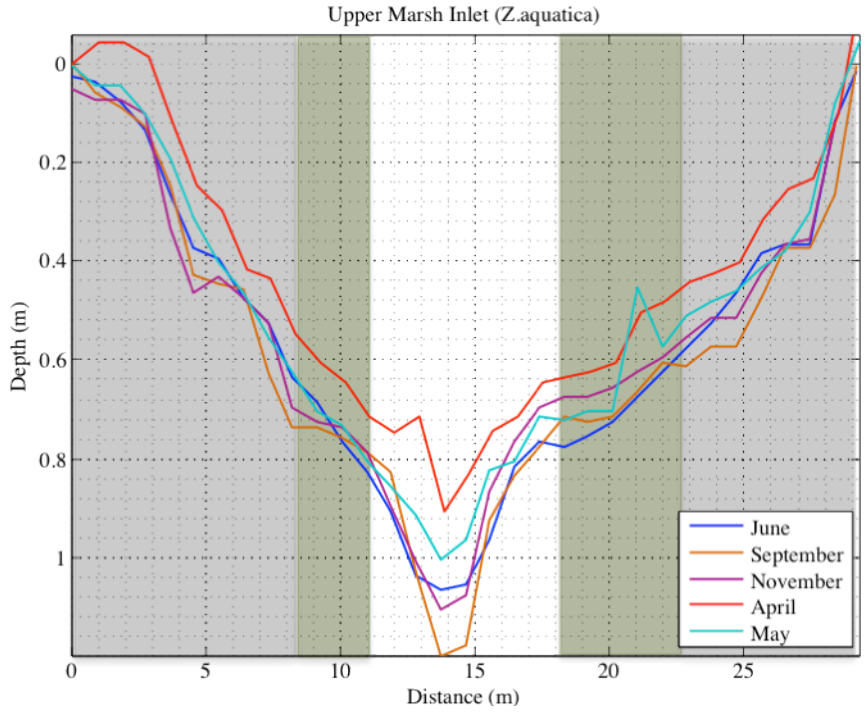

Figure 4.5 Time series of channel form measurements for the Upper Marsh Inlet station, normalized to marsh platform elevation. Grey boxes denote location and extent of *Z.aquatica* as measured in the field. Green boxes represent location and extent of *H.verticullata* as measured in the field. Note significant cross-sectional change occurs across the entire channel.

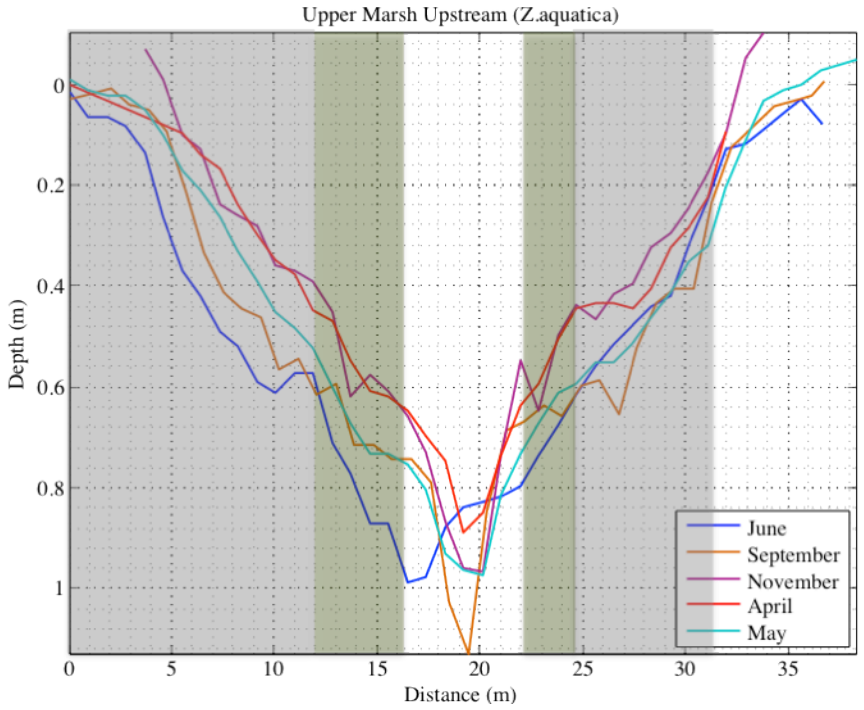

Figure 4.6 Time series of channel form measurements for the Upper Marsh Upstream station, normalized to marsh platform elevation. Grey boxes denote location and extent of *Z.aquatica* as measured in the field. Green boxes represent location and extent of *H.verticullata* as measured in the field. Note significant cross-sectional change occurs across the entire channel.

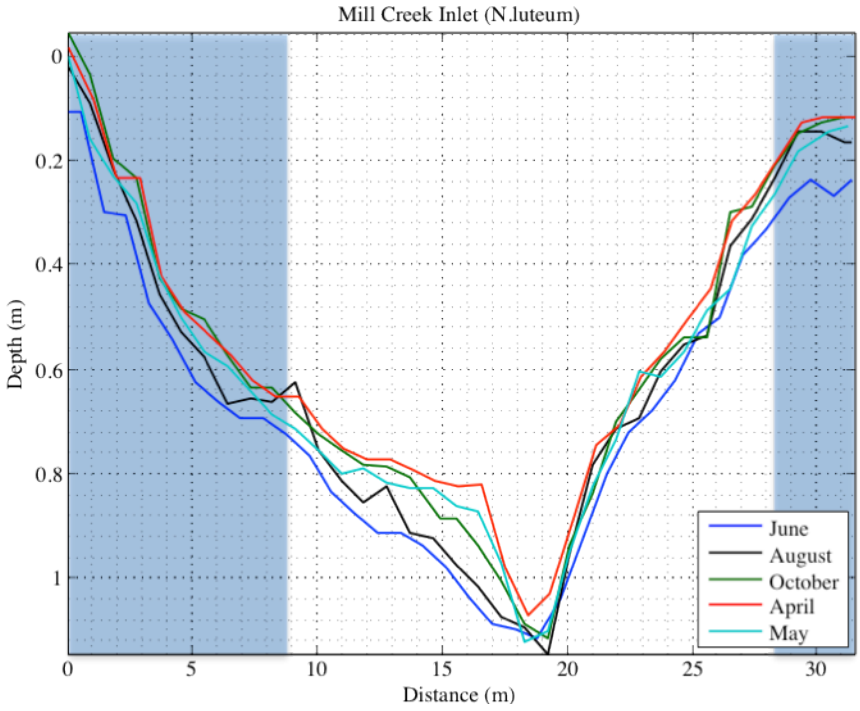

Figure 4.7 Time series of channel form measurements for the Mill Creek Inlet station, normalized to marsh platform elevation. Blue boxes represent location and extent of *N.luteum* as measured in the field. Note significant cross-sectional change occurs across the entire channel.

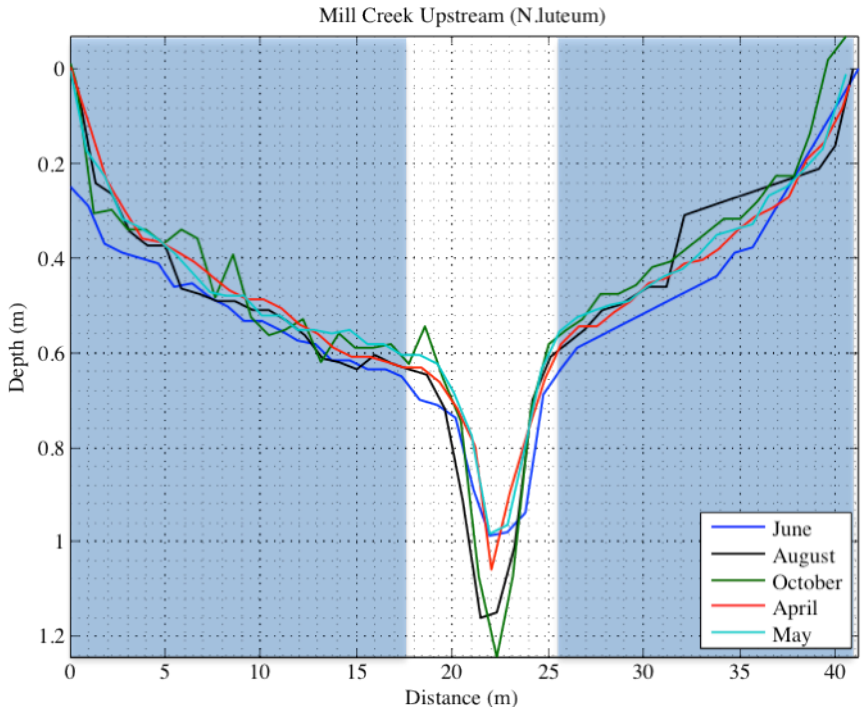

Figure 4.8 Time series of channel form measurements for the Mill Creek Upstream station, normalized to marsh platform elevation. Blue boxes represent location and extent of *N.luteum* as measured in the field. Note significant cross-sectional change occurs across the channel margins, but scour followed by deposition in the central portion.

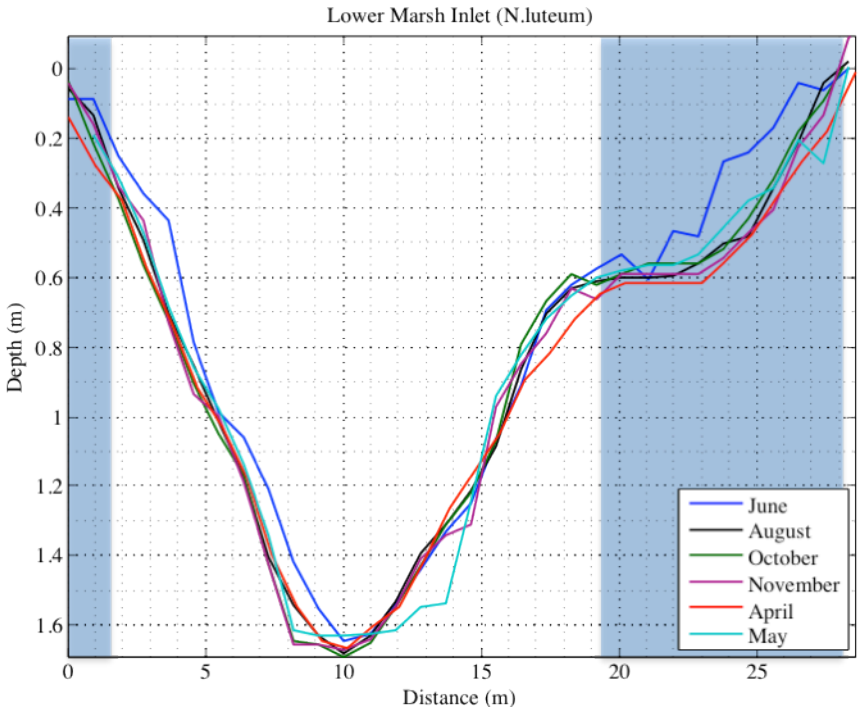

Figure 4.9 Time series of channel form measurements for the Lower Marsh Inlet station, normalized to marsh platform elevation. Blue boxes represent location and extent of *N.luteum* as measured in the field. Note significant cross-sectional change occurs at right channel margin; this section corresponds with the growth of *N.luteum*.

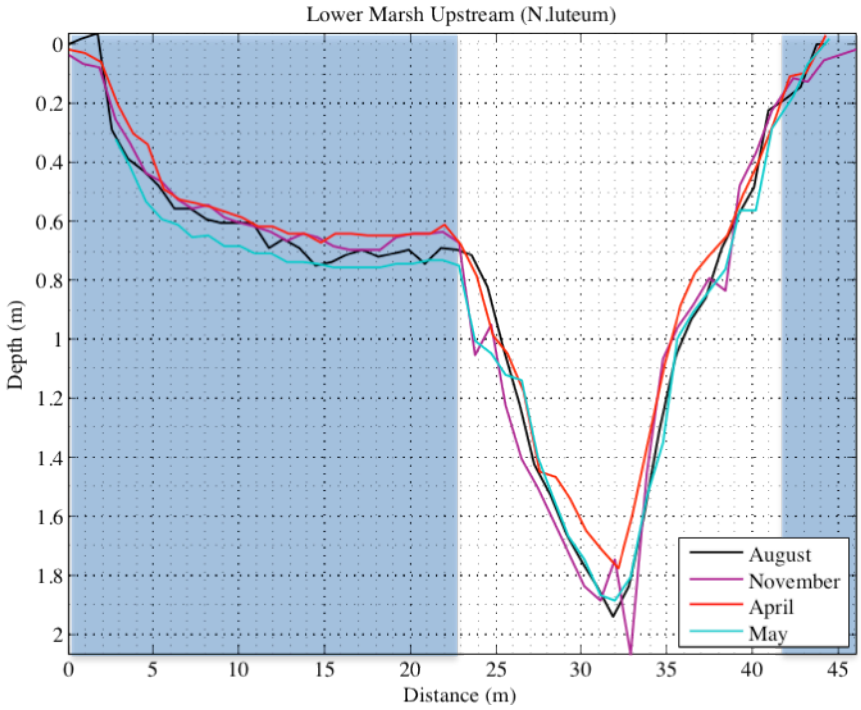

Figure 4.10 Time series of channel form measurements for the Lower Marsh Inlet station, normalized to marsh platform elevation. Blue boxes represent location and extent of *N.luteum* as measured in the field. Note no significant channel change.

trends, which appeared in all cross-sectional time series, include the erosion of the central channel through the summer period and deposition in the same area over the winter season. We also observed deposition over vegetated platforms dominated by both emergent species.

Results of the dimensionless cross-section comparisons appear in figures 4.11-4.12, but few changes are noticeable between summer and winter forms. In the inlet cross-sections (fig. 4.11), no change is observed at the *N.luteum*-dominated marsh. At *N.luteum*-dominated marshes, changes in form occur around the central channel; in the summer, the vegetation platform appears and disappears. The largest inlet change occurs in the *H.verticullata*-dominated marsh, and results from the significant shallowing of the central channel observed over the winter. The winter form appears much more parabolic than the summer configuration.

The upstream cross-sections (fig. 4.12) reveal similar patterns, with small alterations made over the vegetated platforms in *N.luteum*-dominated marshes. The *H.verticullata* upstream cross-section again shows a more parabolic winter form; however, this is likely exaggerated due to difficulty collecting a maximum winter depth. Inconsistencies in the upstream *Z.aquatica* cross-section markers caused the summer and winter forms to be offset. Attempts to correct the data are shown in the diagram below. Extreme apparent shallowing could be caused by the significant changes in maximum depth among season, but differences of this magnitude seem unreasonable based on results shown for other cross-sections; thus, we will disregard this result.

4.4.2 Biogeomorphic Relationships

In addition to observing trends in geomorphic change, we also looked for channel morphologies associated with each plant species. As demonstrated by figures 4.11-4.12, overall channel form does not appear to differ significantly depending on aquatic species present. Table 4.1 lists the summer dimensionless areas of each cross-section. Only sites MC1 and MC2 (*N.luteum*-dominated, shallow marsh) differ significantly from the others. Despite this result, some unique qualities appear in cross-sections dominated by specific aquatic plant species. Marshes populated by both emergent species deviate from the parabolic form associated with non-vegetated channels, but the SAV inlet remains closest to this parabolic state. In each *N.luteum*-dominated inlet, the plant grows in a wide, flat platform while an incised channel appears in the center. The *Z.aquatica* inlet is more triangular than the other inlets; it is characterized by platforms under emergent and submerged vegetation, but the gradient of these slopes is greater than that of the *N.luteum* platforms. These characteristics do not vary seasonally.

4.4.3 Accretion Trends

Analysis of the relationships among annual accretion and vegetation type, vegetated width, and channel shape allow exploration of factors that enhance deposition in TFW channels. Linear regressions of these relationships are shown in

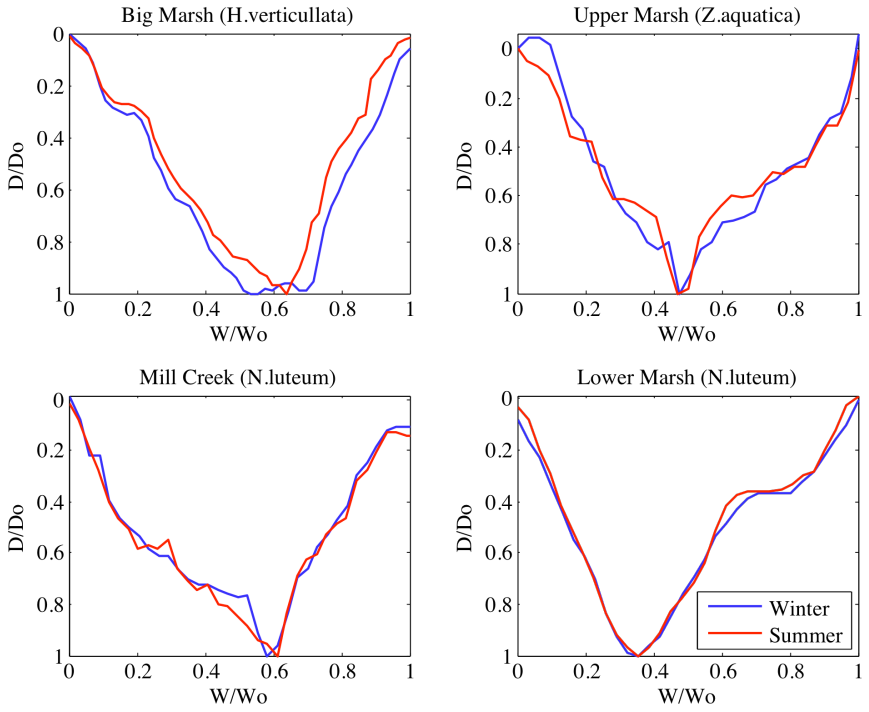

Figure 4.11 Composite of winter and summer dimensionless inlet cross-sections. In order to capture effect of maximum and minimum growing seasons, summer form based on early fall measurements; winter calculated from early spring measurements.

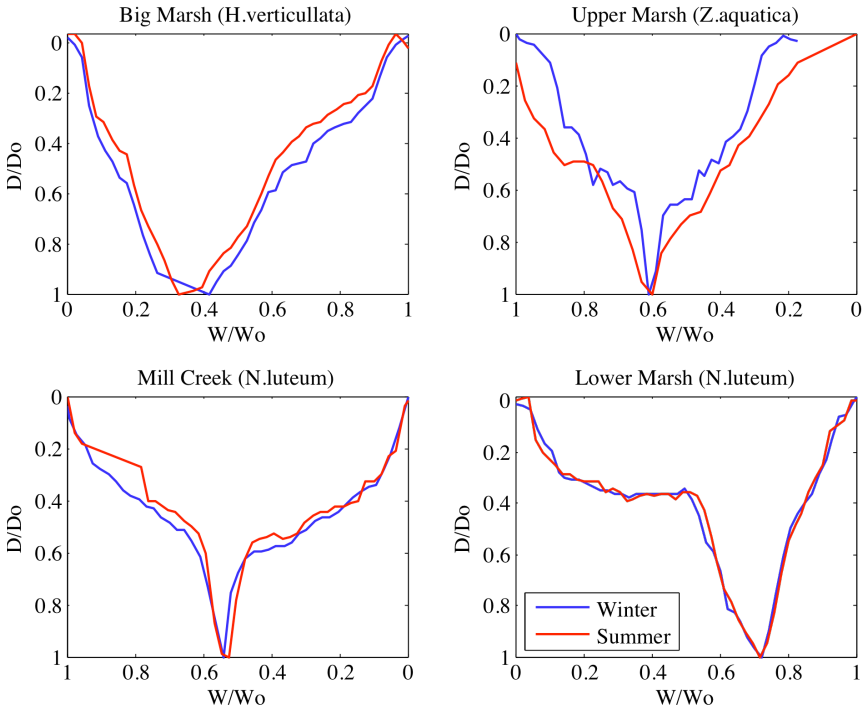

Figure 4.12 Composite of winter and summer dimensionless upstream cross-sections. In order to capture effect of maximum and minimum growing seasons, summer form based on early fall measurements; winter calculated from early spring measurements.

Marsh	BM	MC	UM	LM
Upstream	0.2792	0.1710	0.2626	0.2712
Inlets	0.4045	0.1931	0.4463	0.4976

Table 4.1 Dimensionless areas calculated based on the dimensionless cross-sections in figures 4.11-4.12.

Appendix II. Only one variable (maximum channel depth) exhibited a statistically significant relationship ($r^2 \geq 0.5$) with average annual or summer accretion. As shown by figure 4.13, there is an inversely proportional relationship ($r^2=0.75$, $0.01<p<0.05$) between maximum inlet depth and average annual accretion. The *Z.aquatica* inlet appears to have the highest accretion rates and the *H.verticullata* inlet had the lowest. These conclusions are made with some uncertainty, however, as we are limited by sample size. Figures C-H in Appendix II show results of linear regressions between accretion and plant type; no significant relationship exists between these parameters. Figure 4.14, a bar graph displaying average accretion under each plant type, summarizes these findings. Table 4.2 shows the average annual and summer accretion for each study site; plots of accretion vs. depth for each channel are shown in Appendix II.

Site	LM1	LM2	MC1	MC2	BM1	BM2	UM1
Summer (m)	-0.064	0.135	0.093	0.035	-0.038	0.086	0.008
Annual (m)	-0.078	0.027	0.108	0.062	0.023	0.033	0.117

Table 4.2 Average summer and annual accretion (m) for each cross-section. See Appendix I for a list of site names and codes.

4.4.4 Sediment Characteristics

Results for bulk density and percent organic matter are shown in figures 4.15-4.18. Marshes dominated by *N.luteum* (LM, MC) have the lowest bulk density values (~0.10-0.25g/cm^3), but the highest percent organic matter (~15-22%). It is difficult to define a difference in bulk density between marshes dominated by *H.verticullata* and

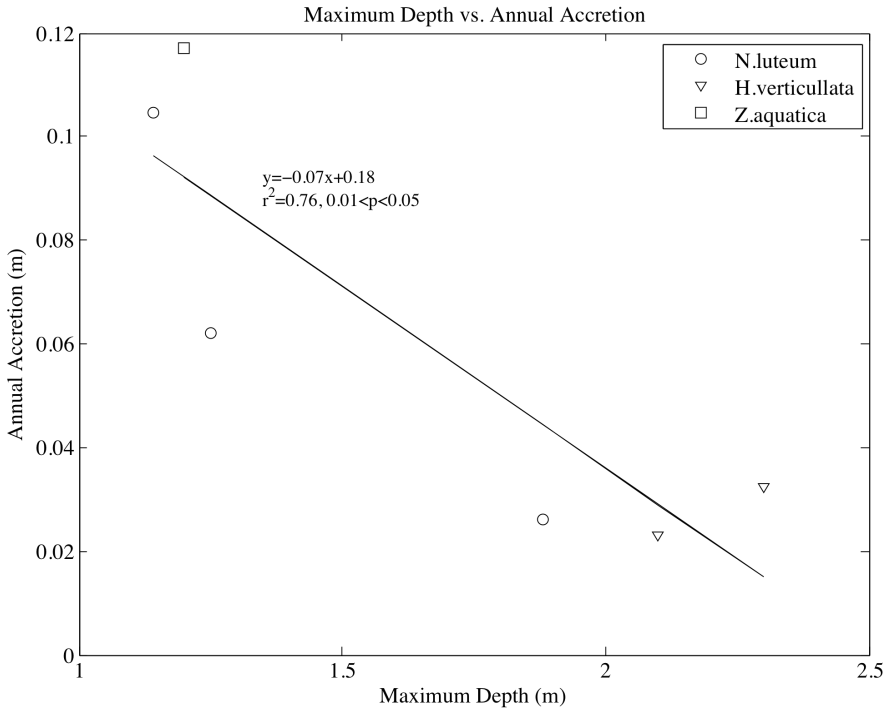

Figure 4.13 Maximum depth vs. average annual accretion for each study site. Trend does not seem to rely solely on plant type.

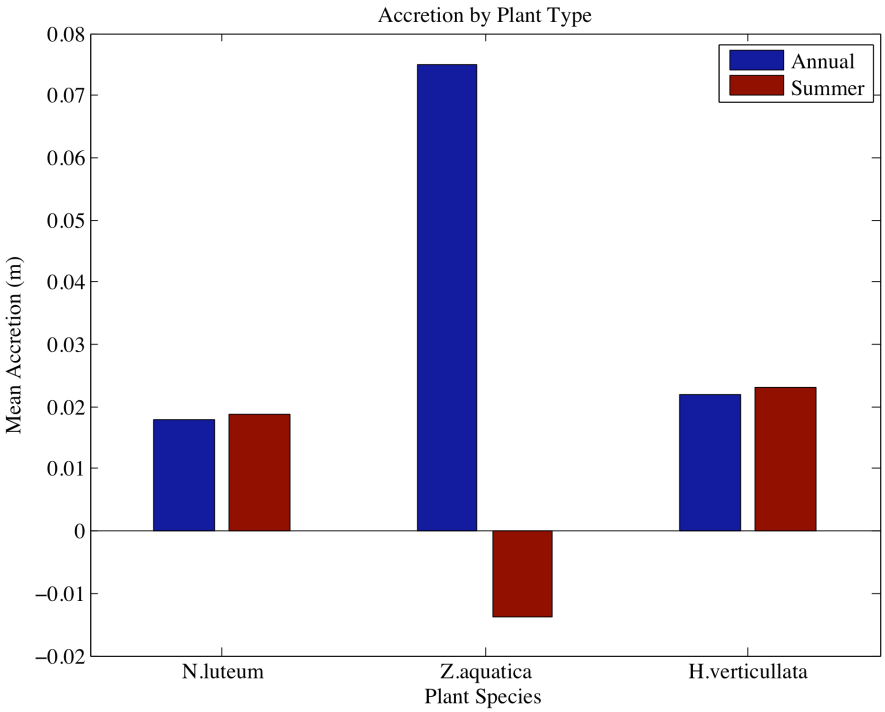

Figure 4.14 Average accretion vs. plant species compiled from both summer and annual accretion data.

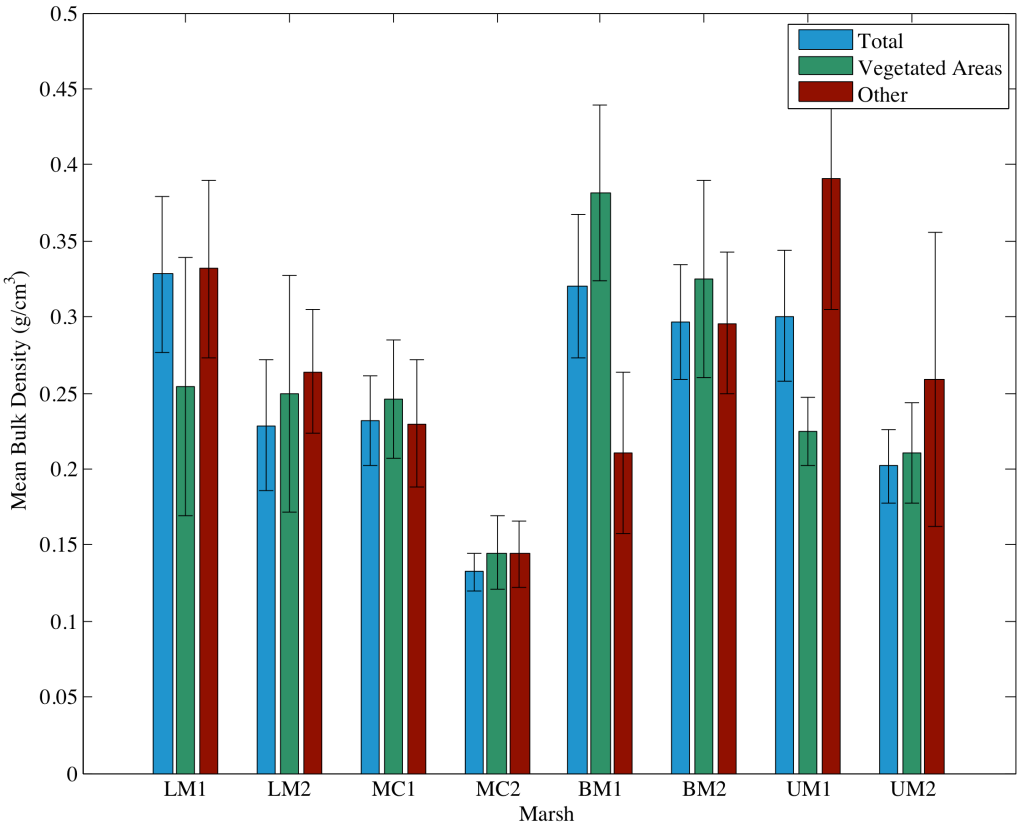

Figure 4.15 Bulk density measurements for each cross-section in study area. Error bars represent ±standard error. See Appendix I for a list of site names and codes.

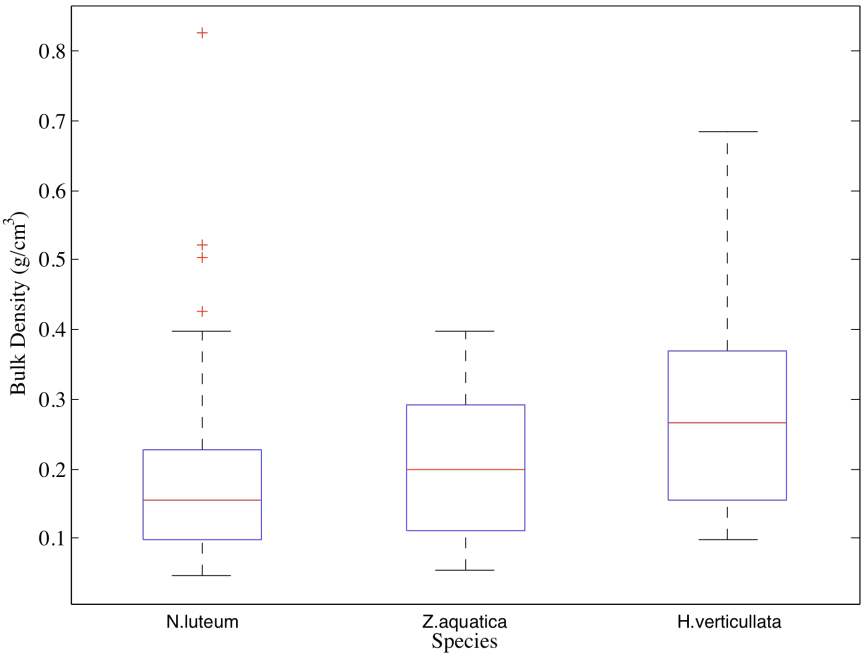

Figure 4.16 Box plots showing distribution of bulk density values for sediment accreted under each aquatic plant species.

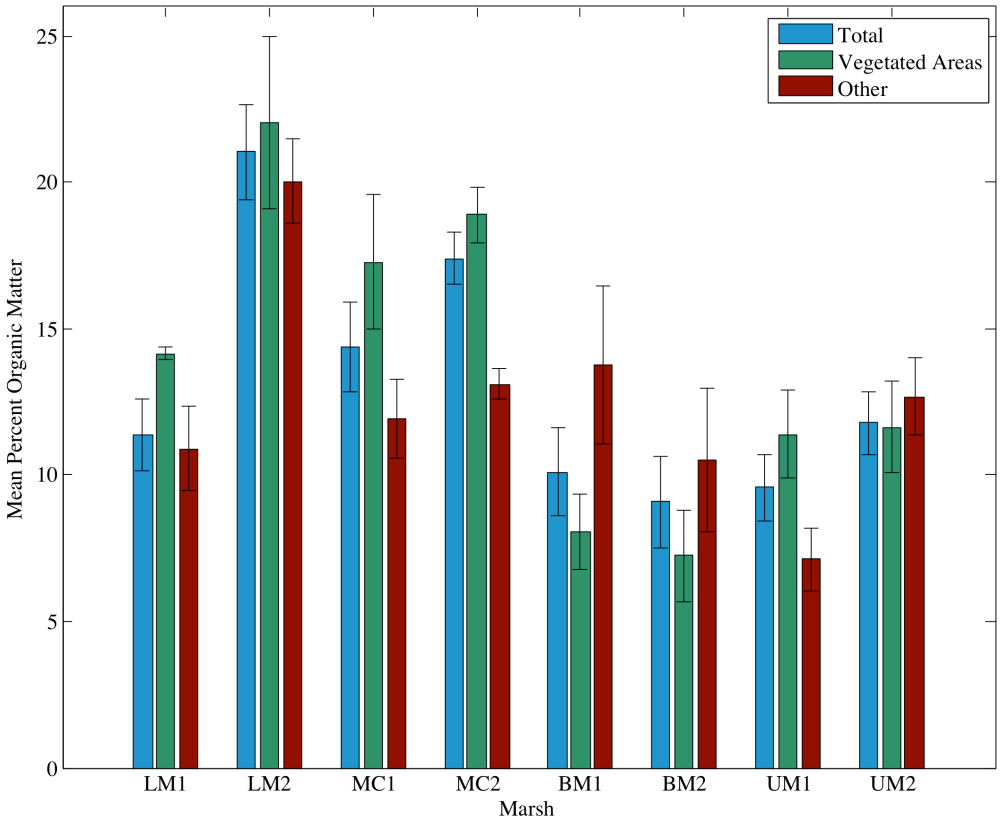

Figure 4.17 Percent organic matter measurements for each cross-section in study area. Error bars represent ±standard error. See Appendix I for a list of site names and codes.

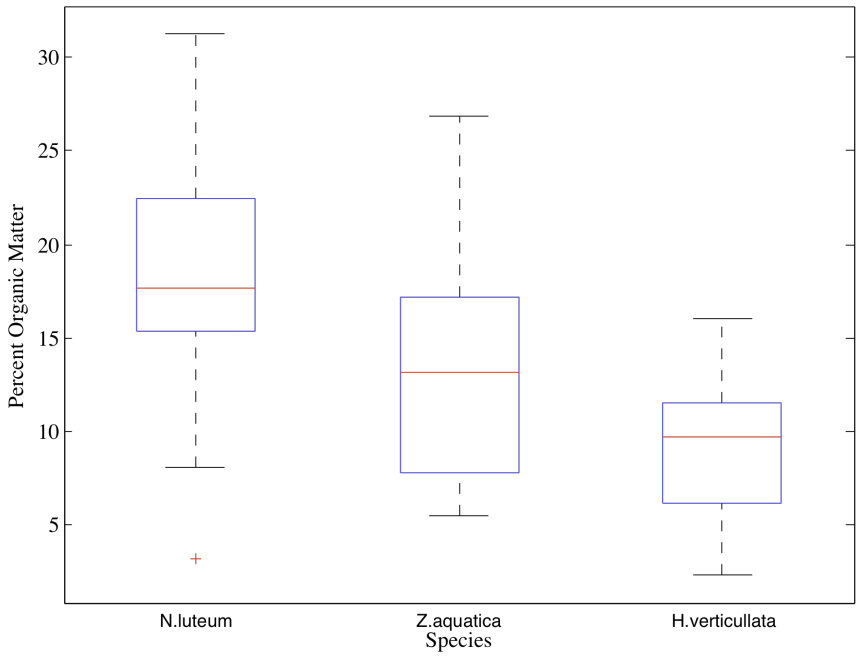

Figure 4.18 Box plots showing distribution of organic content for sediment accreted under each aquatic plant species.

Source of Variation	Sum of Squares	Degrees Freedom	Mean Square	F
Among TFW	0.5960	7	0.0851	4.08***
Within TFW	2.628	126	0.0209	
Total	3.224	133		

Table 4.3 Summary of single-factor ANOVA comparing bulk density of sediment at each study cross-section.

Source of Variation	Sum of Squares	Degrees Freedom	Mean Square	F
Among TFW	2.187×10^3	7	312.4	10.75***
Within TFW	3.661×10^3	126	29.06	
Total	5.848×10^3	133		

Table 4.4 Summary of single-factor ANOVA comparing percent organic matter of sediment at each study cross-section.

Source of Variation	Sum of Squares	Degrees Freedom	Mean Square	F
Among Aquatic Vegetation Types	0.1633	2	0.0816	3.69**
Within Aquatic Vegetation Types	1.903	86	0.0221	
Total	3.224	88		

Table 4.5 Summary of single-factor ANOVA comparing bulk density among sediments accreted under one of the three aquatic vegetation types in the study area.

Source of Variation	Sum of Squares	Degrees Freedom	Mean Square	F
Among Aquatic Vegetation Types	1.413×10^3	2	706.7	20.73***
Within Aquatic Vegetation Types	2.590×10^3	76	34.09	
Total	3.224	78		

Table 4.6 Summary of single-factor ANOVA comparing percent organic matter among sediments accreted under one of the three aquatic vegetation types in the study area.

Percent Organic Matter			
Species	*N.luteum*	*Z.aquatica*	*H.verticullata*
N.luteum	———	4.09***	9.07***
Z.aquatica		———	3.42**
H.verticullata			———
Bulk Density			
Species	*N.luteum*	*Z.aquatica*	*H.verticullata*
N.luteum	———	0.282	3.67**
Z.aquatica		———	2.86*
H.verticullata			———

Table 4.7 Summary table of sediment characteristic a posteriori tests performed after single factor ANOVAs for percent organic matter and bulk density. A series of Tukey tests was performed to highlight specific differences among sediment accreted under each vegetation type.

Z.aquatica, but *Z.aquatica* sediment does appear to have a larger organic content (see fig. 4.18). In these marshes, the vegetated areas had a lower percent organic matter than other portions of the channel. The opposite was true for the *N.luteum* marshes.

A series of single-factor ANOVAs reveal that there is a difference in percent organic matter and bulk density among sediments collected at each cross-section (see tables 4.3-4.4). Tables 4.5-4.6 show results of single-factor ANOVAs comparing the bulk density and organic content of sediment accreted under each vegetation type. In both cases, there is a significant difference among these sediments. A posteriori (Tukey) tests, shown in table 4.7, reveal significant differences in organic content of sediments accreted under each vegetation type. Table 4.7 also shows a significant difference in bulk density between *H.verticullata* sediments and those accreted under emergent vegetation. There is no distinction between the bulk densities of sediments accreted under emergent vegetation.

4.5 Discussion

4.5.1 Accretion Trends

Two notable trends in accretion were observed: (1) a significant relationship exists between maximum inlet depth and annual accretion, and (2) *Z.aquatica* cross-sections experience the greatest accretion. The relationship between inlet depth and annual accretion is a result of the association between inlet geometry and shear stresses generated in the channel. As discussed previously, total boundary shear stress is proportional to depth, so inlets with larger maximum depths will have greater boundary shear stresses. In this situation, fine particles are prevented from settling permanently, and thus, little net accretion will occur. Based on figure 4.13, channels

with a maximum summer depth >1.5m will not produce significant net annual accretion.

In chapter 2, measurements of vegetation morphology and spatial distribution suggested that *N.luteum* occupied a greater channel extent than *Z.aquatica;* however, *N.luteum* is shorter lived and dies back without leaving standing dead. Hydraulic measurements reveal that *Z.aquatica* creates the greatest flow resistance. We see the consequences of these hydraulic differences in channel accretion data, as *Z.aquatica* produced greater annual accretion than *N.luteum* or the submerged *H.verticullata* (fig. 4.14).

4.5.2 Sediment Characteristics

Annual accretion data compare the magnitude of deposition; however, they only reveal short-term patterns of marsh maintenance. Sediment characteristics (percent organic matter and bulk density) provide additional information about deposited material and the long-term capacity for net accretion. Sediments under *N.luteum* had the lowest bulk density and highest organic content. The high organic matter content of these sediments likely derives from the early dieback and fast decomposition of the *N.luteum* plant. Leaves and stems of this vegetation are very friable, thus *N.luteum* is easily incorporated into sediments. This observation has important implications for long-term marsh accretion. Low bulk density means these soils occupy smaller volumes per cm^3 than other soils and will compact under their own weight. Because these soils are also high in organic content, they could decrease in volume due to decomposition.

According to previous studies (Prestegaard *et al.*, submitted 2014), *Z.aquatica* decomposes more slowly than *N.luteum* (likely a result of its tough, fibrous composition), but *H.verticullata* has a faster decomposition rate. As a result of its lifecycle, *H.verticullata* is transported our of the inlet channels, leading to little organic sediment accretion. The resulting sediment has the greatest bulk density, significantly different from sediment under either emergent vegetation species. Emergent vegetation, such as *Z.aquatica* or *N.luteum,* remains as standing dead or decomposes in situ, allowing greater incorporation of organic matter into underlying sediments.

4.5.3 Comparison of Biogeomorphic Observations and Hydraulic Results

Comparison of effective shear stress distributions with channel geomorphic change reveals a complicated view of marsh deposition and erosion processes. At each inlet cross-section, we only observe significant erosion where the effective stress reaches a maximum. Deposition would be expected under emergent and submerged vegetation where the effective stress approaches a minimum. At these locations, where effective stress is much lower than critical and flow resistance is great, emergent vegetation builds platforms near optimum water depths for each species. For example, in each *N.luteum* marsh, the plant grows on a wide platform with an average depth of 0.6 m, regardless of the maximum inlet depth.

While we see hydraulic and geomorphic evidence for the formation of these platforms, current data reveals a slow accretion rate. Of the four cross-sections, which have an associated summer shear stress distribution, only the *Z.aquatica* cross-sections exhibit significant deposition. The *N.luteum* cross-sections reveal positive

accretion, but to a smaller degree. This results from the relationship between depth and effective stress. During winter, deeper inlets are large enough to generate effective stresses over vegetated platforms that exceed critical. These data suggest that perhaps vegetation enhances marsh accretion only during initial vegetation occupation and that subsequent accretion rates are small, but equal to rates of sea-level rise.

4.5.4 Seasonal Differences and Marsh Maintenance Processes

As demonstrated by dimensionless cross-sections, the alternation between vegetated and non-vegetated states does not produce a significant variation in inlet channel form. Previously, we hypothesized that the oscillation in hydraulics and sediment trapping efficiency between the summer and winter states would drive accretion in these marshes; however, this model of marsh maintenance does not fit with observations from this study. Comparison of winter and summer effective shear stress does reveal significant increases during non-vegetated periods, but this does not translate to significant channel change.

To explain this discrepancy, we must consider the relationship between the effective stresses and the critical shear stress at each inlet. The critical shear stress has a variable relationship with the effective stress distribution at each cross-section. In shallow inlets, the critical stress required to erode sediment is only achieved in the central portion of the channel where the effective stress reaches a maximum, thus only a small area of the channel exhibits erosion. This relationship is not seasonally dependent. Deep inlets function differently than shallow inlets; the magnitude of both

summer and winter shear stresses is large, so the channel has little capacity for deposition.

These differences explain the significant correlation between maximum depth and accretion; however, they also contradict the previous hypothesis under which marsh maintenance occurs as a result of the seasonal oscillation in vegetation presence. These observations lead to a new picture of TFW erosion and deposition processes, which place less importance on vegetation presence or absence. The presence of vegetation indirectly controls rate of accretion in these TFW channels. Previously shared vegetation data (Ch. 2) suggests that each aquatic plant engineers an ideal habitat for itself. In the case of *N.luteum* and *Z.aquatica*, the vegetation builds a platform at ideal depths along channel margins. Due to the alteration of the inlet geomorphology (decrease in marginal depths), large effective shear stresses can no longer be generated, even when vegetation is absent. This dynamic preserves the shape of the inlet.

Spring geomorphic change observations further support this hypothesis, as no significant channel change occurred during the major spring flood event even though no vegetation was present. Under the previous picture of marsh maintenance, we would expect a significant change to inlet form during such an event; instead we observed small amounts of erosion evenly distributed across the entire channel (see channel change diagrams for UM1, LM1, LM2, BM1). These observations further confirm the importance of interactions among vegetation, hydraulics, and geomorphology to marsh maintenance processes. Changes in vegetation may drive

initial accretion, but once platforms are formed, the vegetation effects may be less important than the established channel morphology.

4.6 Conclusions

4.6.1 Geomorphology

Geomorphic change measurements agree with previously shared hydraulic data, reflecting spatial differences in channel hydraulics, which produce deposition and erosion in specific locations across each cross-section. In each *N.luteum* and *Z.aquatica* marsh, deposition was observed under emergent vegetation throughout the growing season. These measurements of channel change correlate with shear stress distributions and observations of vegetation flow resistance shown in chapter 3. Another significant trend was the erosion of the central channel over the growing season and deposition in this region over the winter period. These measurements also coincide with shear stress distributions discussed in chapter 3, which show that summer effective stress equals or exceeds overall shear stress in the central channel of marshes dominated by emergent vegetation. The SAV-dominated marsh revealed the same pattern; however, the hydraulic measurements in this channel did not reveal the same increase in effective shear stress as compared to the total shear stress.

On average, most marsh inlets experienced positive elevation changes over the annual cycle (see table 4.2) Those, which experienced negative average accretion, were inlets characterized by large maximum depths. As demonstrated, there is a significant negative correlation between maximum inlet depth and average annual marsh accretion. This association likely results from the positive relationship between depth and shear stress; larger depths translate to higher velocities and thus shear

stresses. In this situation, only large particles can settle to the bed. Although the larger marshes had negative accretion values, they did not necessarily experience erosion across the entire channel, but instead in isolated sections, often associated with summer presence of emergent vegetation. At these locations, flow resistance created by vegetation allows summer deposition, but the large inlet depths allow generation of significant effective shear stresses during the non-vegetated period.

Each aquatic species in the study area had specific geomorphic traits associated with its presence. *N.luteum* inhabits or perhaps engineers wide platforms with extremely small gradients. *Z.aquatica* also builds platforms; however, they have larger gradients directed toward the center of the channel. *H.verticullata* inhabits deeper portions of the inlet channels and does not appear to build any significant features. *Z.aquatica* cross-sections had the greatest average accretion rate, which likely results from the long-lived nature of the plant (it remains as standing dead long after peak growth) and its great affect on flow. *Z.aquatica* provided the greatest flow resistance. These results support our hypothesis that channel erosion will be higher under vegetation that is shorter-lived.

4.6.2 Marsh Maintenance

Because we observed no significant seasonal changes in channel form, our original explanation of annual marsh maintenance processes is invalid. There is no oscillation in form resulting from the seasonal variations in vegetated state. Vegetation alone does not drive the system to the extent that we originally expected. The interaction among vegetation, hydraulics, and geomorphology is complex; naming one of these variables as the driver of the system is difficult. Vegetation plays

an important role upon initial colonization, engineering a preferred habitat; however, the altered geomorphology effectively controls the capacity for erosion and deposition in the channel. Platforms formed under vegetation transform the channel. Often, the maximum winter shear stresses on these platforms do not approach critical. This hypothesis is supported by observations of minor channel erosion after a major spring flood event (refer to channel change figures shown above).

Geomorphology also plays a significant role in the capacity for accretion of individual marshes. The deeper marshes have a wide range of effective shear stress values, most of which exceed the estimated critical value, thus preventing deposition across a large area of the channel. In shallow marshes, the opposite occurs, shear stresses larger than critical cannot be generated across the channel, and deposition occurs across a wide expanse. Despite this relationship, sediment characteristics ultimately determine the long-term capacity for marsh accretion. The *Z.aquatica* marsh exhibited the greatest deposition, moderate bulk density values, and moderate organic matter content. These characteristics allow sediment trapped by the vegetation to contribute more significantly to long-term marsh maintenance. Conversely, the *N.luteum* marshes had fair amounts of deposition, but high organic content and low bulk densities. Not only does each particle contribute less significantly to net accretion, but the organic-rich soils are likely to decompose more quickly.

Chapter 5: Conclusions and Implications: The Influence of Vegetation on Marsh Maintenance and Equilibrium

5.1 Summary Interaction of Vegetation, Hydraulics and Geomorphology

Spatial and morphological measurements of emergent aquatic vegetation reveal significant differences among the habitats and lifecycle of dominant TFW species. *Z.aquatica* occupies smaller depths, and thus smaller channel areas, than *N.luteum,* but has larger stem density and diameter. These plants also exhibit different patterns of dieback: *N.luteum* quickly decreases stem densities after peak growth, *Z.aquatica* remains as standing or fallen dead long after peak growth without reducing population density.

The effects of these growth dynamics are observed in measurements of flow resistance and shear stress distributions in the channels. In all channels, aquatic vegetation creates flow resistance, thus decreasing shear stress over vegetated platforms. Emergent vegetation also acts as a hydraulic wall, funneling water through the central channel, forcing effective shear stresses to equal or exceed overall expected shear stress. While shear stress measurements were not precise enough to differentiate among vegetation types, calculations of flow resistance revealed that each vegetation type affects flow uniquely. *Z.aquatica* imposes significantly greater flow resistance on the channel, while SAV affects flow the least.

These observations have implications for geomorphic change and correlate well with significant observations about channel change over the annual cycle. Biogeomorphic relationships confirm that vegetation indeed builds these platforms at preferred depths. Minimum shear stress values correlate well with locations of platforms in channel cross-sections. While *Z.aquatica* had the greatest impact on flow and largest accretion rate, its platforms were less well defined than those of *N.luteum,* which had platforms with almost no gradient. *Z.aquatica* has the greatest capacity for marsh accretion, but perhaps does not build such defined platforms due to inter-annual variation in vegetated extent. This plant is an annual, which must reseed itself each year, unlike *N.luteum*, which grows from networks of rhizomes each year. *H.verticullata* likely had little affect on marsh geomorphology and accretion because it leaves the marsh upon dieback, taking accreted sediment with it.

Dimensionless cross-sections revealed no oscillation in marsh form with seasonal changes in vegetated extent and shear stress distributions. Accretion trends instead suggest that vegetation is only indirectly linked to marsh maintenance through its control on the geomorphology of the system. Investigation of accretion trends revealed only one significant relationship: decreasing channel change with increasing maximum inlet depth. This relationship results from the proportional increase in shear stress with depth.

These observations, along with hydraulic measurements over vegetated platforms, lead to a new picture of marsh maintenance. Vegetation is initially important, forming platforms by reducing shear stresses upon colonization, but this alteration in channel geometry controls future accretion capacity. Once the vegetated

platforms are established, they cannot be removed or altered easily. Even during the winter, when we would expect the highest effective shear stress, stresses barely equal or exceed critical over these platforms. Vegetation does not play as large a driving role as we initially hypothesized.

5.2 Models of Marsh Equilibrium

Several models of marsh equilibrium exist, which classify TFW based on either hydraulic or geomorphic measurements. Our model of marsh equilibrium sought to combine these to explore how channel hydrodynamics and resulting inlet geometry are controlled by vegetation. Our data did not support this model; however, it also contradicted concepts of equilibrium suggested by previous studies. Seminara *et al.* (2010) stated that an equilibrium marsh channel has a shear stress distribution equal to or exceeding the critical shear stress at each instant at all locations. Our data challenge this hypothesis as the seasonal presence of vegetation causes large variations in effective shear stress. Even though the study marshes may not be in an equilibrium state, these data suggest that marshes occupied by aquatic vegetation will not conform to this model of long-term equilibrium. Because most TFW and other tidal marsh channels are populated by vegetation, this model of equilibrium seems unlikely.

Marsh equilibrium can also be described in a geomorphic context by examining the relationship between marsh geometric traits. In chapter 1, we discussed the model of Friedrichs and Aubrey (1996), which describes a marsh equilibrium in which inlet maximum depth is proportional to channel length:

$$L = \frac{D_o U_{crit}}{A_o W}$$

Because U_{crit}, A_o, and W, will be similar for marshes along short reaches such as those in our study area, we analyzed the relationship between D_o and L for each marsh (fig. 5.1). These data suggest that perhaps these marshes are in equilibrium as they all fit the same trend: as maximum inlet depth increases, channel length also increases.

We furthered the analysis by comparing inlet area to marsh surface area, another geomorphic metric of equilibrium (fig. 5.2). These data do not fit a similar trend; instead the two *N.luteum* marshes appear to have similar inlet areas, but significantly different marsh surface areas. This reflects the alteration of the smaller *N.luteum* marsh (Mill Creek), which was cut in half by the Hills Bridge (rt. 4) over the Patuxent River. As a result of this split, Mill Creek (shown in fig. 5.3) has an inlet area much larger than expected considering its channel length. The comparison of Mill Creek and the larger *N.luteum* marsh yields some clues to how marshes will adjust to changes in discharge over time.

Mill Creek was abruptly cut, resulting in a marsh surface area and channel length much smaller than expected for its inlet size. Current measurements of Mill Creek show that its inlet depth fits proportionally with the abbreviated channel length. This suggests that marsh depth adjusts before marsh width, which fits well with our revised picture of marsh maintenance. Aquatic vegetation stabilizes channel margins, maintaining its ideal depth across a vegetated platform. The large colony of *N.luteum* is likely contributing to the adjustment of channel width. As shown in chapter 2, Mill Creek has the largest fraction of vegetated channel width (75-95%), and most of the

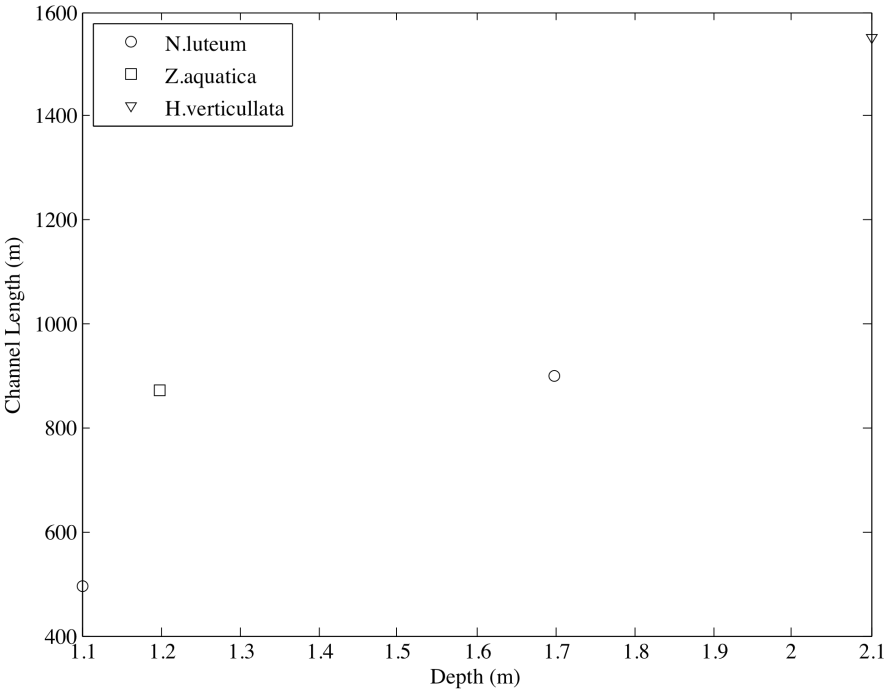

Figure 5.1 Maximum inlet depth (m) vs. channel length (m) for TFW dominated by one of three aquatic vegetation types.

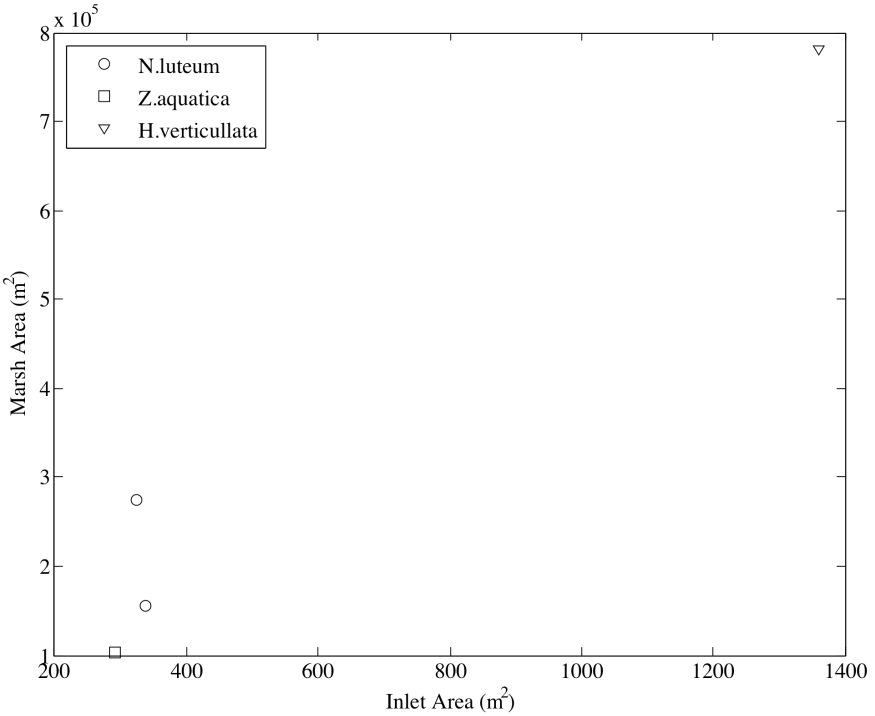

Figure 5.2 Inlet area (m^2) vs. marsh surface area (m^2) for TFW dominated by one of three aquatic vegetation types.

Figure 5.3 Mill Creek cut by Hill's (rt. 4) Bridge over the Patuxent River. White line illustrates extent of channel before marsh alteration. Red box indicates location of inset photo used in subsequent section (5.3). Imagery from 10/12/2012, accessed through GoogleEarth.

channel has adjusted to the preferred *N.luteum* depth. Mill Creek records a small amount of positive accretion each year; eventually channel margins will transform to marsh platform, thus decreasing inlet channel area.

5.3 Timescale of Marsh Alteration and Response to Climate Change

This investigation of seasonal variations in TFW inlet channel vegetation, hydraulics, and geomorphology emphasizes that significant marsh alteration occurs at

timescales much larger than one year. As discussed previously, we did not see significant alteration of the channel from the summer to winter season. These observations leave us to question over what timescale will significant alteration of marsh inlet and channel geomorphology occur? Even though the seasonal variation in vegetation community does not produce significant changes, how long after permanent alterations to the plant community will marsh channel geomorphology respond? These questions are especially salient as we try to predict the fate of coastal areas as sea-level rises.

If no change results from the oscillation between non-vegetated and vegetated states, other drivers of marsh alteration could be large flood events. As discussed previously, our sampling scheme bracketed several flood events (refer to fig. 4.2). Figure 5.4 puts these events on a flood frequency diagram for the Patuxent River at Bowie, MD. The smallest group of flood events, snow melt events, which occurred December 2013 to February 2014, have a recurrence interval of ~1yr and do not seem to have caused a significant reworking of sediment (see geomorphic change diagrams, Ch. 4). In addition to their small size, the effect of these events was further dissipated as a result of ice covering the entire river and frozen floodplain and channel sediments. The medium-sized flood events, with recurrence interval ~1-1.5yrs, again produced few changes (see cross-sections for the lower and upper marshes).

One extreme flood event occurred during our study in May 2014, with flood discharges reaching elevations 1-2.5m above high tide. This event was among the largest ever recorded on the Patuxent River, but we still observed only minor changes in marsh channel elevation. The relationship between our April and May

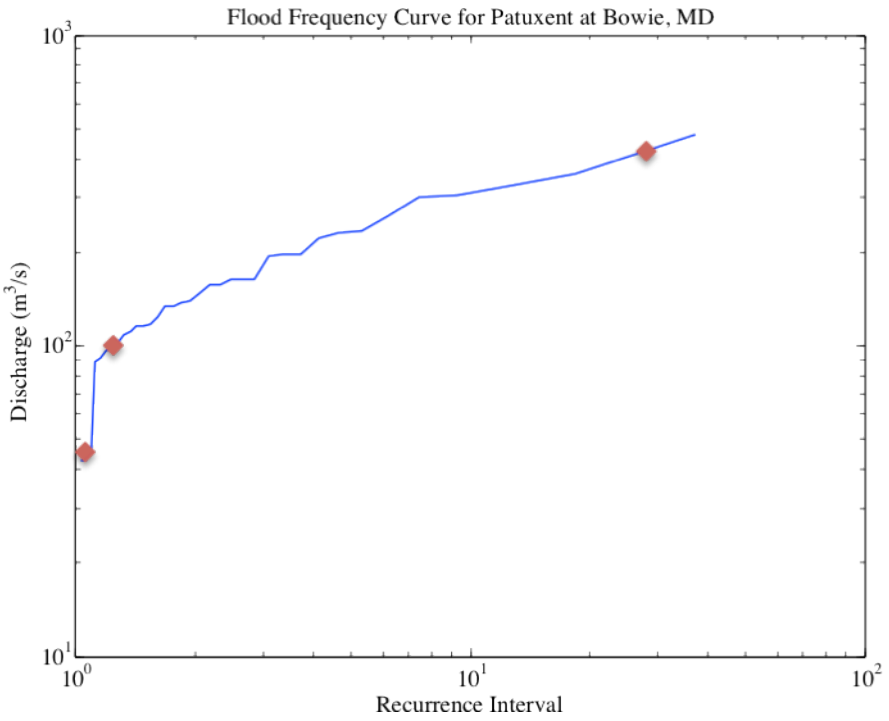

Figure 5.4 Flood frequency curve for Patuxent at Bowie, MD. Note that recurrence intervals are artificially low due a short flood record for this station.

measurements leads to one conclusion: TFW inlet channel morphology changes on very long timescales. These observations support previous conclusions about the role of vegetation in marsh maintenance: plant communities are initially important for establishing an inlet channel form, but the geomorphology then controls the ability for channels to accrete or erode. The shallow depths over vegetated platforms cause channel margins to experience shear stresses below critical even when vegetation is absent, thus TFW inlet forms are fairly static.

Initially, we hypothesized that if marshes could not keep pace with sea-level rise, large areas of open water would form, preventing TFW from performing important ecosystem services. So, what role will vegetation play in marsh survival as sea-level rises and how will TFW inlets respond? To answer this question, we must revisit two important hydraulic observations from chapter 4: (1) summer effective

shear stress reaches a minimum over vegetated platforms, and (2) summer effective stress reaches a maximum (often exceeding possible winter stresses) in the central channel. These relationships cause a funneling of water through the system and result in a scouring of the central channel. Erosion of the central channel increases inlet area and thus the tidal prism volume (discharge) introduced to the marsh. This increased tidal prism exceeds the channel area occupied by a normal high tide. The walls of emergent vegetation prevent overbank flooding, and water that is funneled through the system drives discharge up the marsh, extending the length of the uppermost channels.

This interaction will only magnify with sea-level rise. The tidal prism will greatly increase, further deepening the inlet and thus expanding marsh area by driving TFW inland. Aquatic vegetation will prevent alteration of channel margins, keeping platforms steady, prohibiting the formation of large areas of open water. We already observe the consequences of these relationships in our study area where TFW are creeping into adjacent forested areas to form tidal freshwater swamps (see fig. 5.5). These consequences are particularly prominent in a marsh that was cut in half by the Hills Bridge (rt. 4) over the Patuxent River. The results of >50yrs of disproportionately large discharges are seen as the marsh turns sharply into a previously forested area (as suggested by the abundance of fallen and dead trees). This area has now become a wide, shallow extension of the marsh channel (fig. 5.6).

This type of response may not affect TFW ecosystem services as drastically as previously thought. The creation of open water would prevent nutrient removal,

Figure 5.5 Example of channel lengthening with increased discharge. Red arrows point to incursions of TFW into forested floodplain. Imagery from 10/12/2012, accessed through GoogleEarth.

Figure 5.6 Bend of channel in Mill Creek forced by dramatic reduction of marsh area and channel length. Inset from airphoto in figure 5.3. Imagery from 10/12/2012, accessed through GoogleEarth.

carbon sequestration, and sediment retention; however, if marshes are simply migrating inland without decreasing in size, these functions should be preserved. This migration would affect the ecosystem services of the forested floodplains the TFW are invading. If marshes migrate more slowly than sea-level rise, than services will only be preserved for a short period. Other aspects of climate change, including variable growing season length and increased storm magnitude, could alter the amount of sediment available to these marshes and TFW ability to retain sediment and continue to accrete annually. These relationships would also contribute to accelerated degradation of marsh area and ecosystem services.

5.4 Future Work

While this study revealed important relationships among vegetation, hydraulics, and geomorphology, which contribute to the stability of tidal freshwater marshes, many other processes contribute to net annual accretion. In addition to erosion, other negative impacts on marsh elevation come from decomposition of organic matter and settling and compaction of deposited material. We need to know more about the fate of sediment after deposition in marshes. How much of the material that remains annually decomposes? How much elevation is lost due to the compaction of grains as weight is added to the marsh? There are also other factors contributing to net annual accretion, such as belowground biomass production; do the large networks of *N.luteum* rhizomes offset the magnitude of sediment deposited by seed-generated *Z.aquatica*?

This study focuses on TFW inlet channels, which define much of the marsh capacity for accretion, but does not look at these systems as a whole. Future work

expanding this study to examine upper reaches of marshes could validate some of our new hypotheses and further develop our understanding of marsh maintenance processes. Measurements of geomorphic change at channel heads could demonstrate the validity of our hypothesis concerning the relationship between vegetated hydraulic walls and marsh response to sea-level rise. More channel cross-sections could show whether the observed accretion trends only occur at the inlet where the largest discharges and deepest depths exist, or if plants influence hydraulics and geomorphology in the way across the entire system.

The present study could also be expanded, using numerical models to learn about the timescale of different processes. The response of marshes to changes in vegetation community or climate change may occur over 50-100 years. Field studies are impractical in this case, thus expansion of current modeling efforts with alterations based on field observations would improve our understanding of how these systems evolve.

APPENDIX I: CATALOG OF STATION NAMES, ABBREVIATIONS, PLANT TYPE

Station Name	Station Abbreviation	Plant Cover Type
Big Marsh Inlet	BM1	*H.verticullata*
Big Marsh Upstream	BM2	*H.verticullata*
Upper Marsh Inlet	UM1	*Z.aquatica/H.verticullata*
Upper Marsh Upstream	UM2	*Z.aquatica/H.verticullata*
Mill Creek Inlet	MC1	*N.luteum*
Mill Creek Upstream	MC2	*N.luteum*
Lower Marsh Inlet	LM1	*N.luteum*
Lower Marsh Upstream	LM2	*N.luteum*

APPENDIX II: ACCRETION FIGURES

A. Accretion Summary

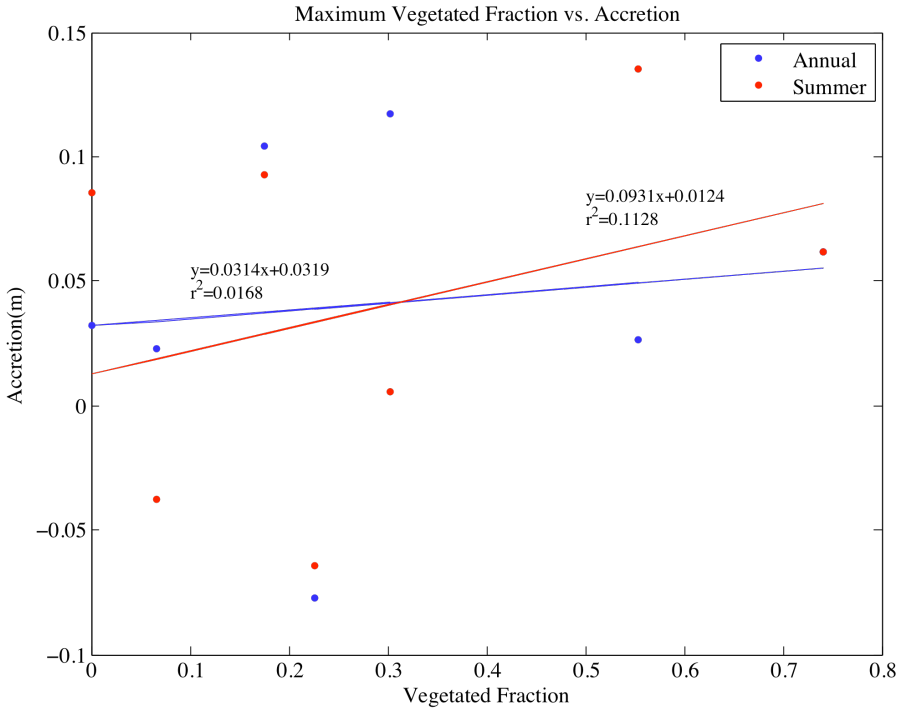

Figure A. Vegetated fraction vs. accretion for each site in study area.

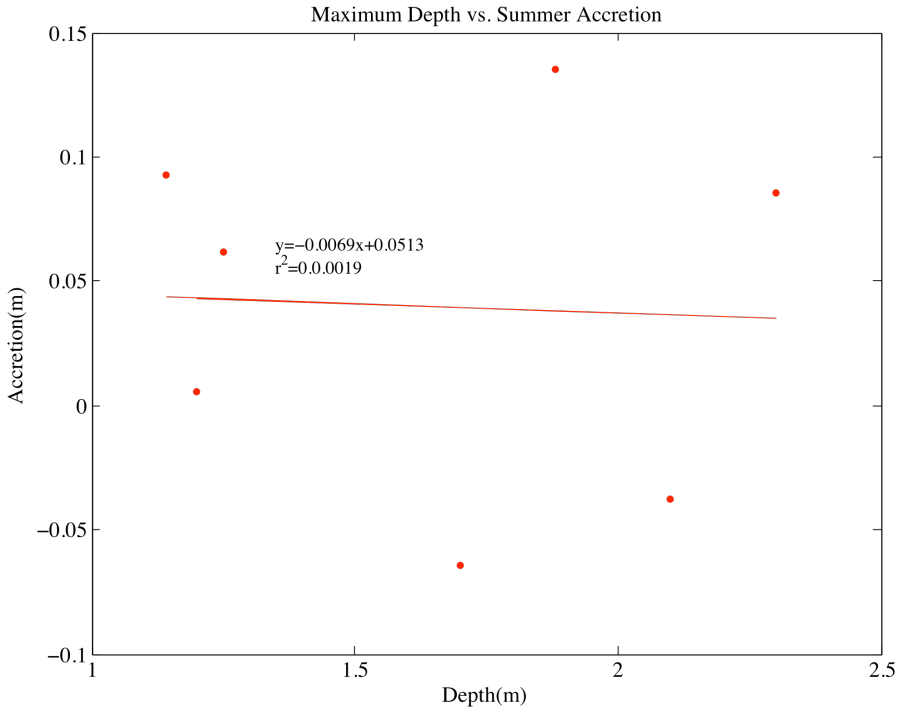

Figure B. Maximum depth vs. average summer accretion for each site in study area.

B. Accretion by Plant Type

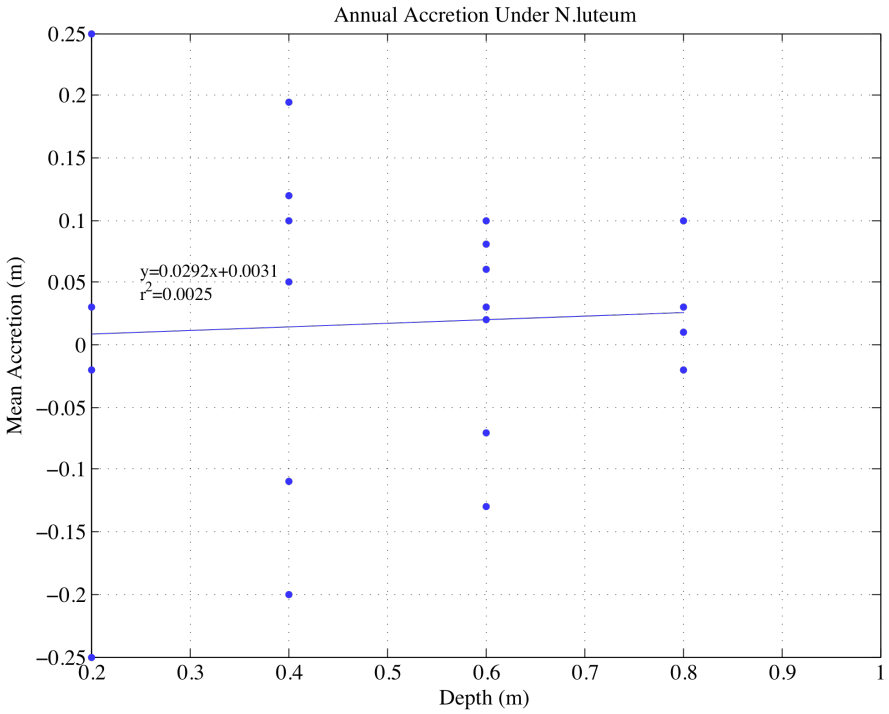

Figure C. Annual accretion under *N.luteum.*

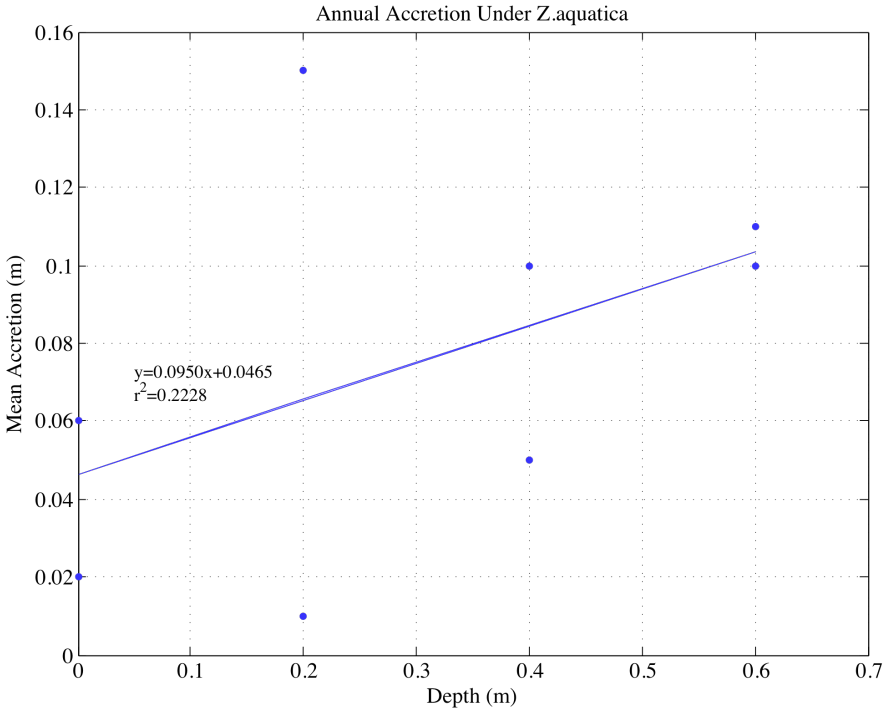

Figure D. Annual accretion under *Z.aquatica.*

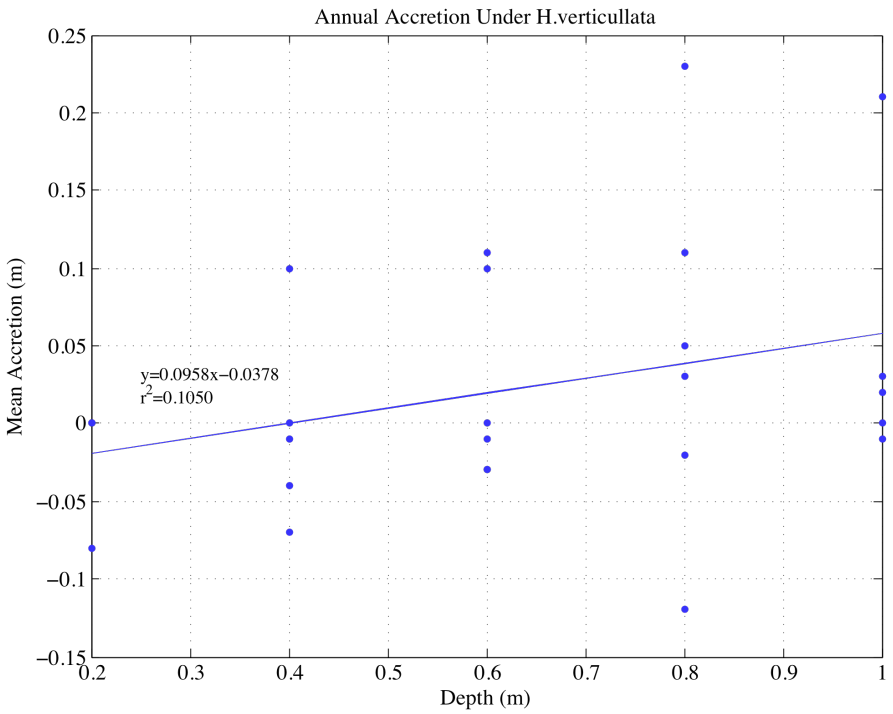

Figure E. Annual accretion under *H.verticullata.*

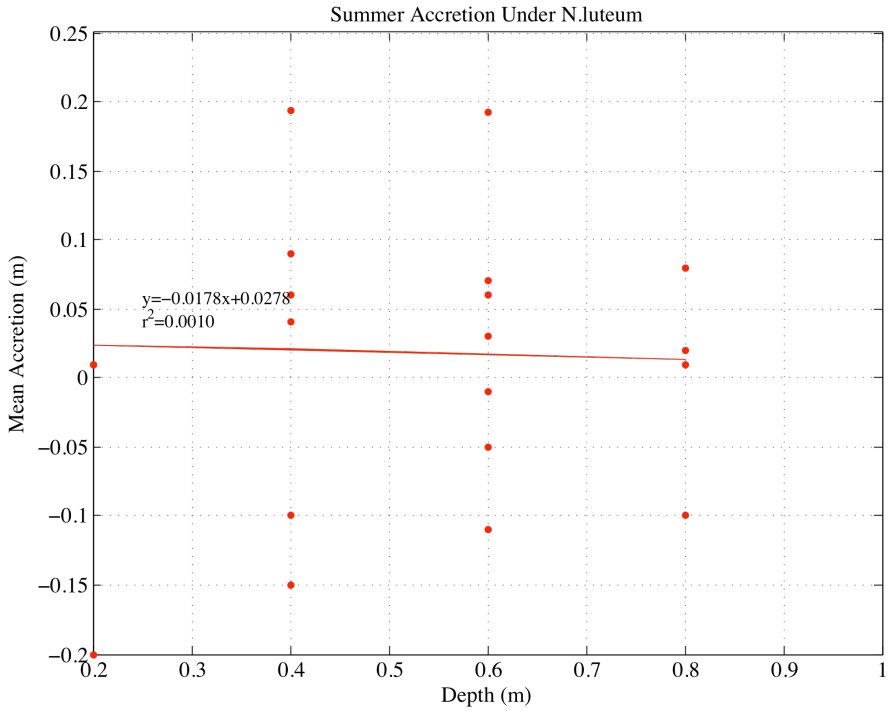

Figure F. Summer accretion under *N.luteum.*

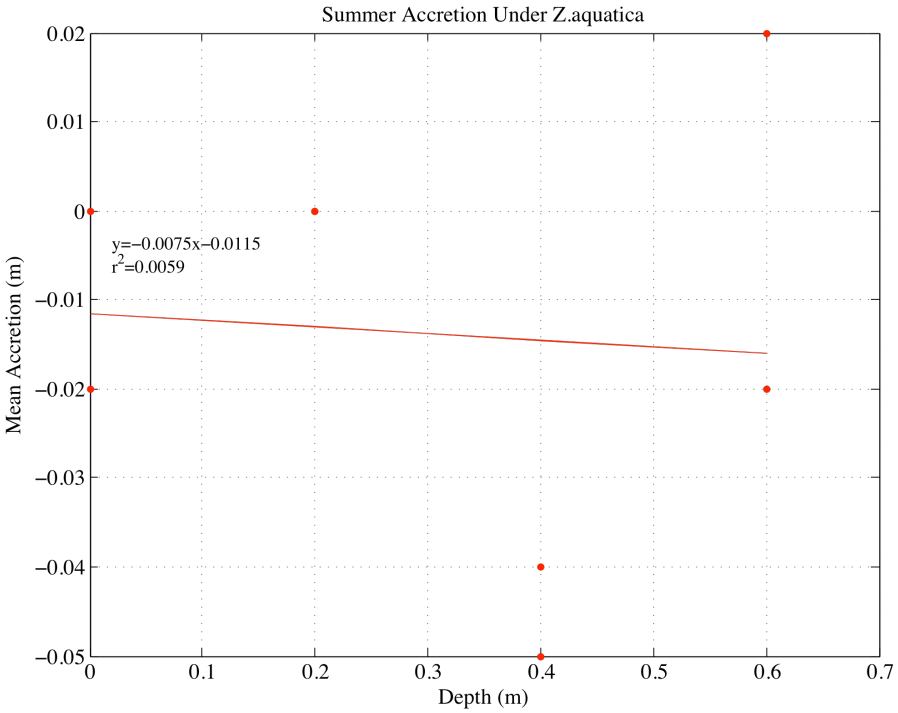

Figure G. Summer accretion under *Z.aquatica.*

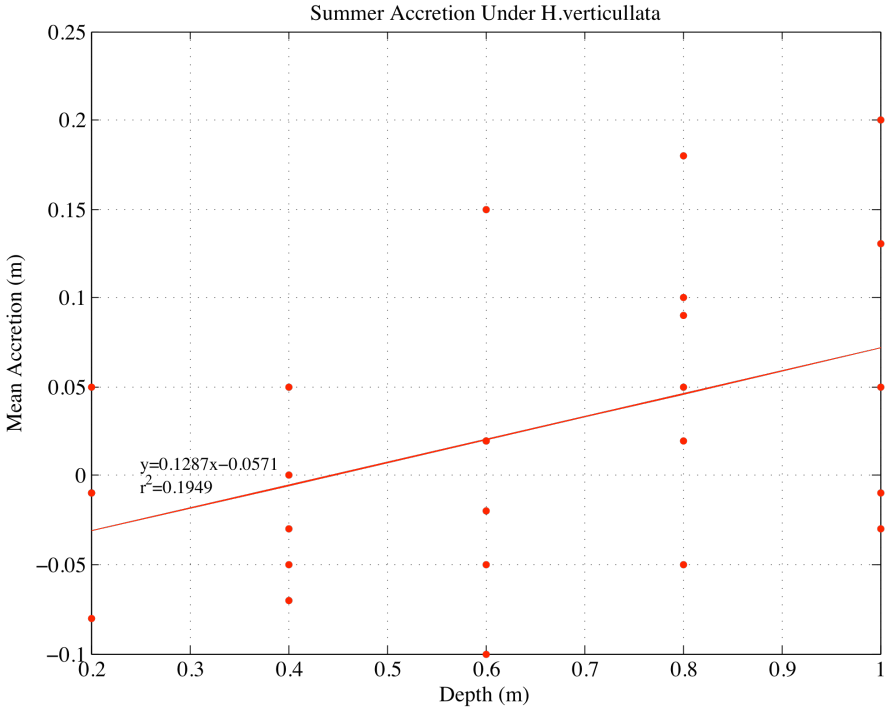

Figure H. Summer Accretion under *H.verticullata.*

C. Accretion By Site

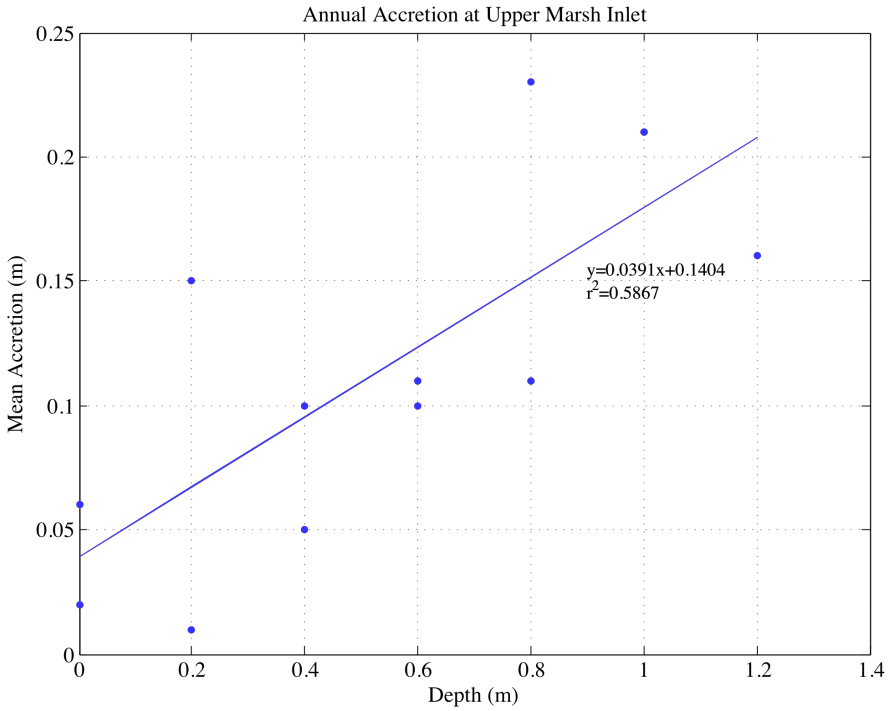

Figure I. Annual accretion at Upper Marsh inlet, dominated by *Z.aquatica.*

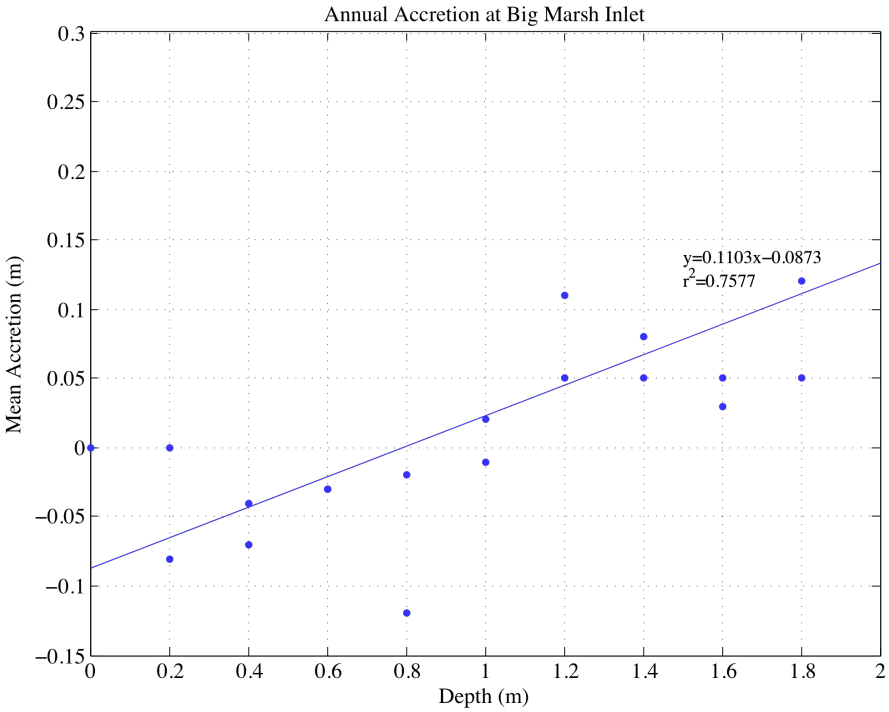

Figure J. Annual accretion at Big Marsh inlet, dominated by *H.verticullata.*

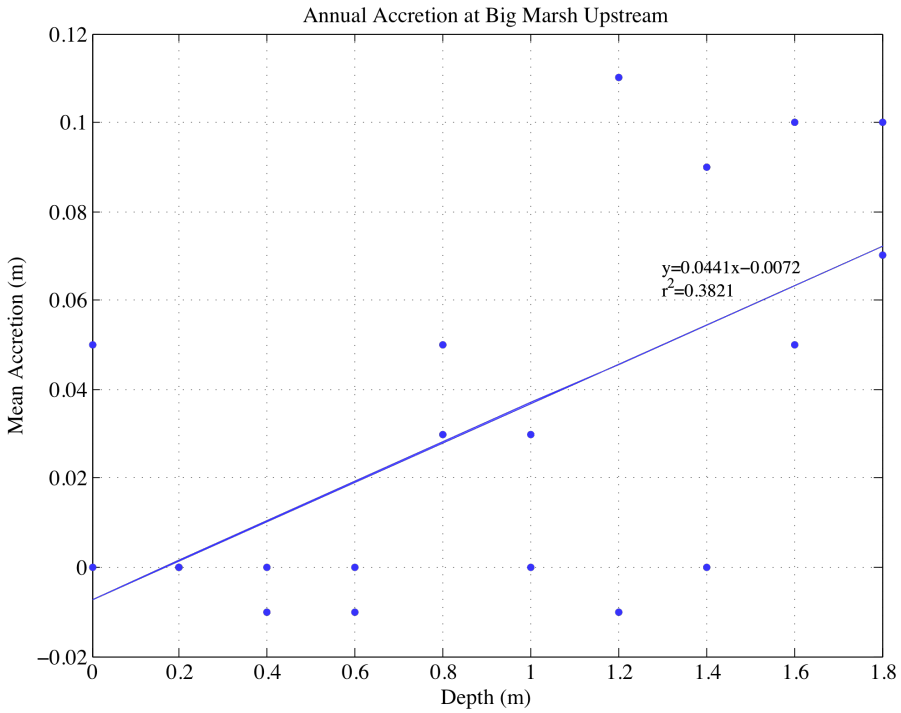

Figure K. Annual accretion at Big Marsh upstream, dominated by *H.verticullata.*

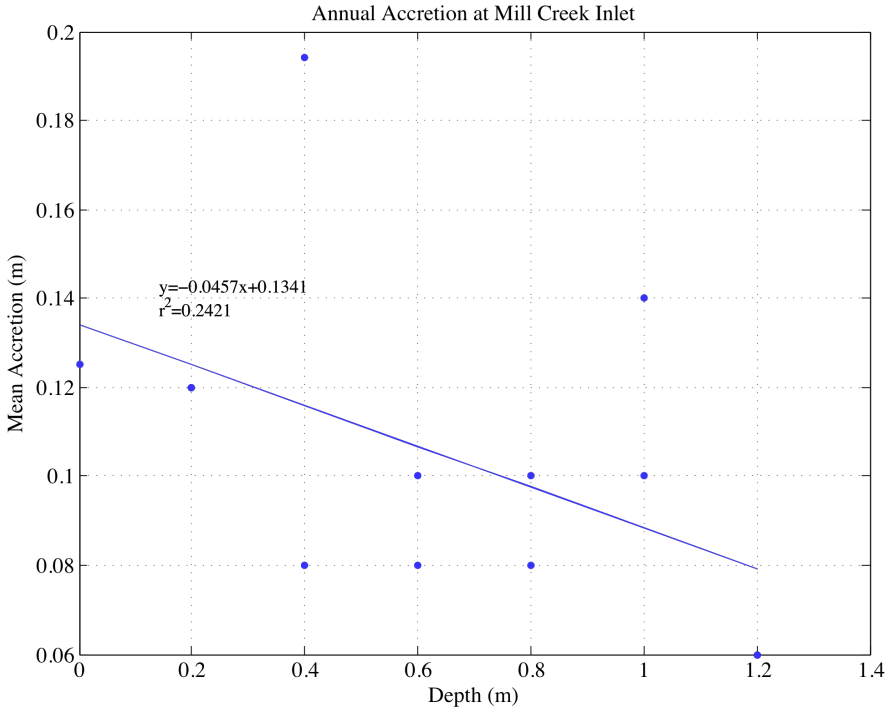

Figure L. Annual accretion at Mill Creek inlet, dominated by *N.luteum.*

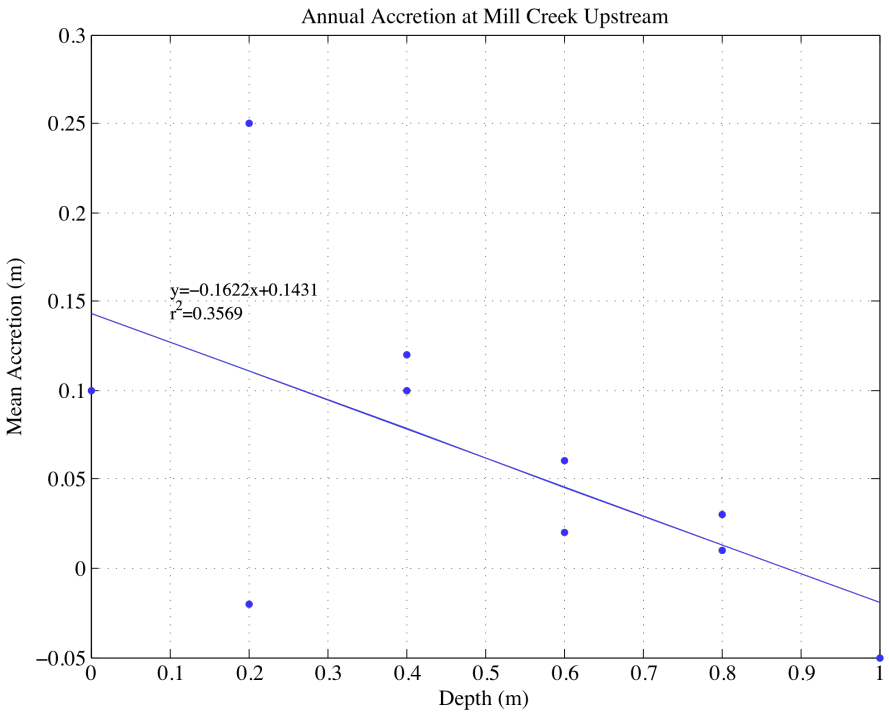

Figure M. Annual accretion at Mill Creek upstream, dominated by *N.luteum.*

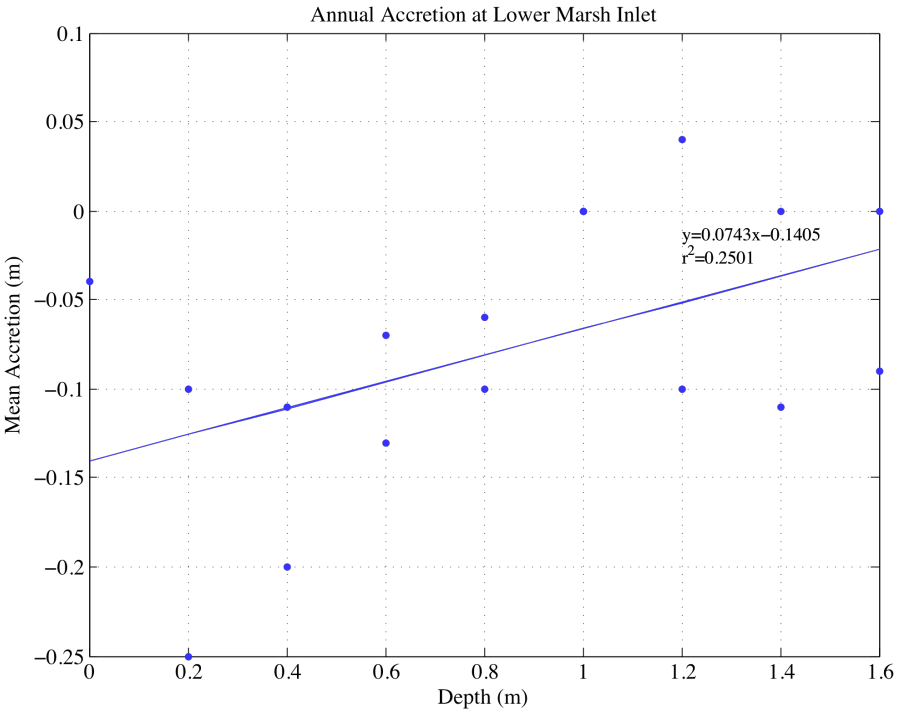

Figure N. Annual accretion at Lower Marsh inlet, dominated by *N.luteum.*

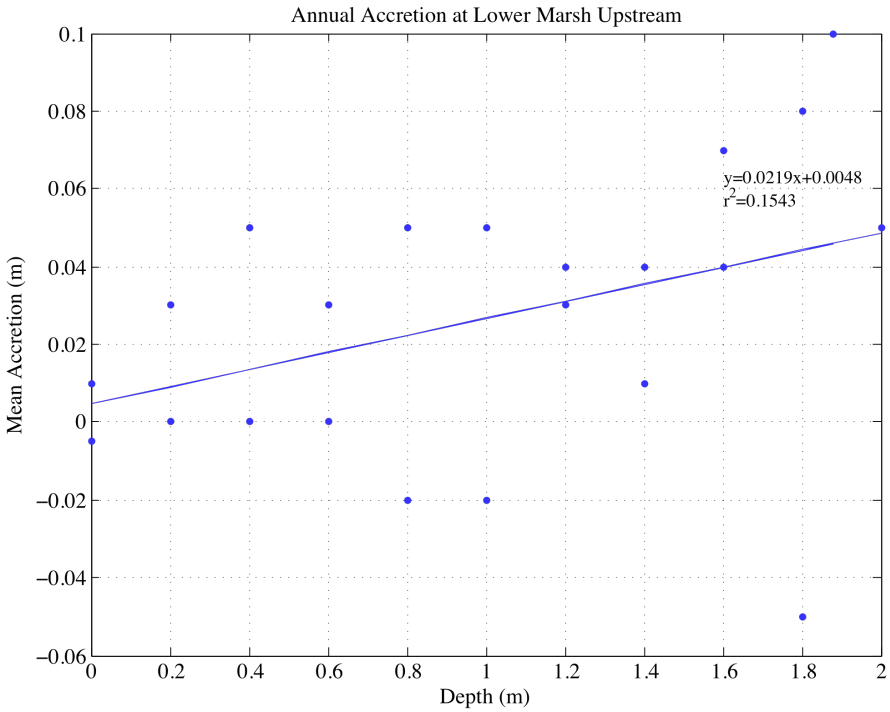

Figure O. Annual accretion at Lower Marsh upstream, dominated by *N.luteum.*

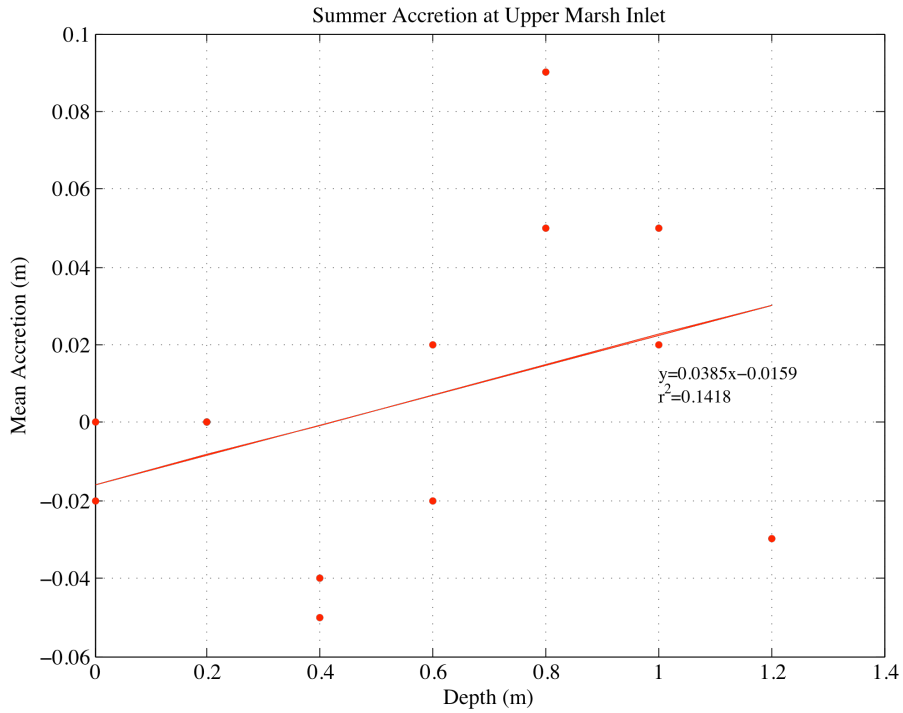

Figure P. Summer accretion at Upper Marsh inlet, dominated by *Z.aquatica.*

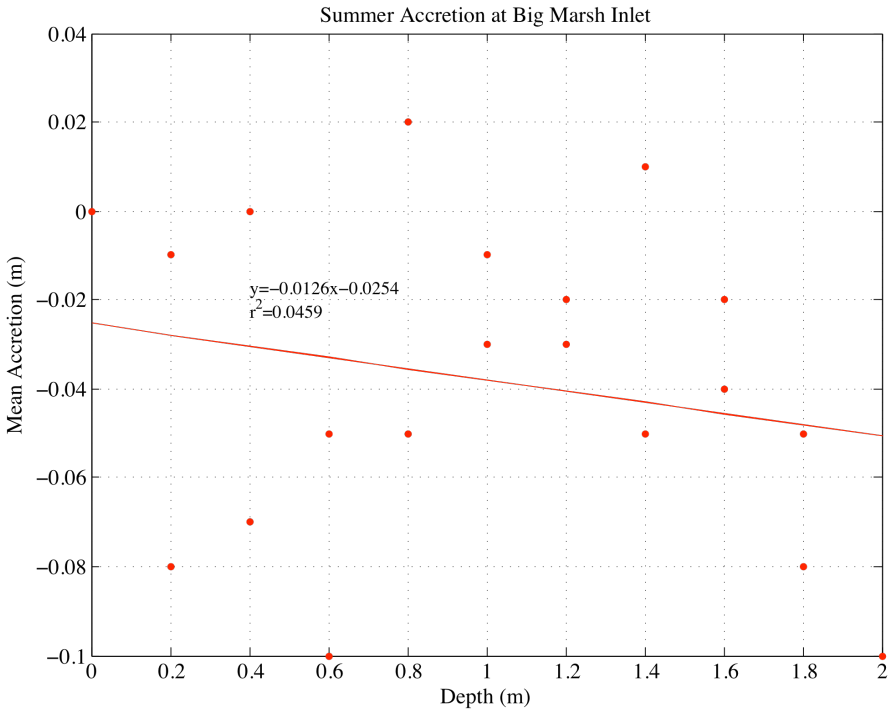

Figure Q. Summer accretion at Big Marsh inlet, dominated *H.verticullata.*

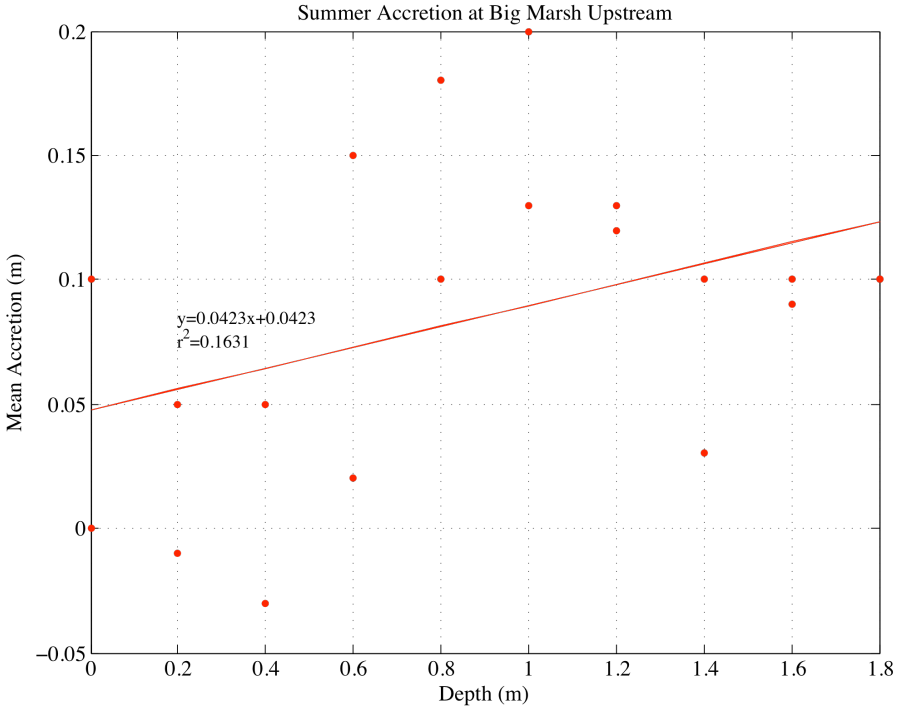

Figure R. Summer accretion at Big Marsh upstream, dominated by *H.verticullata.*

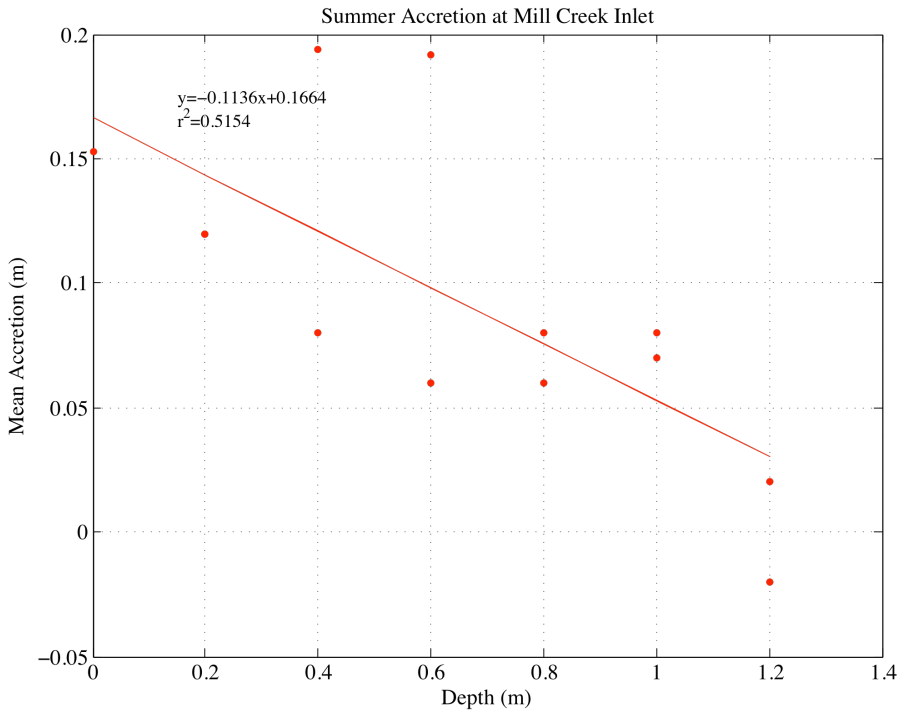

Figure S. Summer accretion at Mill Creek inlet, dominated by *N.luteum.*

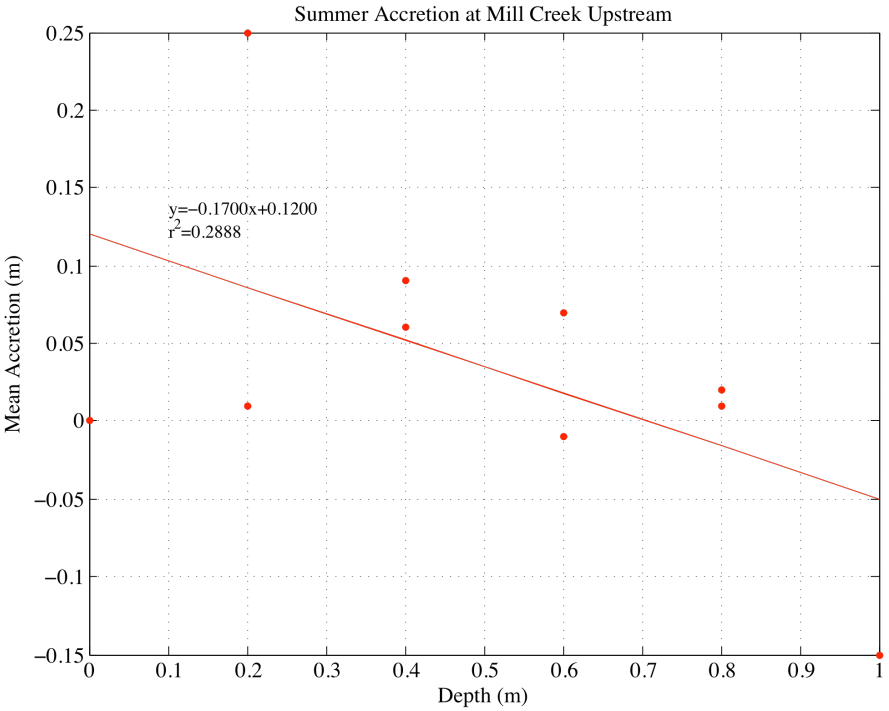

Figure T. Summer accretion at Mill Creek upstream, dominated by *N.luteum.*

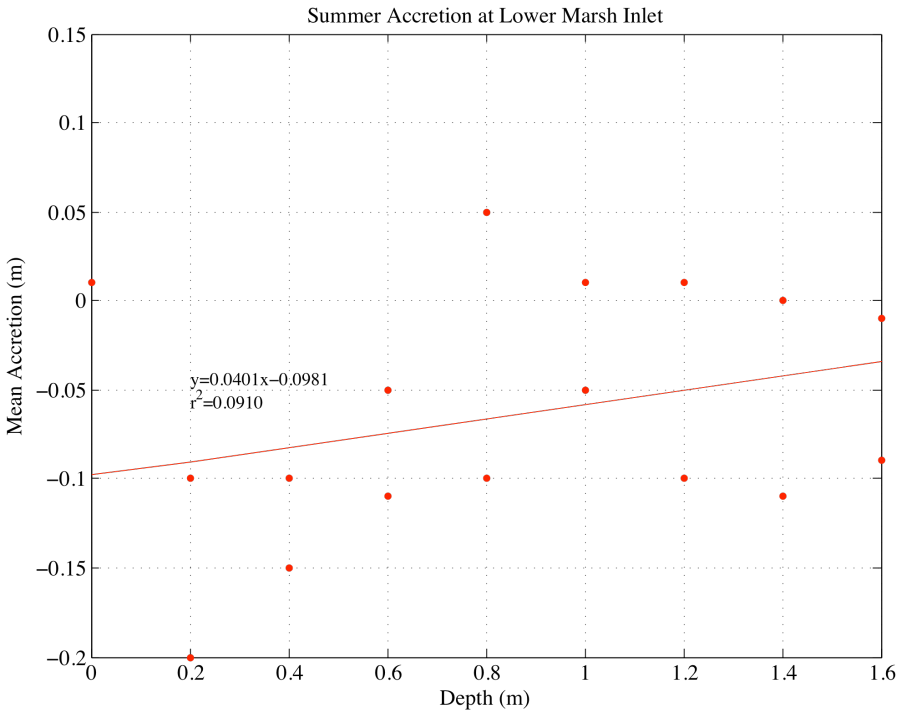

Figure U. Summer accretion at Lower Marsh inlet, dominated by *N.luteum.*

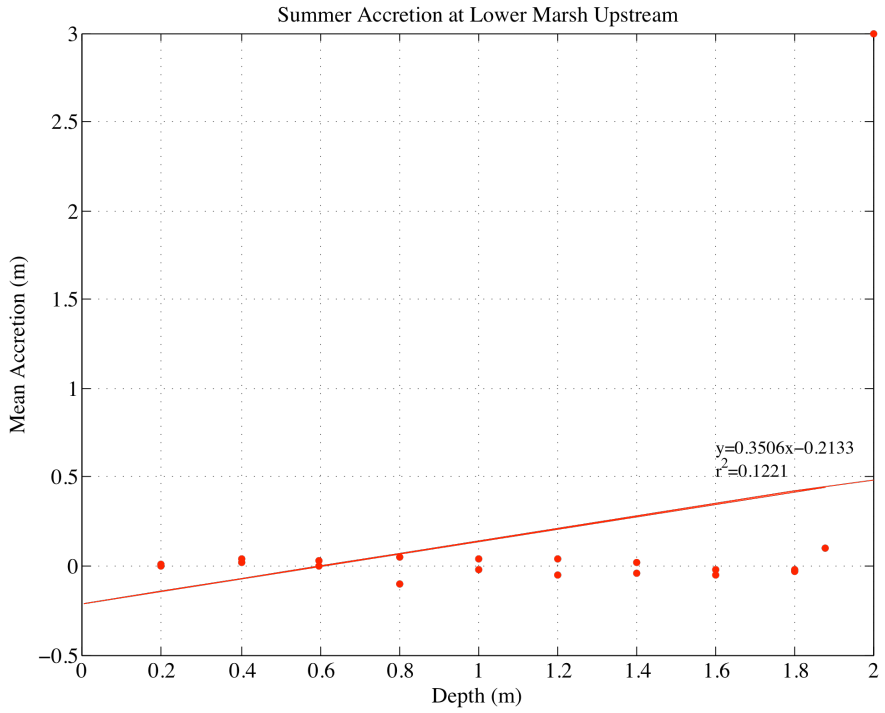

Figure V. Summer accretion at Lower Marsh upstream, dominated by *N.luteum.*

Literature Cited

Boynton, W. R., J. D. Hagy, J.C. Cornwell, W.M. Kemp, S.M. Greene, M.S. Owens, J.E. Baker, and R.K. Larsen (2008) Nutrient budgets and management actions in the Patuxent River Estuary, Maryland. *Estuaries and Coasts*. 31:623-651.

D'Alpaos, A., S. Lanzoni, S.M. Mudd, and S. Fagherazzi (2006) Modeling the influence of hydroperiod and vegetation on the cross-sectional formation of tidal channels.*Estuarine and Coastal Shelf Science*. 20:1-14.

Dietrich, W. E., and J. D. Smith (1984) Processes controlling the equilibrium bed morphology in river meanders, in: *Rivers '83: Proceedings of a Specialty Conference on River Meandering, October, 1983; Am. Soc. Civ. Engineers*. 759-769.

Fagherazzi, S., A. Bortoluzzi, W.E. Dietrich, A. Adami, S. Lanzoni, M. Marani, and A. Rinaldo (1999) Tidal networks: Automatic network extraction and preliminary scaling features from digital terrain maps. *Water Resour. Res*. 35:3891–3904.

Friedrichs, C.T., and D.G. Aubrey (1996) Uniform bottom shear stress and equilibrium hyposymetry of intertidal flats. *Coastal and Estuarine Studies*. 50:405-429.

Friedrichs, C.T., and J.E. Perry (2001) Tidal marsh morphodynamics: a synthesis. *Journal of Coastal Research.* 27:7-37.

Hickin E.J., and G.C. Nanson (1984) Lateral migration rates of river bends. *Journal of Hydraulic Engineering.* 110(11):1557-1567.

Jenner (2011) Geomorphic and hydrodynamic characteristics of small coastal inlets, Chesapeake Bay, Maryland. University of Maryland M.S. Thesis, College Park, MD.

Kent, M. (2011) *Vegetation Description and Analysis: A Practical Approach.* Oxford, UK: John Wiley and Sons, 432 pp.

Keulegan, G.H. (1938) Laws of turbulent flow in open channels. *Journal of Research of National Bureau of Standards.* 21:707-741.

Kirwan, M.L. and A.B. Murray (2007), A coupled geomorphic and ecological model of tidal marsh evolution. *PNAS.* 104(15): 6118-6122.

Kirwan, M.L., A.B. Murray, J.P. Donnelly, and D.R. Corbett. (2011) Rapid wetland expansion during European settlement and its implication for marsh survival under modern sediment delivery rates. *Geology.* 39: 507-510.

Krone, R. B. (1987), A method for simulating historic marsh elevations, in Coastal Sediments'87 edited by N. C. Krause, pp. 316-323, ASCE, New York.

Langbein, W.B., and L.B. Leopold (1968) River Channel Bars and Dunes: Theory of Kinematic Waves. U.S. Geological Survey Professional Paper 422-L.

Larsen, L. G., J. W. Harvey, and J. P. Crimaldi (2009) Prediction of bed shear stresses and landscape restoration potential in the Everglades. *Ecological Engineering.* 35:1773-1785.

Leopold, L.B., and M.G. Wolman (1957) River Channel Patterns: Braided, Meandering, and Straight. U.S. Geological Survey Professional Paper 282-B.

Limerinos, J. T. (1970) Determination of the Manning coefficient from measured bed roughness in natural channels. United States Geological Survey Water Supply Paper 1898-B.

Mackin, J.H. (1948) Concept of the graded river. *Geological Society of America Bulletin.* 59(5):463-512.

Marani, M., A. D'Alpaos, S. Lanzoni, L. Carniello, and A. Rinaldo (2007) Biologically-controlled multiple equilibria of tidal landforms and the fate of the Venice lagoon. *Geophysical Research Letters.* 34:L11402.

Marani, M., C. Da Lio, and A. D'Alpaos (2013) Vegetation engineers marsh morphology through multiple competing stable states. *Proceedings of the National Academy of Sciences.* 110(9): 3259-3263.

Michener, W.K., E.R. Blood, K.L. Bildstein, M.M. Brinson, and L.R. Gardner (1997) Climate change, hurricanes and tropical storms, and rising sea level in coastal Wetlands. *Ecological Applications*. 7:770-801.

Mitsch, W. J., and J. G. Gosselink (2000) *Wetlands*. New York, New York: Van Nostrand Reinhold. 600 pp.

Mudd, S.M, A. D'Alpaos, and J.T. Morris (2010) How does vegetation affect sedimentation on tidal marshes? Investigating particle capture and hydrodynamic controls on biologically mediated sedimentation. *Journal of Geophysical Research*. 115:F03029.

Nepf, H. and M. Ghisalberti (2008) Flow and transport in channels with submerged vegetation. *Acta Geophysica.* 56(3):753-777.

Nixon, S.W. (1982) The ecology of New England high salt marshes: a community profile. U.S. Fish and Wildlife Service. FWS/OBS-81/55. 70 pp.

Odum, W.E. (1988) Comparative ecology of tidal freshwater and salt marshes. *Annual Review of Ecology and Systematics.* 19:147-176.

Odum, W.E., and J.K. Hoover (1987) A comparison of vascular plant communities in tidal freshwater and salt water marshes. In *Ecology and Management of Wetlands,* ed. D.D. Hook *et al.* London: Croom Helm.

Palmer, M.R. H.M. Hepf, and T.J.R. Pettersson (2004) Observations of particle capture on a cylindrical collector: Implicatiosn for particle accumulation and removal in aquatic systems. *Limnology and Oceanography*. 49, 76-85.

Parker, G. (1978) Self-formed straight rivers with equilibrium banks and mobile bed, Part 1, the sand-silt river. *Journal of Fluid Mechanics*. 89(1): 109-125.

Prestegaard, K., A.J. Kaufman, E. Fowler, A. Statkiewicz, and R.Plummer (2014) Comparison of plant decomposition rates, and isotopic composition of sedimentary organic matter in *Zizania* and *Nuphar* zones of tidal inlets. Submitted for Publication.

Redfield, A.C. (1965) Ontogeny of a salt marsh estuary. *Science.* 147: 50-55.

Schulte, E.E. and B.G. Hopkins (1996) Estimation of soil organic matter by weight loss-on-ignition, In *Soil Organic Matter: Analysis and Interpretation.* SSSA Special Publication no. 46.

Seldomridge, E. and K. Prestegaard (2012) Use of geomorphic, hydrologic, and nitrogen mass balance data to model ecosystem nitrate retention in tidal freshwater wetlands. *Biogeosciences*. 9:2661-2672.

Seldomridge, E. (2009) Importance of channel networks on nitrate retention in freshwater tidal wetlands, Patuxent River, MD. University of Maryland M.S. Thesis, College Park, MD.

Tambroni, N. and G. Seminara (2012) A one-dimensional eco-geomorphic model of marsh response to sea level rise: Wind effects, dynamics of the marsh border and equilibrium. *Journal of Geophysical Reseach*. 117.

Wang, Q., Y. Li, and Y. Wang (2011) Optimizing the weight-loss-on-ignition methodology to quantify organic and carbonate carbon of sediments from diverse sources. *Environ. Monit. Assess.,* 174: 241-257.

Wolman, G. (1967) A cycle of sedimentation and erosion in Urban River Channels.

Geografiska Annaler. Series A, Physical Geography. 49(2/4): 385-395.

Zedler, J.B. (1977) Salt marsh community structure in the Tijuana estuary, California. Estuarine Coastal Marine Science. 5:39-53.